The Development and Application of Taste Sensor Using Lipid-Impregnated Membrane and Strongly Hydrophobic Lipid Polymer Membrane

巫, 霄

https://doi.org/10.15017/1931937

出版情報：九州大学, 2017, 博士（工学）, 課程博士
バージョン：
権利関係：

The Development and Application of Taste Sensor Using Lipid-Impregnated Membrane and Strongly Hydrophobic Lipid Polymer Membrane

脂質含浸膜及び疎水性の強い脂質高分子膜を用いた味覚センサに関する研究

Xiao Wu

2018

Kyushu University
Graduate School of Information Science and Electrical Engineering
Department of Electrical and Electronic Engineering

Contents

Figure List

Table List

Chapter 1
Introduction

1.1 Taste

1.1.1 Taste reception

The dorsal surface of the mammalian tongue is covered with four kinds of papillae: circumvallate, foliate, fungiform, and filiform papillae. The fungiform, foliate and circumvallate papillae are known as the gustatory papillae, which contain taste buds and work as sensory organs. The gustatory papillae are distributed over the tongue surface in a distinct spatial pattern. [1,2]. As shown in Figure 1.1, taste buds exist in the soft palate, tongue, pharynx and larynx surrounding the oral region. About 5,000 taste buds cover the surface of the human tongue [3]. A single taste bud contains 50-100 taste cells that respond to compounds that elicit sweet, bitter, sour, salty, and umami tastes and transmit this information to cerebral cortex in the brain [4]. The receptor cells for each taste quality function as dedicated sensors wired to elicit stereotypic responses [5].

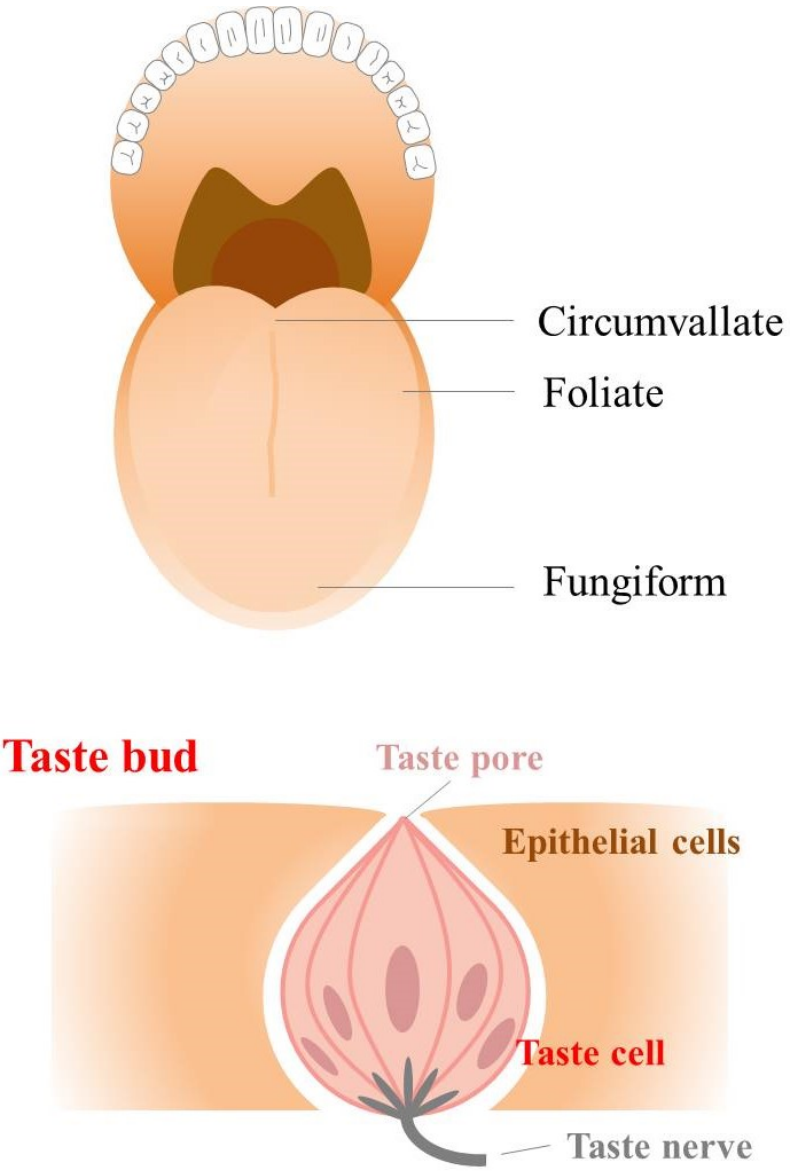

Figure 1.1: Taste-receptor cells, buds and papillae.

1.1.2 Basic tastes

In the human senses, the sense of taste is essential for the animals to identify which food is accepted or which food is unpalatable. To most mammals like human, taste consists of five basic taste qualities: saltiness, sourness, umami, sweetness, and bitterness. A study published in 2015 indicates that fat may be a sixth basic taste [6].

The taste system, or gustatory system provides valuable information about nutritive and hedonic values of foods and beverages. Taste also prevents us from consuming potentially harmful substances.

Saltiness

Saltiness is a taste produced by the presence of sodium chloride (and to a lesser degree other salts). Many studies have suggested that the ions of salt, especially Na+ can pass through Na^+ channels on the apical surface of the cell and cause an action potential. Although the ENaC receptor for sodium detection was proposed in drosophila, the identity of the salt receptor for humans has not been fully revealed yet [7,8,9]. To humans, sense of saltiness is an important signal of the mineral source that affects the maintenance of the electrolytes balance and fluid balance in human body [10].

Sourness

Sourness is a signal of corruption, produced by hydrogen ions (H^+) derived from acids. Many ion channels have been proposed to mediate sour taste transduction, including a transient receptor potential (TRP) channel PKD2L1 and its partner PKD1L3. In 2015, scientist reported a potassium (K^+) channel as a key component of sour taste transduction [11].

Bitterness

Bitterness serves as a warning signal against the ingestion of potentially harmful

substances. Bitter compounds are recognized by T2R receptors. Although the types of bitter substances are too diverse to find the consistency in the chemical structures of bitter substances, they have relatively strong hydrophobicity in common. The main interaction between bitter substances and the bitterness receptor sites involve hydrophobic interaction and electrostatic interaction. The bitter substances such as plant alkaloids, caffeine, denatonium, cyclohexamide cause bitterness stimulation when combining with the G protein coupled receptors (GPCRs) in taste bugs, which have seven transmembrane helices structures [12].

Sweetness

Sweetness indicates the presence of sugar or sweeteners as the energy source of the human body. There are many kinds of sweet substances in different chemical structures and sizes, such as sugar (sucrose, glucose etc.), sugar alcohol (xylitol etc.), peptides (aspartame etc.), sulfonylamide (saccharine sodium etc.) and so forth. Sweet taste receptor is heterocomplex receptor combined with T1R2 and T1R3 (GPCRs), which can widely accept various kinds of sweet substances [13,14].

Umami (or savory taste)

Umami was a basic taste since Kikunae Ikeda first proposed its existence in 1908. It is a Japanese word meaning "savory" or "meaty" and thus applies to the sensation of savoriness. Umami taste is elicited by many small molecules, providing necessary amino acids (glutamate and aspartate) and nucleotides (monophosphates of inosinate or guanylate, inosine 5'-monophosphate and guanosine-5'-monophosphate) to livings. These receptors include 2 glutamate-selective G protein-coupled receptors, mGluR4 and mGluR1, and the taste bud-expressed heterodimer T1R1+T1R3 have been proposed to underlie umami detection in taste buds [15].

1.2 Electronic tongue

Sensory test is often carried out by trained panelists to evaluate taste in food and pharmaceuticals. However, sensory test has some problems such as low objectivity, low reproducibility due to individual differences, physical conditions, and human fatigue. Muramoto et al. [16] have proposed that people taste the chocolate with more delicious and weaker bitter when in a high-stress state. In addition to the mental state, the age also affects so-called five senses including taste. Cowart et al. [17] found that the taste threshold of the elders to quinine and isohumulone increased compared to young people. In sensory test, the cost of selecting and training panelists with sharp sensation also cannot be ignored. Therefore, an objective method of evaluating taste using an electronic tongue has been expected. The research on taste sensing started in the mid-1990s, before the elucidation of the principle of vertebrate taste receptors [18-20]. Since then, many studies on electronic tongues (e-tongue) [21-27] and bioelectronic tongues [28, 29] have been carried out for taste assessment. The sensitivity of traditional electronic tongues is higher than bioelectronics tongue on the whole. However, traditional electronic tongues consist of a number of sensors whose selectivity are lower than bioelectronic tongues, and uses advanced mathematical procedures for signal processing based on the pattern recognition (PARC) and /or multivariate data analysis [30]. In the multivariate data analysis, the meaning of each principal component has to be explained. Although there is a disadvantage that the taste of an unknown sample cannot be objectively evaluated, the current e-tongue is superior in comparison between control samples and the application to quality management has also been expected.

1.3 Taste sensor (TS-5000Z)

1.3.1 Characteristic

In 1989, Toko et al. proposed the prototype of the taste senor (SA401, Anritsu Co. Ltd.) using the lipid polymer membrane as taste receptors. In 2007, the evolved taste sensor in Figure 1.2 (TS-5000Z, Intelligent Sensor Technology Inc., Kanagawa, Japan) has been invented and could measure all five basic taste qualities and astringency, respectively. This sensor has an unique characteristic called 'global selectivity', which means that each sensor does not distinguish each chemical substance, but distinguishes taste quality and taste intensity [31,32]. For example, the bitter substances are strongly hydrophobic while the salty taste substances are hydrophilic and contain a metal cation or a chloride ion in solution. The sensing principle of the taste sensor utilizes these physicochemical properties of taste qualities in Figure 1.3. Although this type of taste sensor utilizes fundamentally different principle from the receptor principle in human taste cells, it has been used widely because of the advantage of better selectivity than other electronic tongues, as well as better sensitivity and durability than bioelectronic tongues in the objective evaluation of the taste of food and pharmaceutical products (e.g., beer, coffee, traditional Chinese medicines) [32-34].

The lipid polymer membrane is composed of three elements: lipid, plasticizer and support material. Each sensor membrane is designed using different types and amounts of lipids and plasticizers. The lipid molecules are amphiphilic and have the role of adjusting the density of electric charges on the surface and the hydrophobicity of the membrane. The plasticizers and PVC basically have no charge and are added to form the membrane with softness and toughness [22,35,36 ,37].

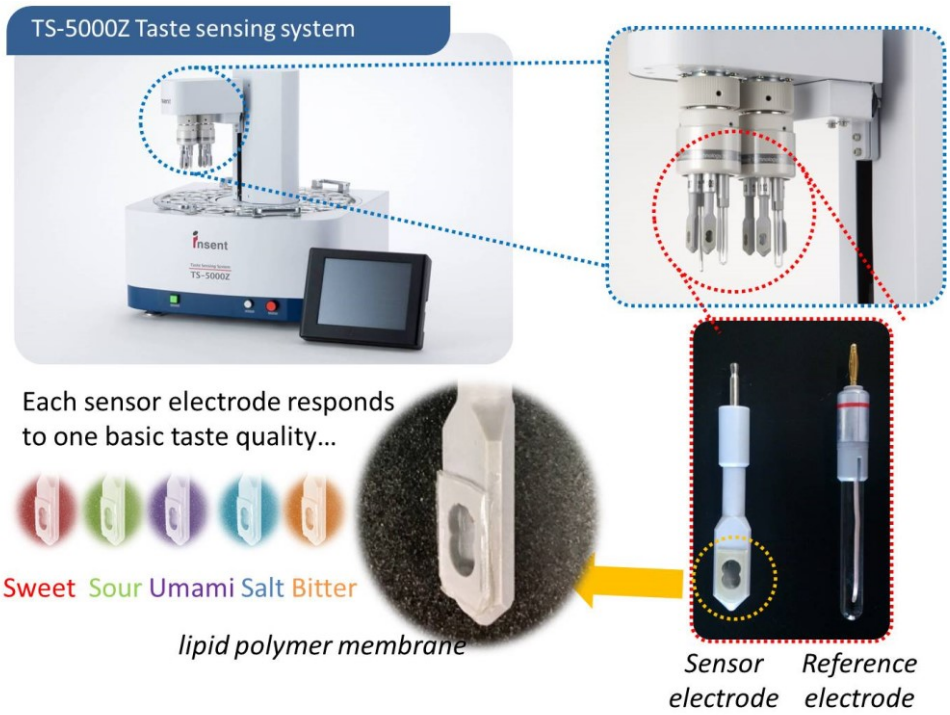

Figure 1.2: Taste sensor (TS-5000Z)

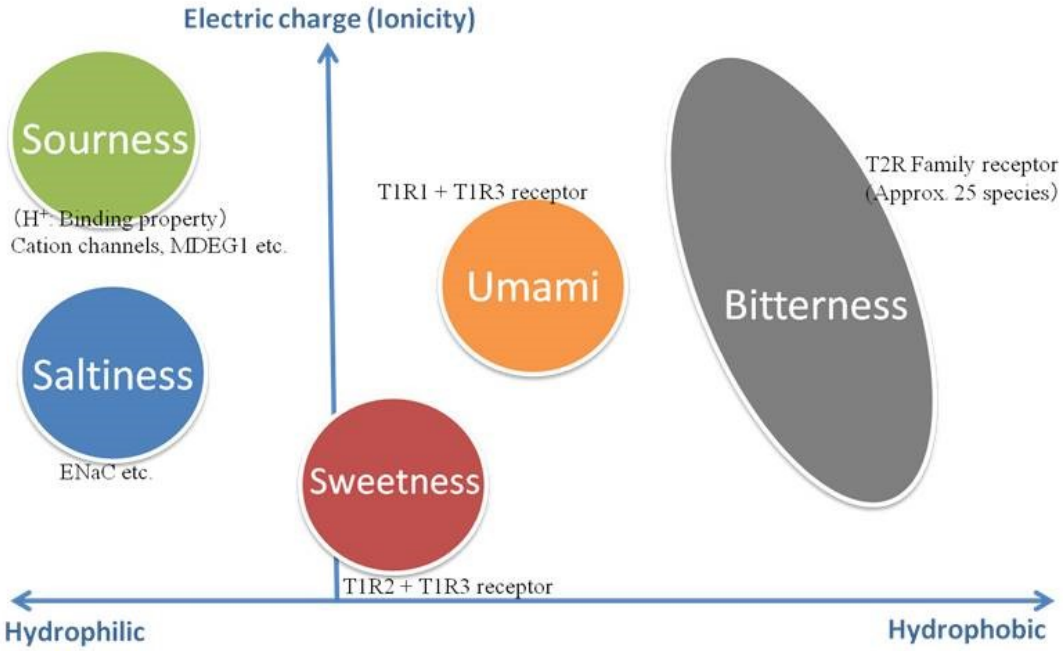

Figure 1.3: Physicochemical properties of the five basic taste substances

1.3.2 Mechanism of taste sensor response

It is well known that an electrical double layer is formed on a charged membrane in accordance with classical Gouy-Chapman theory [38,39]. When the lipid polymer membrane is immersed in an aqueous solution, an electrical double layer is formed on the membrane surface by dissociation of lipid molecules, causing membrane potential. The higher the sample concentration, the shorter the distance between the bulk and membrane becomes [32,40]. As an example of a positively charged film in an aqueous solution (Figure 1.4), the electric field E in the solution and the potential difference V satisfy the following integral equation.

$$V = \int_0^d E dx \quad \text{(1.1)}$$

Here, d is the distance from the surface of the membrane. As the amount of the taste substance contained in the sample is larger, the reduction in the potential difference due to the shielding effect becomes greater. Therefore, taste substances contained in the sample can be quantified.by using a certain solution as a reference and comparing the potential difference between the reference solution and each sample.

The substance exhibiting sour taste ionizes to hydrogen ions and other anions, so the aqueous solution shows the acidic property. When we immerse a negatively charged lipid polymer membrane in an acidic solution, the suppression effect of the dissociation of hydrogen ions from lipid molecules happens and causes a change in membrane potential (Figure 1.5). Therefore, since the dissociation of hydrogen ions is suppressed, the electric charge of the lipid polymer membrane decreases and the potential difference changes.

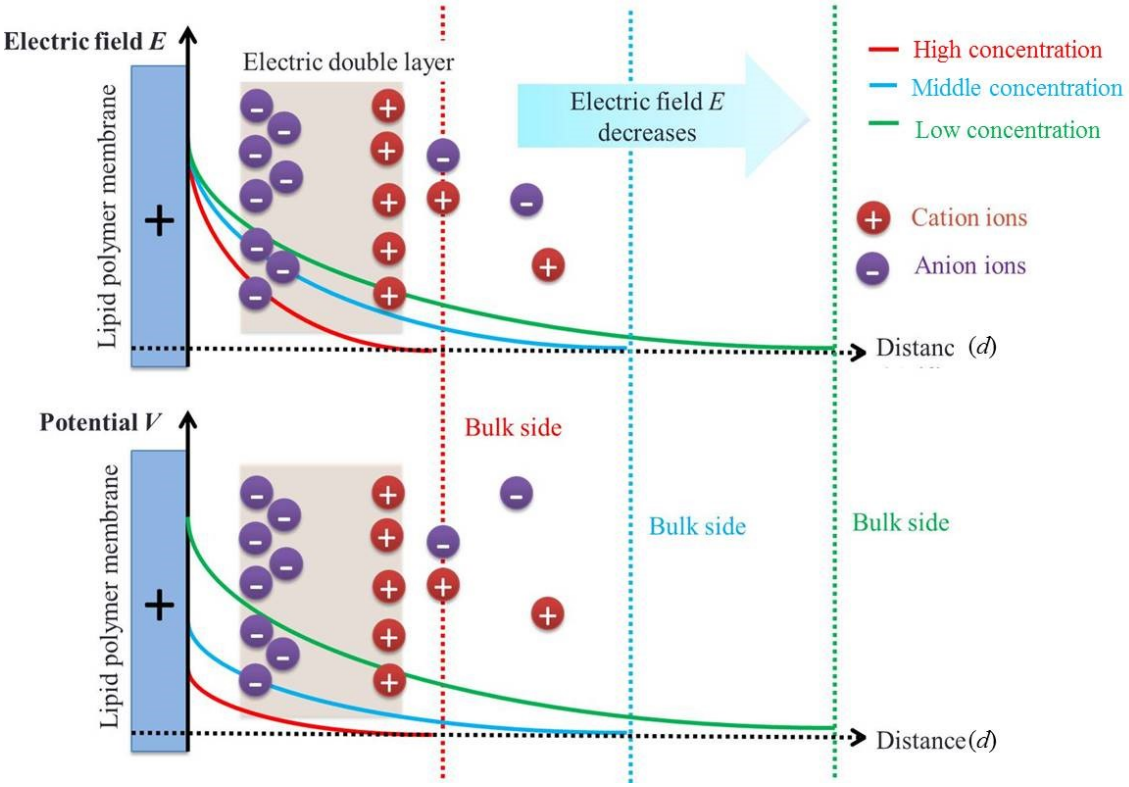

Figure 1.4: Shielding effect.

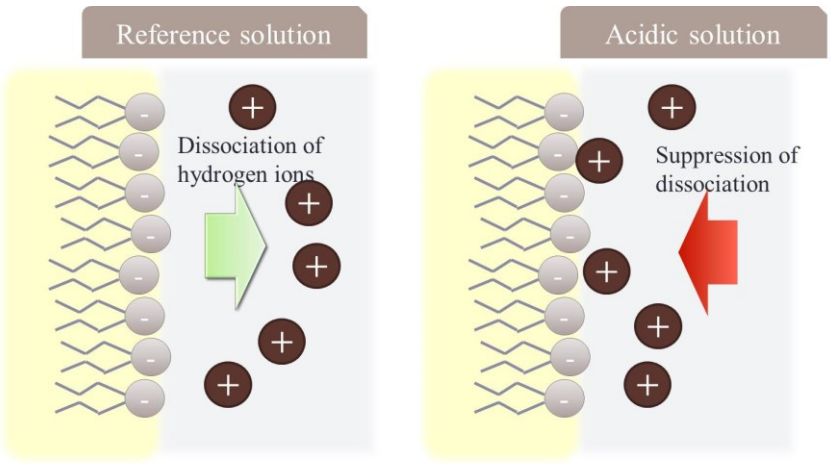

$$RP(O)OH \rightleftharpoons RP(O)O^- + H^+$$

Figure 1.5: Dissociation by pH and suppression of dissociation.

In addition to electrostatic interaction, there is hydrophobic interaction between the taste substances and the lipid polymer membrane. Hydrophobicity means the property of (a part of) a substance or molecule that has low affinity for water and is difficult to dissolve in water or mix with water. Among the hydrophobic substances exhibiting tastes, there are quinine (bitter), iso-α-acid (bitter), and tannic acid (astringency). Since these substances are ionized in an aqueous solution, they are positively or negatively charged. When the hydrophobic membrane is immersed into a hydrophobic taste solution, the ionized hydrophobic substance causes physical adsorption due to hydrophobic interaction with the hydrophobic group of lipid or plasticizers in the lipid polymer membrane to change the charge state.

1.3.3 Measurement of taste sensor

The difference of membrane potential between sensor electrode and reference electrode caused by the electrical and hydrophobic interactions is measured to evaluate the taste samples. Figure 1.6 shows the diagram of taste sensing system with sensor electrode and reference electrode. First, the sensor electrode and reference electrode are immersed in the reference solution of 30 mM KCl and 0.3 mM tartaric acid to obtain the membrane potential V_r after the membrane pretreatment. The reference solution has almost no taste and mimics human saliva. Second, the electrodes are moved to the sample solution to obtain the potential V_s. Third, the sensor electrodes are slightly rinsed by the reference solution and moved to a reference solution again to obtain V_r'. As shown in Figure 1.7, the difference in potential (Vs – Vr) is called the relative value. The difference in potential (V_r' – V_r) is called CPA (change of membrane potential caused by adsorption) [41]. The relative value and CPA value (change of membrane potential caused by adsorption) are two outputs of the taste sensor used at the taste evaluation. The relative value approximates the initial taste derived from hydrophilic taste substances at sensory evaluation, including sourness, saltiness, and umami. On the other hand, the CPA value approximates the after taste derived from hydrophobic taste substances including bitter and astringent substances, providing change of membrane potential due to the adsorption on the lipid polymer membrane [42]. In recent years, as the relationship between CPA value and adsorption amount has been clarified, the evaluation of bitterness using the taste sensor has been placed great expectations in food and pharmaceutical industries.

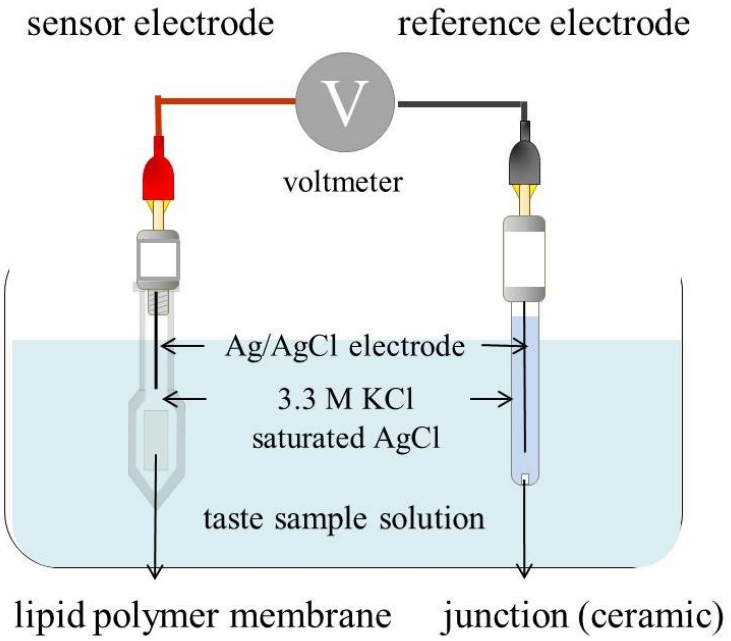

Figure 1.6: Diagram of taste sensing system.

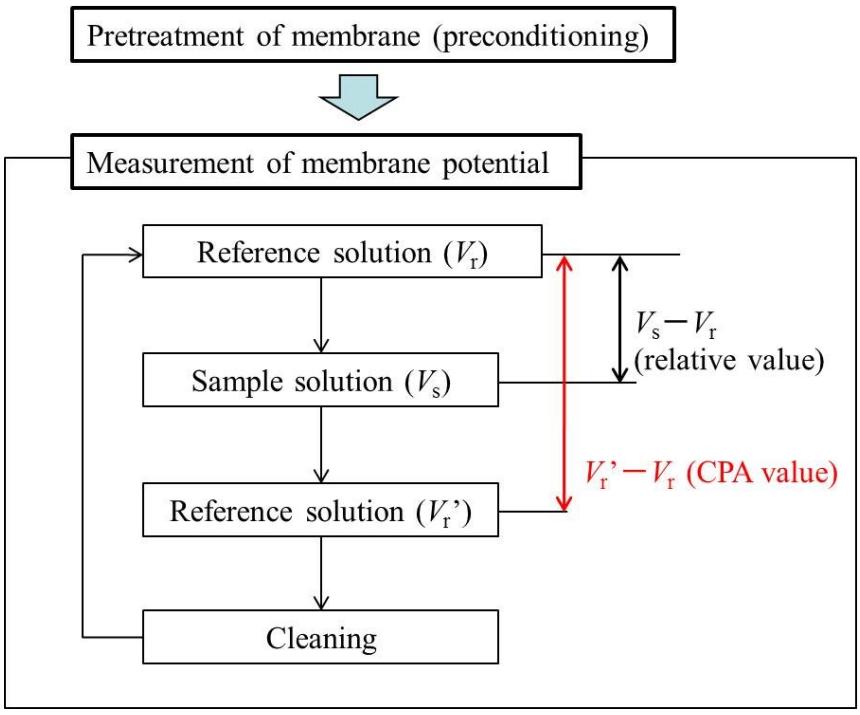

Figure 1.7: Measurement procedure of taste sensor.

1.4 The purpose of this study

The purpose of this paper is to enhance the performance of the taste sensor for education with a lipid-impregnated membrane as well as the taste sensor with a strongly hydrophobic lipid polymer membrane. We hope to promote the application of the taste sensor in the field of education, agriculture, and bitterness evaluation through this research.

First, we discussed about a simple taste sensor used for education, which uses a lipid-immersed Teflon filter as the sensing material. This sensor could be made easily by the students but has low selectivity. However, we thought the selectivity is important for the students to recognize the usefulness of the taste sensor. So in **Chapter 2**, we aimed to develop a do-it-yourself (DIY) taste sensor set for education with better sensor selectivity. As a result, we proposed a fabrication method of the taste sensor for education using cheap and commonly used materials which can be easily realized by the students of middle school or high school. The taste sensor for education was improved to respond selectively to salty and sour samples by adjusting the composition of lipids and plasticizers.

Second, we aimed to improve the performance of the taste sensor in sensitivity and durability. In **Chapter 3**, we discussed the influence of the pretreatment process on the taste sensor with the strongly hydrophobic membrane. As a result, we found that the sensor response has a great correlation with the pretreatment time and both the adsorption amount and the surface charge density of the lipid polymer membrane affect the CPA value. In **Chapter 4**, we investigated the reason for the deterioration in the response of the BT0 sensor by measuring the membrane potential, contact angle, and adsorption amount, as well as by performing gas chromatography-mass spectrometry

(GC-MS), liquid chromatography-tandem mass spectrometry (LC-MS/MS). We found that the change in the surface charge density caused by the hydrolysis of plasticizer led to the deterioration of the response. The acidic environment generated by lipid promoted plasticizer hydrolysis. Finally, we succeeded in fabricating a new membrane for sensing the bitterness of medicines with higher durability and sensitivity by adjusting the proportions of the lipid and plasticizers.

Third, we attempted to evaluate the interaction between two taste qualities with multiple sensor electrodes. In **Chapter 5**, we develop a quantitative prediction method to evaluate the bitterness of medicines suppressed by high-potency sweeteners using the taste sensor. As a result, we proposed a quantitative prediction method to evaluate the bitterness masking effect of high-potency sweeteners using the taste sensor. The quantitative prediction method showed a good correlation between the estimated bitterness scores and the sensory scores.

Finally, in Conclusion, we summarized the results of Chapter 2~5, and stated the future prospects.

Chapter 2

Taste Sensor for Education with Selectivity to Salt and Citric Acid [43]

2.1 Background

2.1.1 Attitudes towards science among students

According to the results of the Trends in International Mathematics and Science Study (TIMSS) conducted in 2015 by the International Association for the Evaluation of Educational Achievement (IEA), 37% of grade-two junior high school students in Japan do not like learning science, while the proportion of all the 29 participating countries is 19% in average. Japan ranked second to the last. Another investigation on students confident in science was also carried on these 29 countries. 68% of grade-two junior high school students in Japan do not confident in science, while the average is 40%. Japan ranked the last. Not only Japan, many countries in Asia ranked behind. The result pointed out that lack of interest and confidence in science among students is still a serious problem in Asia, especially in Japan [44]. In addition, Programme for International Student Assessment (PISA) conducted in 2006 by the Organization for Economic Co-operation and Development (OECD), reported that only 42% of grade-one high school students in Japan clearly understood the contribution science could do to human life. While the proportion of all the 57 participating countries is 67% in average, which showed lack of awareness of the close contact between science study and human life [45]. Therefore, it is significant to let the students recognize the usefulness of the science subjects such as physical, biological and chemistry.

Characteristics of Taste Sensor	***Subjects***	***Context of Science in High School***	***Context of Science in Junior High School***
Utilization of lipid membrane	Biology	Hydrophilic & hydrophobic	Cell and cell membrane
Interaction with taste substance	Chemistry	Ionization equilibrium	Chemical change and ion
Measurement of voltage	Physics	Current and electrical circuit	Current and voltage

Table 2.1: Relationship between taste sensor and science education.

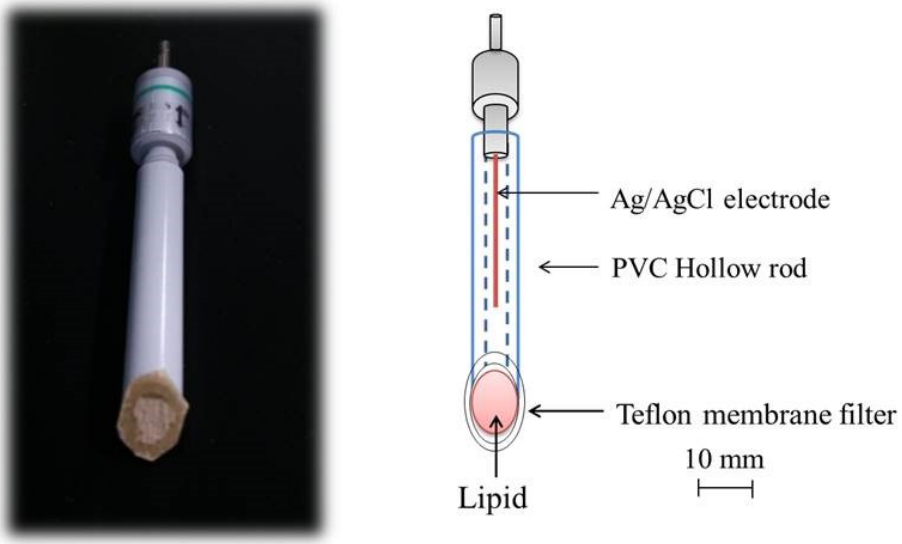

Figure 2.1: The electrode of taste sensor for education.

2.1.2 Problems of current taste sensor and purpose of this chapter

At this moment, many events on science education targeting high school students have been held in an attempt to solve the problem of lacking of interest and confidence in science [46]. In this study, we also attempted to apply the taste sensor into a Japanese science class, because the features of taste sensors are related to the science subjects of high school and junior high school, which are showed in Table 2.1.

The idea of taste sensor for education has been proposed to let the students make a taste sensor and use this sensor to measure taste qualities [47]. The fabrication and measuring process might help students to understand the related science knowledge and stimulate their enthusiasm for scientific experiments. However, it is unrealistic to make a commercial taste sensor in a science class, because the fabrication process takes 3 days in order to completely dry the solvents in the membrane. Moreover, the organic solvent, tetrahydrofuran (THF) used in the fabrication of the lipid polymer membrane, distributes a bad smell and may cause stimulus and nausea to human's mucosa [48]. Therefore, the fabrication method of the do-it-yourself (DIY) taste sensor for students which can be made easily in a short time without THF is as follows [49].

The detailed method is as follows.

(1) Cut the Teflon membrane into about 1 cm^2

(2) Paste the cut Teflon membrane onto the head of a hollow bar using an instant adhesive

(3) Dry the instant adhesive for 1 minute

(4) Immerse the attached Teflon membrane in the lipid solution (single lipid with ethanol) for 30 seconds

(5) Dry the solvent of lipid for 10 minute

(6) Inject the inner solution containing 3.3 M KCl and saturated AgCl into the PVC hollow rod by using a pipette

(7) Completed by attaching an Ag/AgCl electrode to the PVC hollow rod

The photo and structure of taste sensor electrode for education is shown in Figure 2.1. The above process takes about 20 minutes without using THF at all. In addition, the lipid solution was diluted by the ethanol, which reduces the risk during the fabrication. We used this sensor to measure different concentrations of salt and citric acid solution. The sensor response showed good concentration dependence to both salt and citric acid [49]. However, there is no sensor selectivity to salt or citric acid using this sensor. In order to let the students realize the usefulness of the educational taste sensor, we intended to improve the sensor selectivity to saltiness and sourness. Moreover, although the above fabrication method excludes the risk of THF, fixation of the Teflon membrane still needs an instant adhesive, which may cause danger to children. Therefore, we prefer a new method without using an instant adhesive. In order to increase the fun of the experiment and reduce the cost of production, the stationery around children is taken into consideration as much as possible [50].

In this chapter, we reported a simple taste sensor for education with the selectivity to saltiness and sourness as well as a new fabrication method which can be made easily in a short time without THF and instant adhesives. In the end, we carried out science classes using handmade taste sensors and evaluated the educational effect of the class [43].

2.2 Experiment

2.2.1 Materials

The Teflon membrane filter (80 μm thick) purchased from Advantec Co. Ltd., Tokyo, Japan is used as a lipid-holding membrane. The polyvinyl chloride hollow rod is replaced by a pencil cap, which can be easily available from a stationery store. The terminal cap purchased from Morigin Co. Ltd., Tokyo, Japan is used to fix the membrane onto the top of the hollow rod. TOMA (trioctylmethylammonium chloride) and PAEE (phosphoric acid di(2-ethylhexyl) ester) purchased from Tokyo Chemical Industry Co., Ltd. As shown in Figure 2.2, TOMA is positively charged in solution due to the hydrolysis of chloride ions; PAEE is negatively charged in solution owing to the ionization of phosphate group.

2.2.2 Selectivity improvement

Because TOMA and PAEE are ionized in solution and charged positively and negatively, respectively, the charged state of the sensor membrane can be controlled by adjusting the amount of TOMA and PAEE. In this way, we considered that the balance of positive and negative charges is important for the response to saltiness and sourness. In the electrostatic interaction, attraction or repulsive force expressed by Coulomb's law works between positive and negative charges. Therefore, in this experiment, TOMA and PAEE were mixed at a volume ratio of 3: 1, 2: 1, 1: 1, 1: 2, 1: 3 (corresponding to molar ratios: 2.16, 1.44, 0.72, 0.36, 0.24). The ethanol used for dilution accounts for 50% of the total lipid solution. The lipid mixed solution was stirred with a stirrer for 1 hour.

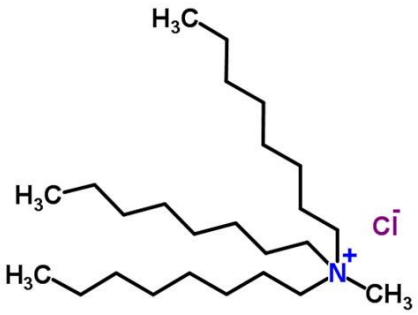

trioctylmethylammonium chloride
TOMA

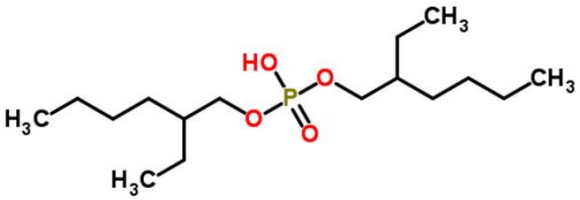

phosphoric acid di(2-ethylhexyl) ester
PAEE

Figure 2.2: Chemical structures of TOMA and PAEE.

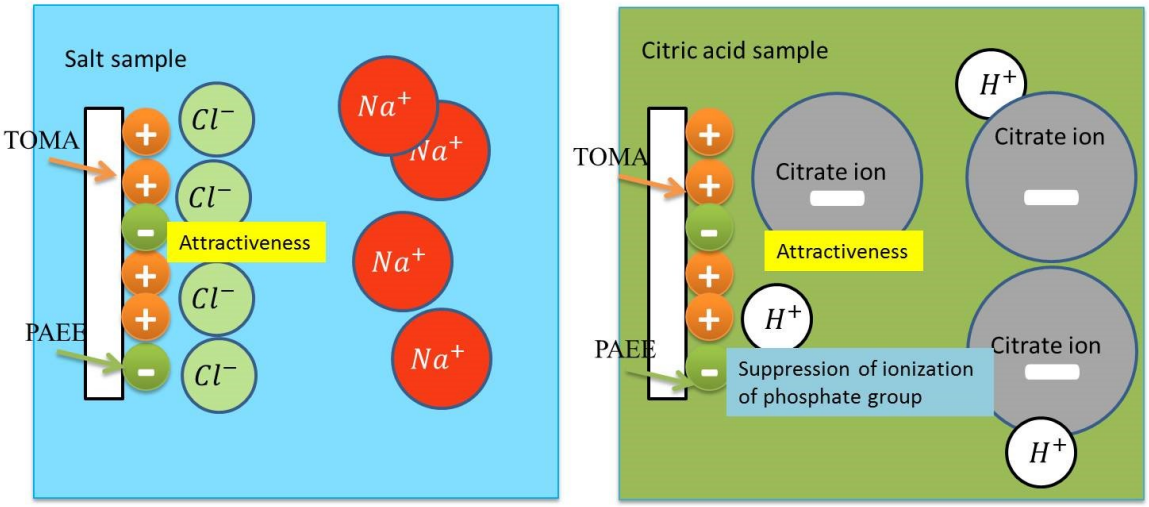

Figure 2.3: Design concept of the charged lipid membrane for salt.

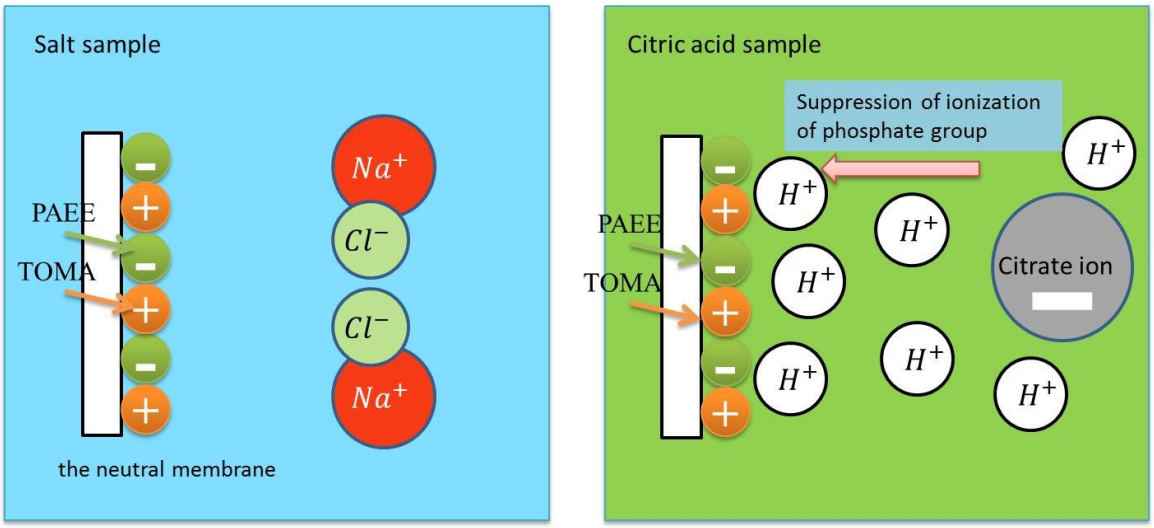

Figure 2.4: Design concept of the charged lipid membrane for citric acid.

As shown in Figure 2.3, on the one hand, the membrane for saltiness is designed to be positively charged and attract chloride ions. The membrane potential decreases owing to the electrostatic interaction of negatively charged chloride ions. On the other hand, we want to find the balance of attractiveness to citrate ions and the suppression of ionization of phosphate group in the citric acid solutions. Therefore, the membrane is considered to respond to only salt but not to citric acid.

As shown in Figure 2.4, on the one hand, the membrane for sourness is designed to show electricity in nearly neutral. Therefore, the membrane is considered not to attract any sodium ions or chloride ions. On the other hand, the membrane potential increases because of the suppression of ionization of phosphate group in the citric acid solutions. Therefore, the membrane is considered to respond to only citric acid but not to salt.

2.2.3 Sensory test

Six mixed samples #1 ~ #6 with salt and citric acid (# 1 salt 2.0 g / 500 mL, citric acid 0.25 g / 500 mL; # 2 salt 4.0 g / 500 mL, citric acid 0.25 g / 500 mL, # 3 salt 8.0 g / 500mL, citric acid 0.25 g / 500 mL; # 4 salt 2.0 g / 500 mL, citric acid 0.5 g / 500 mL, # 5 salt 4.0 g / 500 mL, citric acid 0.5 g / 500 mL; # 6 salt 2.0 g / 500 mL, citric acid 1.0 g / 500 mL) were used in the sensory test. The concentration difference among these samples was set to close to 1.2 times, which is called the minimum concentration difference people can distinguish in taste. The panelists were general college students who have not received any special training on sensory testing. Based on sample #1, we randomly sorted the samples #2 to #6 and let the panelists map the results in the following two-dimensional answer sheet (Figure 2.5).

2.2.4 Improvement of fabrication procedure

In the fabrication of the conventional taste sensor for education, the sensor membrane can be completed in 20 minutes without using THF. However, in order to prevent the accidents such as mischief of children and gluing fingers caused by usage of the instant adhesive, we renewed the fabrication method by using a terminal protective cap instead of the instant adhesive. In the science class we conducted before, the students often failed to complete the sensor electrode because bubbles entered when inserting the inner solution. By using the transparent pencil cap instead of the PVC hollow rod, the students can make sure there is no bubble in during the fabrication of sensor electrode. First, a hole about 0.5 cm^2 was cut in the head of two terminal protective caps. Then fix the smaller terminal protective cap to thread part of Ag/AgCl electrode. Cut the Teflon membrane filter into about 2×2 cm and sandwich the Teflon membrane between the pencil cap and the bigger terminal protective cap. (Expose the Teflon membrane through the hole). Make sure there was no gap between Teflon membrane and the pencil cap. Then drop a dropwise of lipid onto the exposed part of membrane using a pipette and naturally dry the membrane for 10 min. Next, inject the inner solution containing 3.3 M KCl and saturated AgCl into the pencil cap by using a pipette. Finally, fix an Ag/AgCl electrode to the pencil cap (Figure 2.6). The completed taste sensor for education is shown in Figure 2.7 [43].

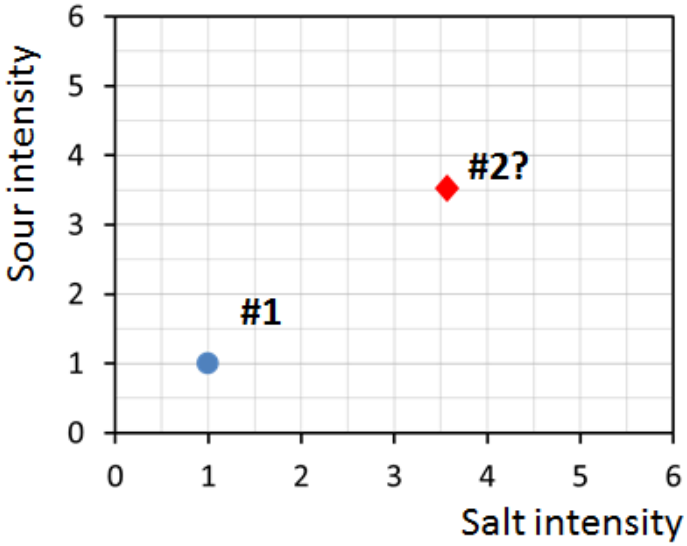

Figure 2.5: The answer sheet for sensory test

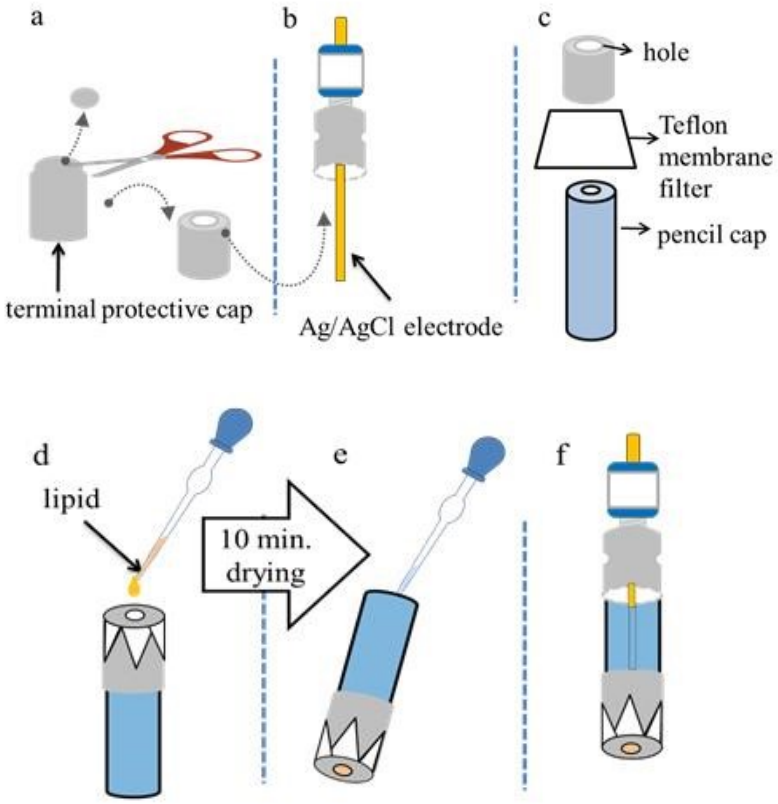

Figure 2.6: The fabrication procedure of taste sensor used in science class [51].

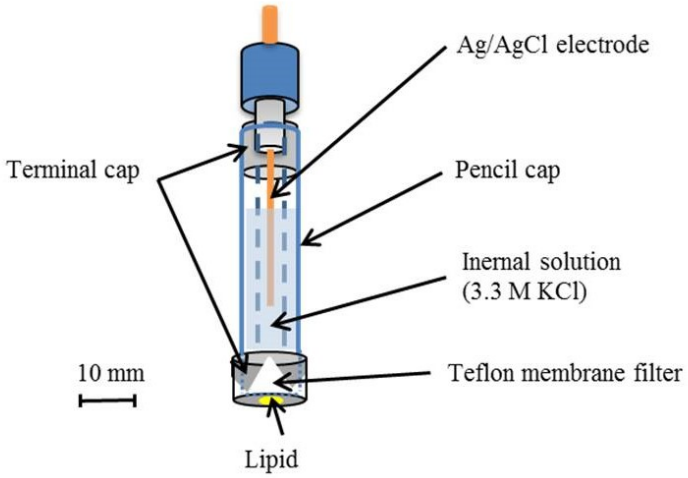

Figure 2.7: The completed taste sensor for education.

2.2.5 Measurement method

As shown in Figure 2.8, to record the time to reach a stable membrane potential during the development of the sensor kit, we connected the sensor electrode to the positive terminal of the voltmeter and the reference electrode to the negative terminal of the voltmeter. We used a computer to observe the voltage between the electrode and the reference electrode. Firstly, we measured the membrane potential V_r in a reference solution comprising 30 mM KCl and 0.3 mM tartaric acid. Then the sensor electrodes were moved into a sample solution based on the reference solution and the potential V_s is obtained. We defined value difference (V_s - V_r) as the sensor response. Finally, the electrodes are subsequently rinsed with a reference solution again for about 3 seconds before the next measurement.

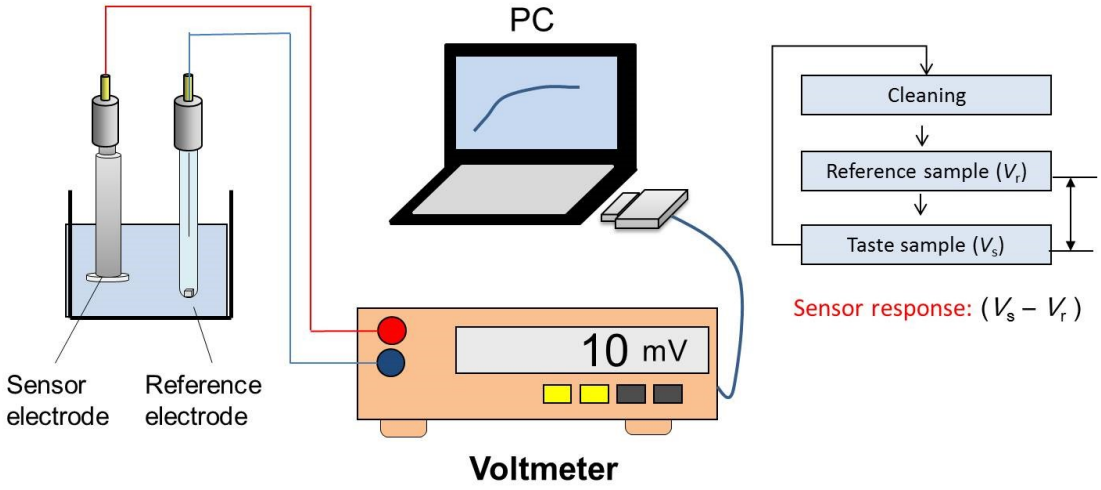

Figure 2.8: Schematic of measurement system at developing stage.

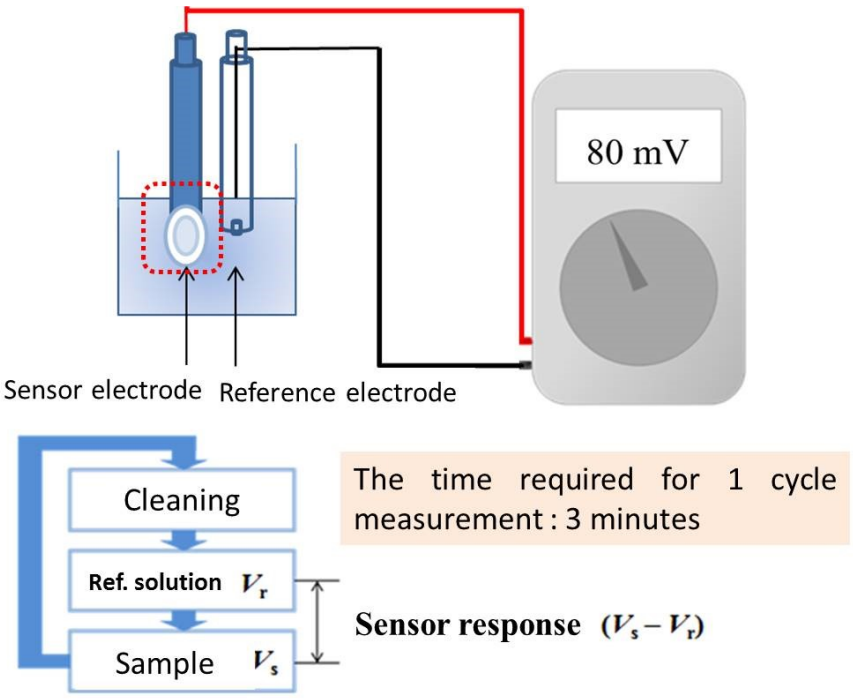

Figure 2.9: Schematic of measurement system at science classes.

2.2.6 Application in Science class

In order to prove the usefulness of the improved taste sensor for education, we applied the sensor fabricated by the above method in a science class in Japan. In the science class, we use a small tester instead of a digital voltmeter, which was easier to carry. The objects of the science class were 28 high school students (11 boys and 17 girls). The students were divided into five groups with five or six students in every group. Five TA students from our lab were assigned to each group to guide the experiment.

The goal of each group was to fabricate one saltiness sensor and one sourness sensor using the method in section 2.2.4. Only the student volunteers participated in the sensory test. The method of the sensory test was the same to that of section 2.2.3 except for the adjustment in citric acid concentrations. Four mixed samples A ~ D with salt and citric acid were used in the sensory test. The concentrations were shown in Table 2.2. The commercial mineral water was used as the reference solution. All the samples were made based on the reference solution (RS). At the end of the science class, we conducted a survey based on the following questions, which focus on student attitudes about fabricating the new taste sensor for education. *Q1*: Do you think today's science class was a good opportunity to know more about the field of science subjects? *Q2*: Do you think it was difficult to fabricate a sensor by yourself? *Q3*: Do you like to make up something by yourself? *Q4*: What function do you want to improve the sensor?

Sample/500 mL	#1	#2	#3	#4	RS
Salt	2 g	4 g	2 g	4 g	0 g
Citric acid	1 g	1 g	2 g	2 g	0 g

Table 2.2: Schematic of measurement system in science classes.

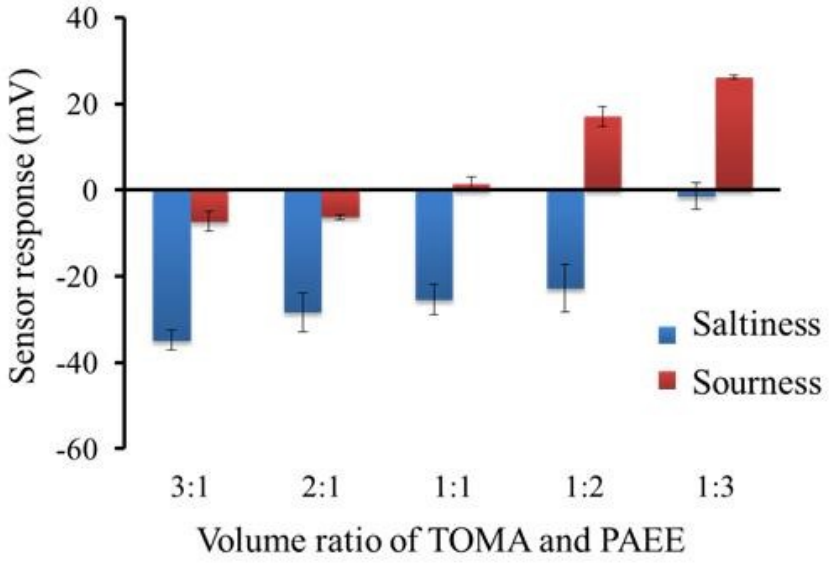

Figure 2.10: Response characteristics of saltiness and sourness [43].

2.3 Results and discussion

2.3.1 Improvement on sensor selectivity

In Figure 2.10, the vertical axis means the changes in the membrane potential (mV/dec) between high concentration sample and low concentration sample with ten times difference. The horizontal axis shows the volume ratio of TOMA: PAEE. The result showed that when TOMA and PAEE were mixed in the volume ratio of 1:1, the sensor response showed good selectivity for salty solution (saltiness sensor). When TOMA and PAEE were mixed in the volume ratio of 1:3, the sensor response showed good selectivity for citric acid solution (sourness sensor).

In Figure 2.11, the vertical axis means the relative value. Since the sensor response of the conventional taste sensor follows the Nernst equation, the logarithmic scale is adopted on the horizontal axis. From Figure 2.11, when TOMA : PAEE = 1: 1, the relative value was proportional to the logarithm of the sodium chloride sample concentration. On the other hand, when citric acid was added to the salt sample, the relative value kept almost unchanged. Therefore, when TOMA: PAEE = 1: 1, this sensor showed good selectivity to saltiness and can be used as saltiness sensor for science class. As shown in Figure 2.12, when TOMA: PAEE = 1: 3, the relative value was proportional to the logarithm of the citric acid sample concentration. On the other hand, when the sodium chloride was added to the citric acid sample, the relative value kept almost unchanged. Therefore, when TOMA: PAEE = 1: 3, the sensor showed good selectivity to sourness and can be used as sourness sensor for science class.

We considered the principle of the selectivity of saltiness and sourness sensor. The saltiness sensor has a positively charged membrane because TOMA was positively charged in a solution. Therefore, the sensor membrane attracts Cl^- of NaCl and showed

a negative potential. However, the citric acid ions have little interaction with this positively membrane because of the repulsion. On the other hand, the sourness sensor has a neutrally charged membrane because the charge of both TOMA and PAEE were neutralized. Therefore, the sensor membrane cannot attract Na^+ or Cl^-. However, the pH decreased when the sensor membrane was put into a citric acid solution, which leads to a suppression of dissociation of H^+ from PAEE. Therefore, the sensor membrane showed a positive potential in citric acid solutions.

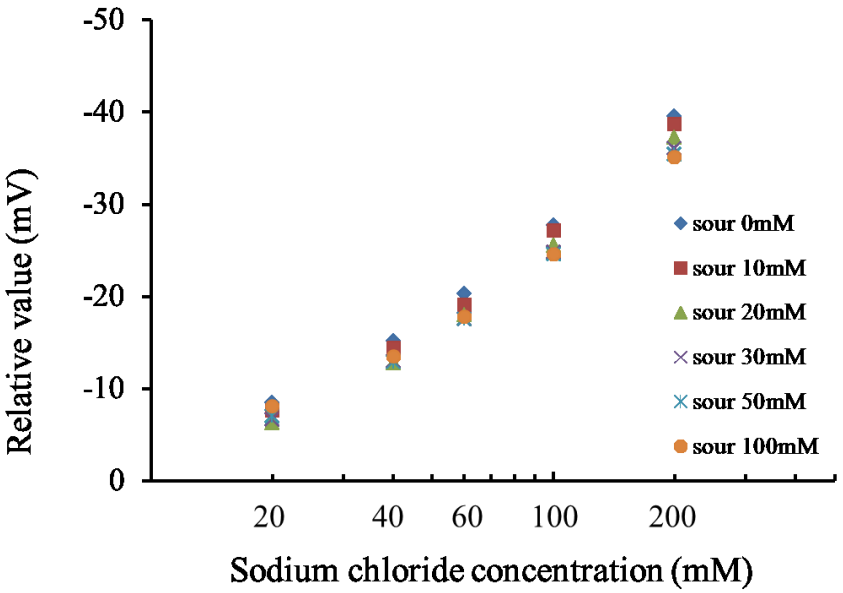

Figure 2.11: The relative value with increasing sodium chloride (Mixing ratio, TOMA: PAEE = 1: 1) [43].

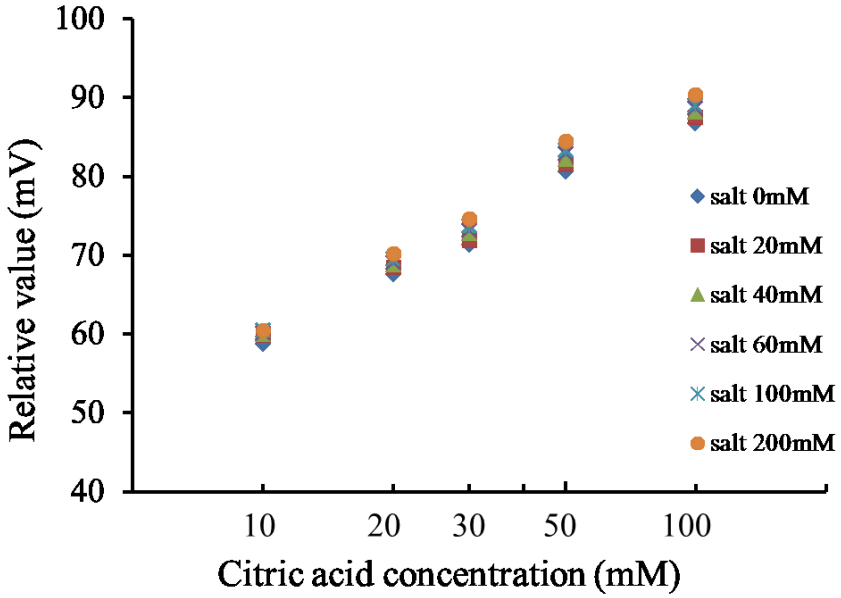

Figure 2.12: The relative value with increasing citric acid (Mixing ratio, TOMA: PAEE = 1: 3) [43].

2.3.2 Result of sensory test

The high standard deviation showed in Figure 2.13, indicated that different people have different sense of taste intensity. The Figure 2.14 shows the results of the taste sensor for education fabricated by the above method. The positional relationships in Figure 2.13 and Figure 2.14 are in good agreement. In addition, the standard deviation of the sensor response is much lower. By comparing the result of the sensory test and the result of the educational taste sensor, it is considered that the taste sensor could be a good experimental example that makes the students realize the ambiguity of human senses and the usefulness of the taste sensor.

2.3.3 Science class

As shown in Figure 2.15 and Figure 2.16, the relationship of the positions of the samples between sensory test and the sensor response were the same, which proved that both saltiness sensor and sourness sensor were successfully made by students themselves.

According to the result of questionnaire, more than 92% students thought the science class was a good opportunity to know more about the field of science subjects. On the evaluation of the new fabrication method, half of the students thought it was difficult while half don’t think so. After the science class, more than 92% students thought they like making up something by themselves. The function the students most want to improve is to measure the commercial drinks using the taste sensors.

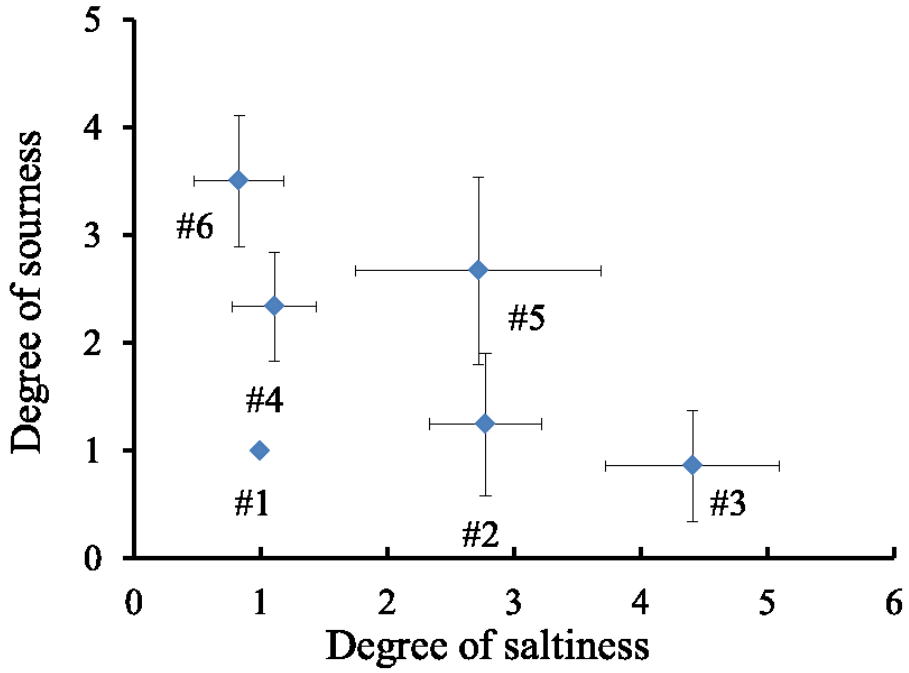

Figure 2.13: Result of sensory test [43].

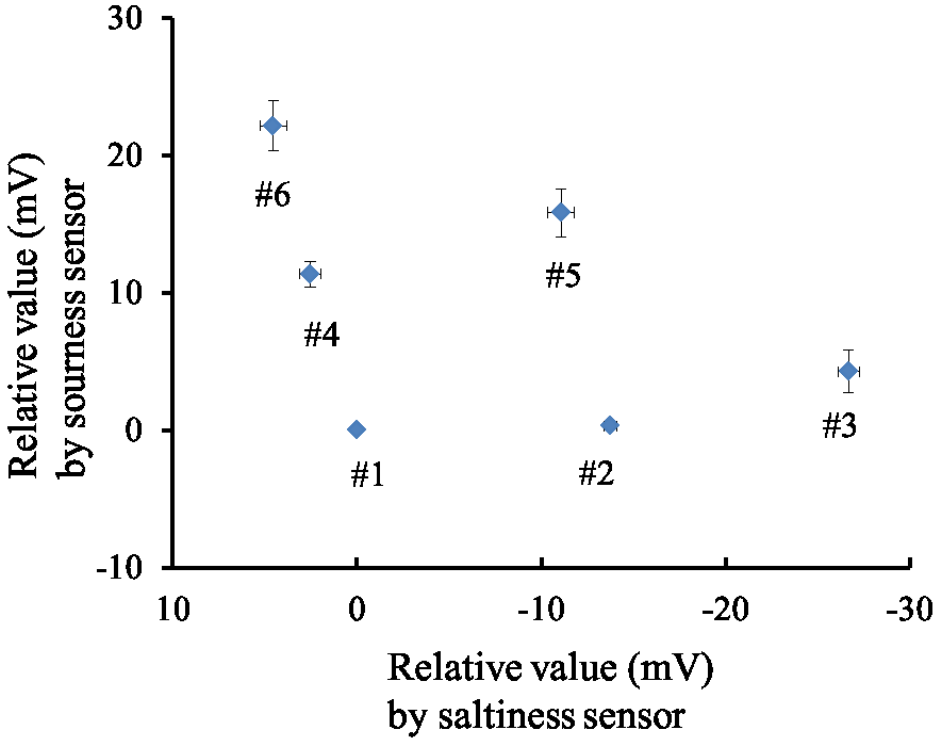

Figure 2.14: Relative values of saltiness and sourness sensors [43]

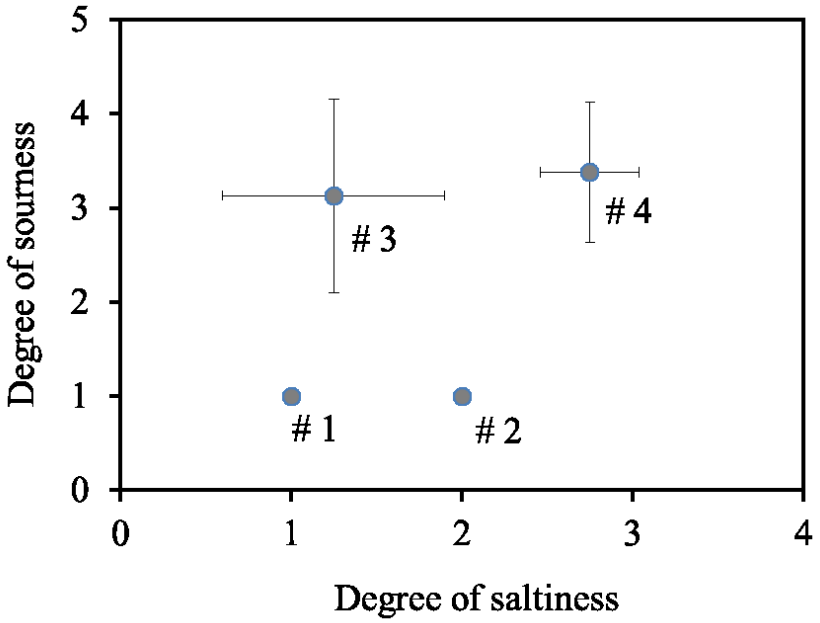

Figure 2.15: Result of sensory test of students

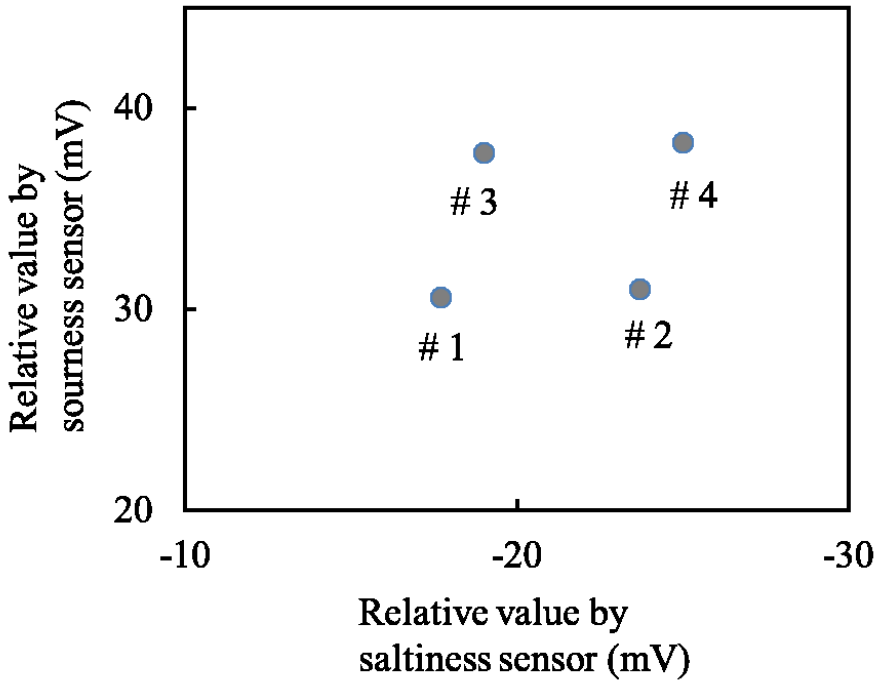

Figure 2.16: Relative values of saltiness and sourness sensors of students

2.4 Conclusion

So far we have developed the sensor membrane by impregnating the Teflon membrane into a single lipid. In the chapter, we succeeded in providing selectivity to saltiness and sourness by adjusting the mixing ratio of lipid TOMA and PAEE. Furthermore, we developed a method to fabricate taste sensors for education using more safe and normal stationeries.

To demonstrate the usefulness of this taste sensor for education, we applied this taste sensor into a science class for high school students. The students succeeded in the fabrication of the saltiness sensor and sourness sensor and used the sensors to measure mixture samples of salt and citric acid, which is proved a useful teaching material for science class.

Chapter 3
Preconditioning Process for Taste Sensor with a Strongly Hydrophobic Membrane [52]

3.1 Background

3.1.1 Hydrophobic membrane of taste sensor

As we introduced in Chapter 1, the membranes of the commercial taste sensor (TS-5000Z) consist of lipid, plasticizer and polymer. The lipid is used to adjust the charge density on membrane surface. The plasticizer is used to improve the softness and toughness of membrane. Both lipid and plasticizer can affect hydrophobicity of the membrane. Polyvinyl chloride is used to form the membrane as a supporting material [22].

Because the lipid has both hydrophobic and hydrophilic groups, the surface of the membrane shows hydrophilic when the lipids are arranged with the hydrophilic part facing the water. As shown in Figure 3.1, although saltiness sensor and bitterness sensor (-) for acidic bitterness adopted the same kind of lipid, they have different characteristics. The bitterness sensor (-) has a hydrophobic membrane surface because the amount of lipid is relatively small while the saltiness sensor has a hydrophilic membrane because the amount of lipid is relatively large.

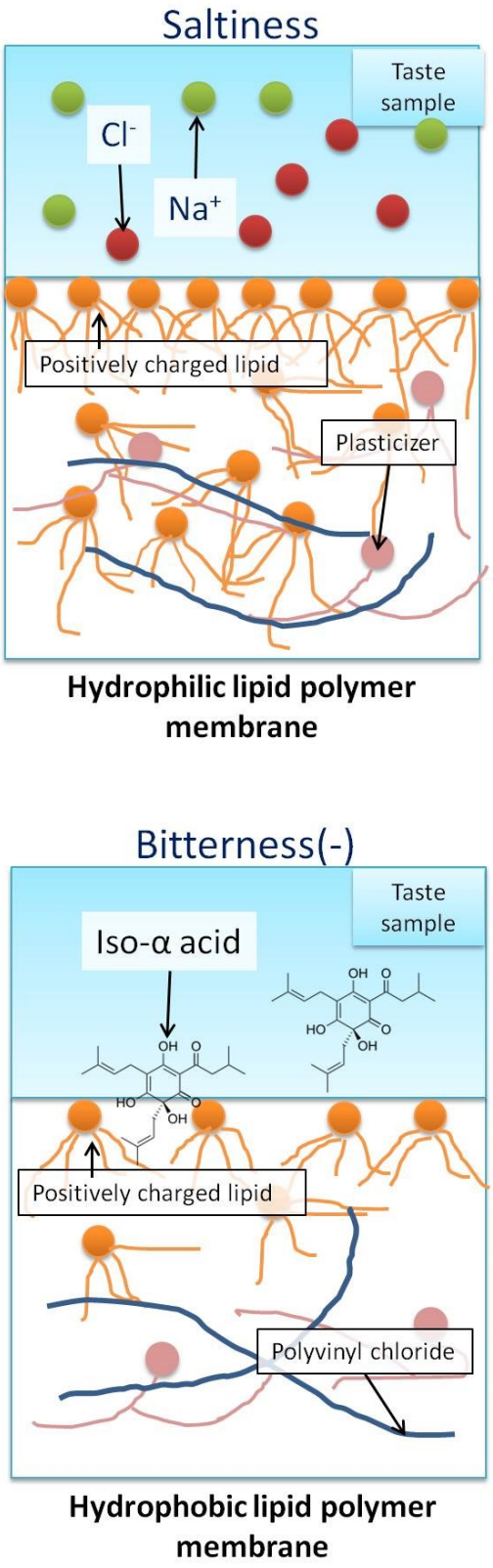

Figure 3.1: The lipid polymer membranes for saltiness and bitterness (-)

3.1.2 Detection of pesticide surfactants

As food safety issues attract more and more attentions, the sensor with a lipid polymer membrane has been used to detect agriculture chemicals [53], cyanide [54] and organic substances [55]. In agriculture production, pesticide residues have always been an important issue. As we know, pesticides consist of active ingredients (AIs) and pesticide adjuvant. The pesticide adjuvant is composed of carriers and surfactant. The carriers are used to carry AIs and facilitate pesticide handling while the surfactant is used to emulsify, disperse and spread AIs and diluents as well as increase their solubility. Because there are too many types of AIs and the physiochemical properties are quite different from each other, the conventional methods can only detect very few kinds of pesticide species. There are 799 types of pesticides registered in total in Japan. For example, ELISA (enzyme-linked immunosorbent assay) targets about 30 types of pesticides [56]. Cholinesterase inhibition assay targets approximately 20% pesticides registered in Japan [57]. In 2012, a screening method for pesticide residues by detecting anionic surfactants used as pesticide adjuvants was examined by membrane measurement using a surfactant-sensing membrane composed of tridodecylmethylammonium chloride (TDAB). It is reported that the sulfonate anionic surfactant, sodium dodecyl sulfate (SDS), was detected under 10 ppb. The Chemical structures of TDAB and SDS are shown in Figure 3.2. The sensor showed a specific response to a coexisting surfactant, but no response to the AIs [58]. More pesticides could be detected by indirectly measuring the amount of SDS contained in pesticides because an anionic surfactant accounts for approximately 70% of registered pesticides. [59].

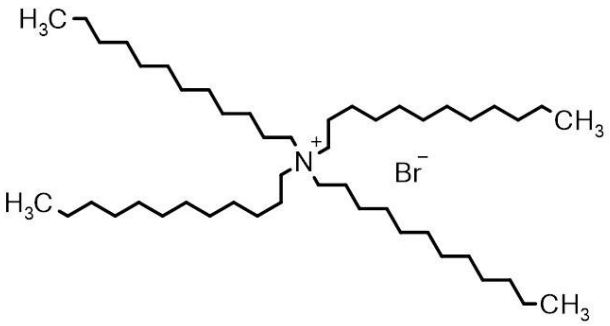

tetradodecylammonium bromide (TDAB)

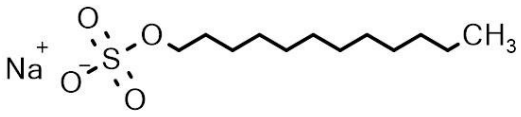

sodium dodecyl sulfate (SDS)

Figure 3.2: Chemical structures of TDAB and SDS.

3.1.3 Preconditioning process of lipid polymer membrane

The sensor electrode and a reference electrode were used in the measurement of membrane potential. Before measuring the membrane potential, there is an important pretreatment step for the lipid polymer membrane. The bottom of the sensor electrode with the membrane and the reference electrode were immersed in a solution for several days. The immersion process in reference solution (30 mM KCl and 0.3 mM tartaric acid) is called reference preconditioning. The immersion process in monosodium glutamate (MSG) solution (10 mM MSG, 30 mM KCl and 0.3 mM tartaric acid) is called MSG preconditioning (usually for strongly hydrophobic membranes).

As shown in Figure 3.3, before the preconditioning, there is a messy distribution of lipids in the membrane. After the preconditioning, the lipids will arrange regularly on the surface of the membrane with the hydrophilic part facing to the solution, because of self-organization. The preconditioning process can help improve the membrane properties such as surface structure and charge density of the lipid polymer membrane. The reference preconditioning is used for most of the taste sensor electrodes while the MSG preconditioning is used for a bitterness sensor (-) (for acidic bitterness), which equipped with a hydrophobic membrane [60].

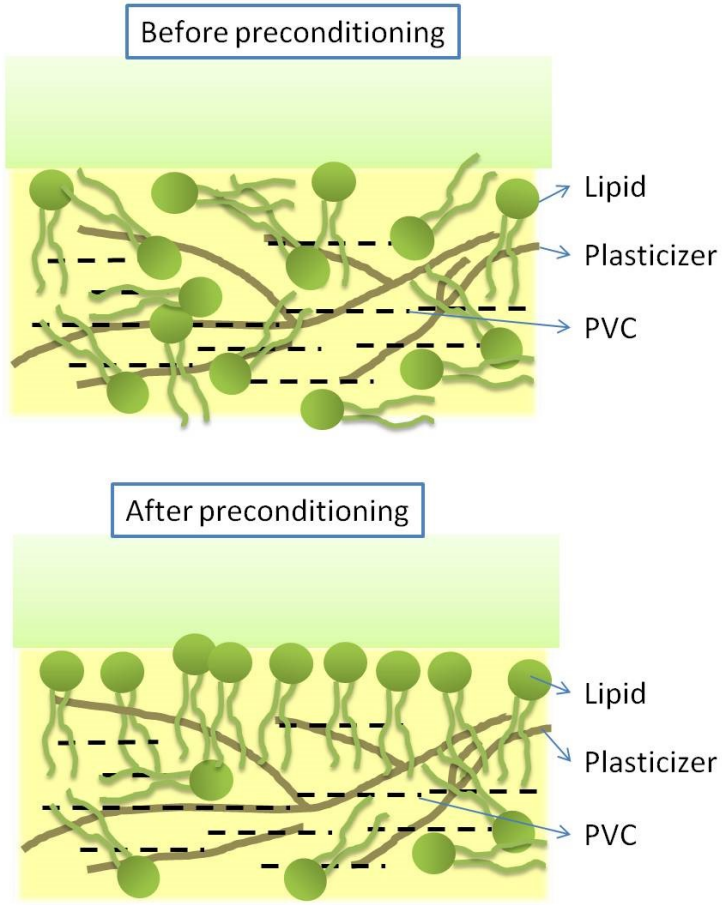

Figure 3.3: The diagram of the preconditioning process

3.1.4 The current problem and the purpose of this chapter

Although the relative value of the pesticide sensor showed good concentration dependence on SDS concentration, the CPA did not respond to SDS even after a reference preconditioning. As shown in Figure 3.4, when the sensor membrane was pretreated by MSG preconditioning for one day, the CPA value showed good concentration dependence on SDS concentration. If you look at Figure 3.5 you will find that the reference potential kept stable with the measurement times after the MSG preconditioning. On the other hand, the reference potential decreased to minus without the reference preconditioning. We think the research will contribute to the development of high-sensitivity sensor for hydrophobic substances if we know the response properties during the MSG preconditioning. Therefore, the purpose of this chapter is to reveal the membrane properties during MSG preconditioning using a strongly hydrophobic membrane for SDS detection. In this chapter, we investigated the relationship between the CPA value of the sensor for SDS and period of MSG preconditioning. The amount of adsorbed SDS and MSG was also measured to figure out whether the CPA value is related to the amount of adsorption.

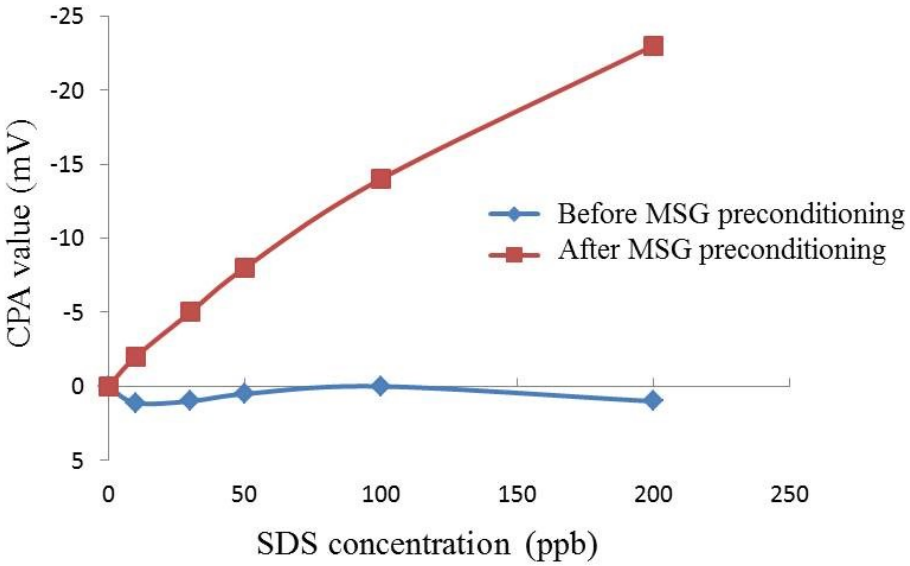

Figure 3.4: Relationship between CPA value and SDS concentration

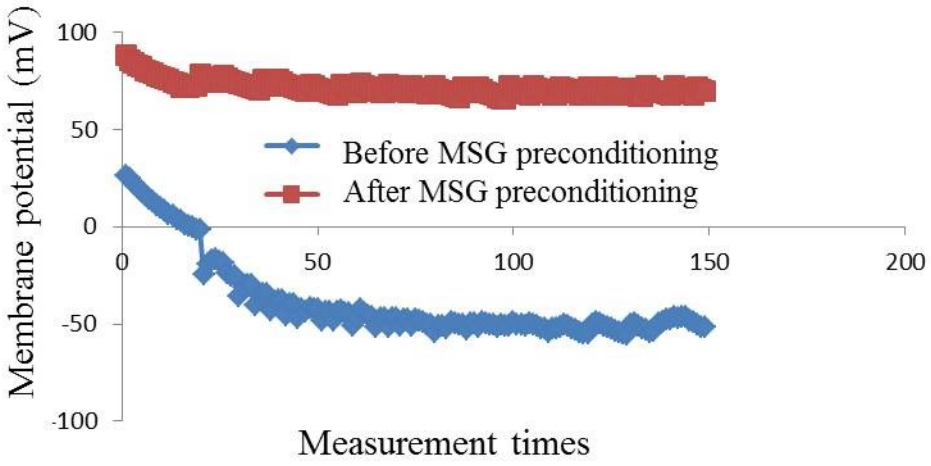

Figure 3.5: Relationship between reference potential and SDS concentrtion

3.2 Experiment

3.2.1 Chemicals

TDAB was purchased from Sigma-Aldrich, Inc. (St. Louis, MO, USA). 2-Nitrophenyloctyl ether (NPOE) was purchased from Dojindo Laboratories (Kumamoto, Japan). Polyvinyl chloride (PVC) and SDS were purchased from Wako Pure Chemical, Ltd. (Osaka, Japan). MSG, KCl and tartaric acid were obtained from Kanto Chemical Co., Inc. (Tokyo, Japan). TDAB (log P = 15.55) shows strong hydrophobicity in the monomeric state. TDAB can be ionized into TDA^+ and Br^- in solutions. Therefore, the membrane with TDAB positively charges and can detect the negatively charged SDS in samples. All aqueous solutions were prepared with deionized water. The chemical structures of these substances are showed in Figure 3.6 PONALKIT-ABS was purchased from Dojindo Laboratories and YAMASA L-Glutamate Assay Kit was purchased from YAMASA Co., Ltd (Tokyo, Japan).

3.2.2 Fabrication of lipid polymer membrane

The fabrication steps are as follows. Firstly, TDAB, NPOE and 800 mg PVC were dissolved by 10 ml THF and stirred for one hour. Secondly, the above solution was poured into a 90 mm glass Petri dish and the THF volatized off and the membrane formed. Thirdly, the membrane was cut into about 1×1 cm and stuck to the sensor probe using an adhesive of 10 mL THF and 800 mg PVC. Fourthly, 0.2 mL inner solution of 3.3 M KCl and saturated AgCl was filled into the sensor probe using a syringe. Finally, the sensor electrode was completed by attaching an Ag/AgCl electrode to the sensor probe.

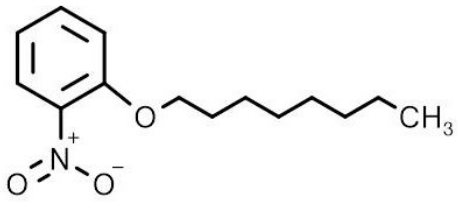

NPOE (plasticizer)

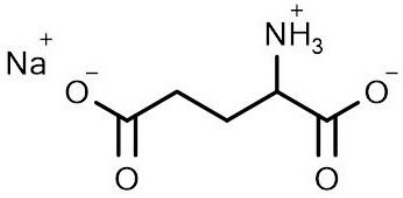

MSG

Figure 3.6: Chemical structures of NPOE and MSG

3.2.3 Membrane potential measurement

First, the sensor electrode was immersed in the MSG preconditioning solution (10 mM MSG, 30 mM KCl and 0.3 mM tartaric acid) from 0 to 5 days before the measurement. Second, the sensor electrode and reference electrode were immersed in the reference solution comprised of 30 mmol/L KCL and 0.3 mmol/L tartaric acid and obtain membrane potential V_r. Third, the sensors were immersed into a sample solution and obtain membrane potential V_s. Finally, the sensors were immersed into the reference solution again and obtain membrane potential V_r' after being lightly rinsed by the reference solution. Here, we defined the difference between potential (V_s - V_r) the relative value and the difference between potential (V_r' - V_r) the CPA (the Change in the membrane Potential caused by Adsorption) value [61,62]. Finally, the membrane potential retuned to V_r, when the membrane rinsed with a sensor-rinsing solution (30 vol% ethanol, 100 mM KCl and 10 mM KOH).

3.2.4 Measurement of adsorbed SDS

The lipid membrane used for measurement of adsorbed SDS was made in 45 mm glass Petri dish. Before the measurement, the MSG preconditioning solution was poured onto the membrane in 45 mm Petri dish for the certain days (0, 1, 2, 3, 4 or 5 days). PONALKIT-ABS kit was used to measure the amount of adsorbed SDS. In PONALKIT-ABS kit, the ion pair of Co-5-Cl-PADAP and SDS is extracted to the organic phase, which made the organic phase colored. The SDS concentration can be calculated by measuring the absorbance of the organic phase. The chemical structure of Co-5-Cl-PADAP and organic solvents are shown in Figure 3.7 and Figure 3.8. The coloring principle of organic solvent is shown in Figure 3.9.

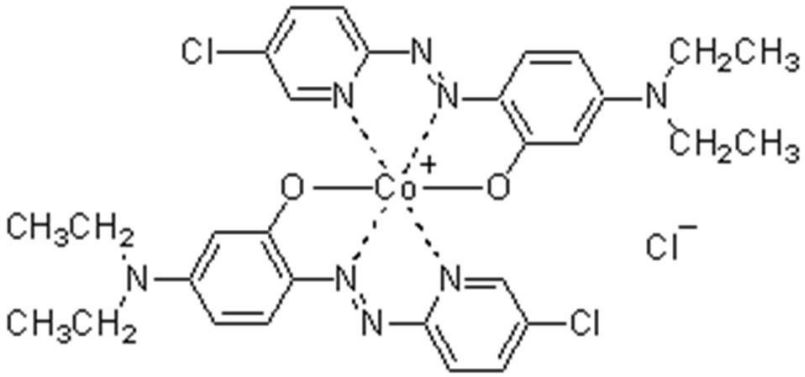

$C_{30}H_{32}Cl_3CoN_8O_2$=701.92

Figure 3.7: Chemical structure of Co-5-Cl-PADAP (colorimetric reagent)

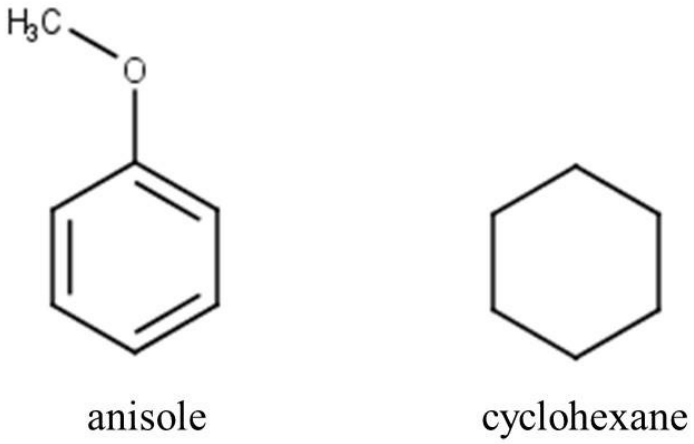

Figure 3.8: Chemical structure of anisole and cyclohexane (organic solvent)

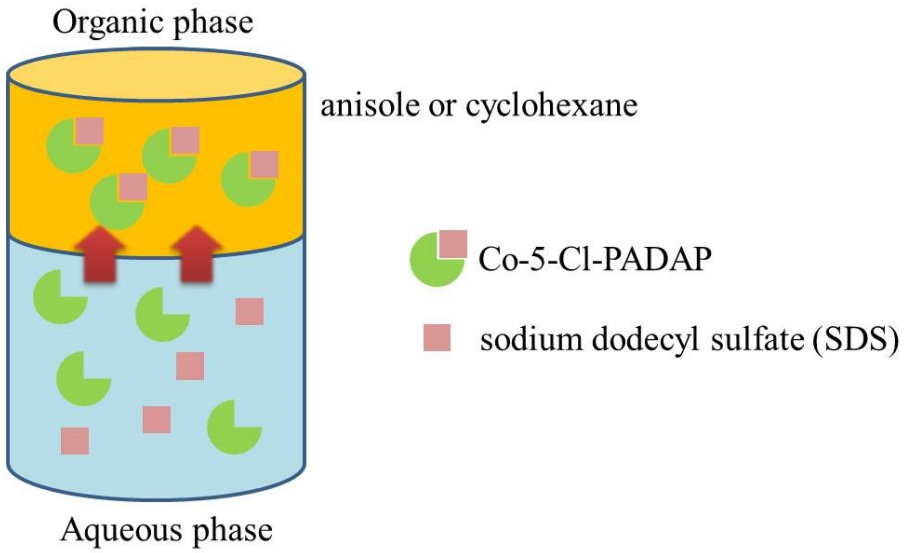

Figure 3.9: Coloring principle of organic solvent

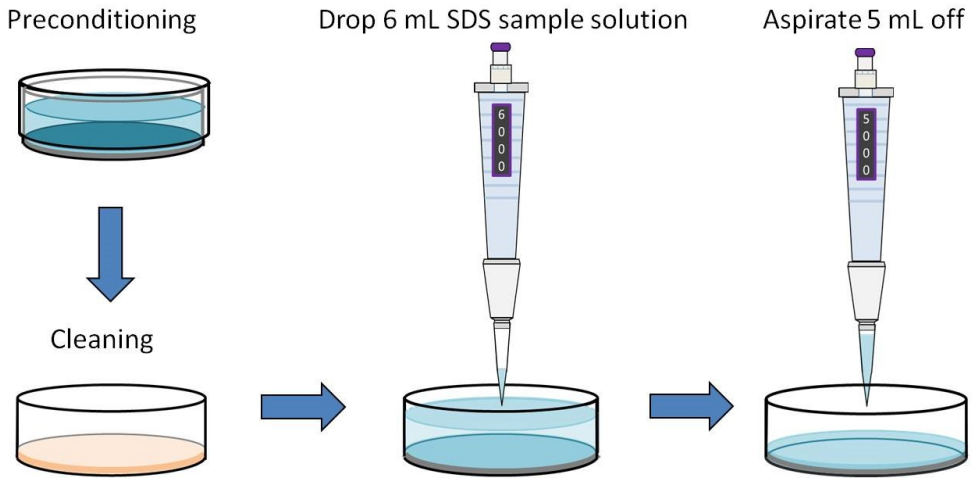

Figure 3.10: Measurement procedure of adsorbed SDS

The measurement procedure of adsorbed SDS is shown in Figure 3.10. First, calibration curves were obtained by measuring the standard solutions of SDS in known concentrations. Second, 6 mL of SDS solution was dropped onto the lipid polymer membrane in the 45 mm glass Petri dish. SDS was allowed to absorb onto the membrane for 60 s. Then, 5 mL of SDS solution was taken from the Petri dish using a pipette. The absorbance of the extracted 5 mL of sample solutions was measured and the corresponding concentration was calculated using the calibration curve. The amount of the adsorbed substance by the membrane was calculated from the difference between the amounts of SDS before and after adsorption.

3.2.5 Measurement of adsorbed MSG

YAMASA L-Glutamate Assay Kit was used to measure the amount of adsorbed MSG. YAMASA L-Glutamate Assay Kit is a test kit for determination of L-glutamate using L- glutamate oxidase specific to L-glutamate.

Hydrogen peroxide is produced due to oxidation reaction of L-glutamic acid oxidase. The enzymatic reaction among peroxidase, 4-Aminoantipyrine (4-AA) and DAOS causes the blue dye. The MSG concentration can be calculated by measuring the absorbance of the blue dye. The measurement principle is shown below.

① Oxidation reaction of L-glutamic acid oxidase:

L-glutamic acid + H_2O + O_2 → α-ketoglutaric acid + NH_3 + H_2O_2

② Blue dye formation by peroxidase:

H_2O_2 + DAOS + 4-AA → blue dye (600 nm)

The measurement procedure of MSG is similar to that of SDS. First, calibration curves were obtained by measuring the standard solutions of MSG in known concentrations. Second, 5 mL MSG were dropped onto the lipid polymer membrane in the 45 mm glass Petri dish. MSG was allowed to absorb onto the membrane for 30 s. Then, 5 mL of MSG solution was taken from the Petri dish using a pipette. The absorbance of the extracted 5 mL sample solutions was measured and the corresponding concentration was calculated using the calibration curve. The amount of the adsorbed substance by the membrane was calculated from the difference between the amounts of MSG before and after adsorption.

3.3 Results and discussion

3.3.1 Change of CPA value with the preconditioning time

As shown in Figure 3.11, the CPA value increased with the period of MSG preconditioning in the beginning. It reached a peak on the first day and then decreased gradually to a certain value during the second day and fifth day. In addition, on the same day, CPA value increases with the concentration of SDS solutions from 10 ppb to 300 ppb after MSG preconditioning. The results indicated that the period of MSG preconditioning has a great effect on the magnitude of CPA value.

3.3.2 Amount of absorbed SDS

As shown in Figure 3.12, although the CPA value increased in Figure 3.11, the amount of absorbed SDS kept unchanged with the period of MSG preconditioning. It indicates that the increase of CPA with the period of MSG preconditioning was not caused by the change in the amount of SDS adsorption. On the other hand, SDS absorption increased with the SDS concentration at the same MSG preconditioning time. It indicates that the sensor showed good concentration dependence with the SDS after MSG preconditioning.

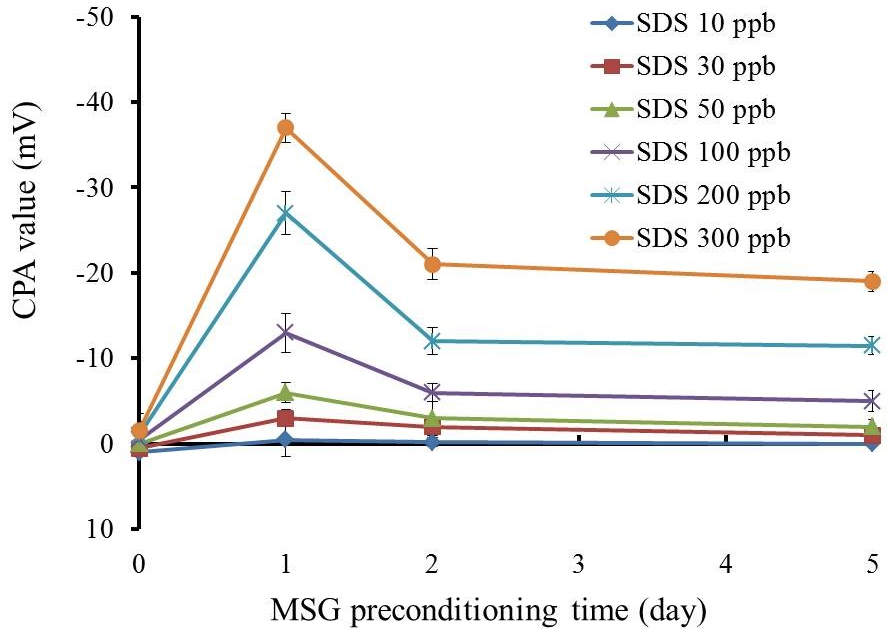

Figure 3.11: The relationship between the CPA value and preconditioning time [52]

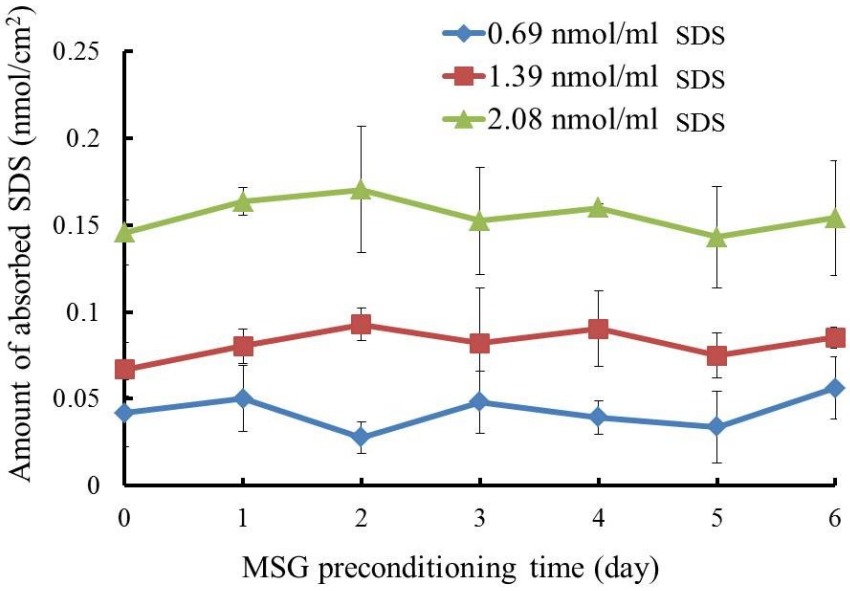

Figure 3.12: The relationship between the amount of adsorbed SDS and the preconditioning time [52]

3.3.3 Amount of absorbed MSG

As shown in Figure 3.13, the amount of absorbed MSG increased with the period of MSG preconditioning in the beginning and reached a maximum on the second day. If you look at the graph you will find approximately 350 nmol/cm^2 adsorbed MSG onto the membrane. The adsorption amount decreased when the period of MSG precondition continued to the fourth day, but subsequently kept constant beyond the fourth day.

3.3.4 Reference potential

Figure 3.14 shows although the reference potential increased with the period of MSG preconditioning, the increasing rate decreased from one day of MSG preconditioning. The reference potential showed negative values of approximately -25 mV before MSG preconditioning. Then it tended to increase to a positive value of approximately 80 mV when experienced MSG preconditioning for one day, and gently increased to about 140 mV after 5 days of MSG preconditioning.

With the above results, we could explain the following phenomena.

(1) Why was the CPA value almost zero before MSG precondition?

In our previous studies [62,63,64], we found very few lipid molecules TDAB, deposited to the surface of the membrane before MSG preconditioning, which led to a low sensitivity of the sensor. Moreover, the SDS absorbed was also too few to make an apparent change in membrane potential in such a low-lipid-concentration region in Figure 3.14. The impurity, phenylphosphonic acid monooctyl ester contained in NPOE caused the negative reference potential before MSG preconditioning [35].

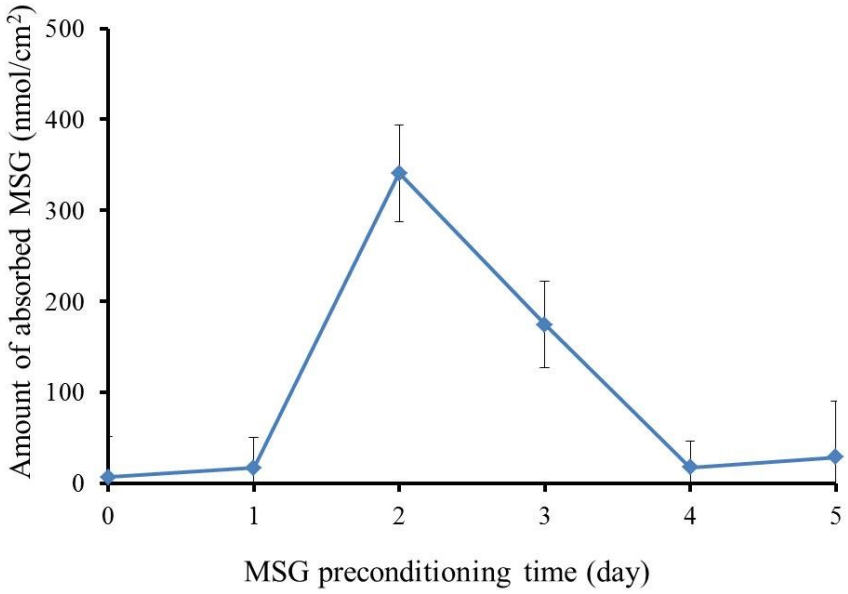

Figure 3.13: The relationship between the amount of adsorbed MSG and preconditioning time [52]

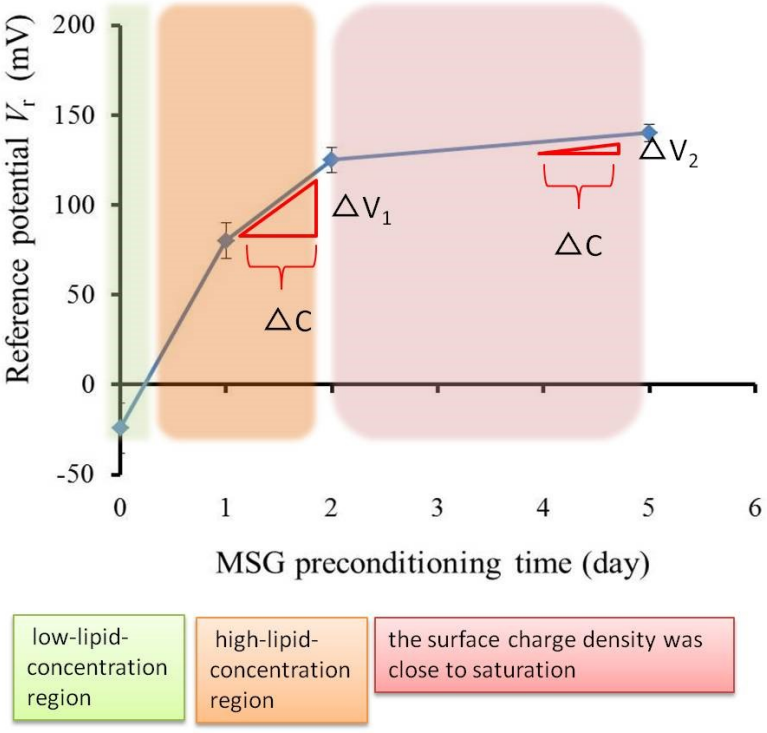

Figure 3.14: Relationship between the reference potential and preconditioning time

(2) Why did the CPA value increase to a maximum and decreased to a certain value?

As shown in Figure 3.13, MSG molecules gathered around the membrane due to preconditioning. Then negatively charged MSG concentrated the positively charged TDAB (ionized into TDA^+ and Br^-) in the membrane to the surface of membrane [64]. As shown in Figure 3.14, more and more positively charged TDAB makes the surface charge density positive, which made reference potential from negative to positive value after reconditioning. However, the adsorbed MSG neutralized the positive charge on the membrane surface led to the decrease of the surface charge density. As MSG preconditioning proceeding, increasing TDA^+ gathered onto the membrane surface, which made the membrane hydrophilic. MSG gradually separated from the membrane due to the change of hydrophobicity of membrane (Figure 3.13). On the other hand, the reference potential became relatively stable after two days of MSG preconditioning because the surface charge density increased and was close to saturation (Figure 3.14). We found that although the adsorption of SDS did not change, change of membrane potential becomes smaller due to the saturation of the surface charge density. As a result, the CPA value began to decrease significantly from the first day to the second day during the period of MSG preconditioning.

In addition, as showed in Figure 3.11 and Figure 3.12, both the CPA value and the SDS adsorption increase with SDS concentration after MSG preconditioning. These results suggested that the CPA value is related to the amount of absorbed SDS when the number of surface charge density reaches a certain amount. As we reported in our previous study [35], the CPA value is affected by both adsorption amount and the surface charge density.

(3) Why did the peak of the amount of MSG appear during period of MSG

preconditioning?

Negatively charged MSG molecule was gathering and absorbed to the positive membrane after MSG preconditioning. However, as the hydrophobicity of membrane decreased, MSG can be hardly absorbed onto the membrane. The balance between the electrostatic interaction and hydrophobic interaction led to the peak of MSG. Although the decease of hydrophobicity of membrane caused the fall of MSG, the amount of adsorbed SDS did not change due to the stronger hydrophobicity than MSG.

3.4 Conclusion

This chapter aimed at clarifying the influence of MSG preconditioning on the lipid polymer membrane. A pesticide sensor for SDS detection with a strongly hydrophobic membrane was used in the study. In conclusion, we found out that the sensor's sensitivity improved by MSG preconditioning because the TDA^+ gathered onto the surface of membrane and caused a higher surface charge density. This study succeeded in improving the sensitivity of the pesticide sensor using lipid polymer membrane for detecting SDS in CPA measurement. We also confirmed that the CPA value is affected by both adsorption amount and the surface charge density of lipid polymer membrane. The adsorption amount is affected by both surface charge density and hydrophobicity of the membrane. Furthermore, it provides a new design idea for pretreatment process when using hydrophobic membranes of the taste sensor. The sensitivity of the taste sensor, especially for hydrophobic taste qualities such as bitterness (quinine hydrochloride or iso-α acid) or astringency (tannic acid), may be improved by the pretreatment such as MSG preconditioning.

Chapter 4

Improved Durability and Sensitivity of Bitterness Sensing Membrane for Medicines [65]

4.1 Background

4.1.1 Bitterness sensor for hydrochloride medicines

The bitterness sensor (BT0) is one of the sensor electrodes of the taste sensor (TS-5000Z) used for the bitterness quantification of hydrochloride medicines. The lipid polymer membrane uses phosphoric acid di-n-decyl ester (PADE) as the lipid, bis(1-butylpentyl) adipate (BBPA) and tributyl o-acetylcitrate (TBAC) as the plasticizers [66]. The membrane is negatively charged in the taste solution, because PADE produces negative charges on the surface of the membrane owing to the ionization of phosphate group. On the other hand, the function of BBPA and TBAC is to adjust the flexibility and hydrophobicity of the membrane. The sensitivity and selectivity to bitter substances depends on the contents of PADE, BBPA, and TBAC [66]. As shown in Figure 4.1, the BT0 sensor possesses good sensitivity to the bitterness of medicines and don’t respond to any other taste quality. The BT0 sensor also has high correlation with bitterness sensory scores [32,67].

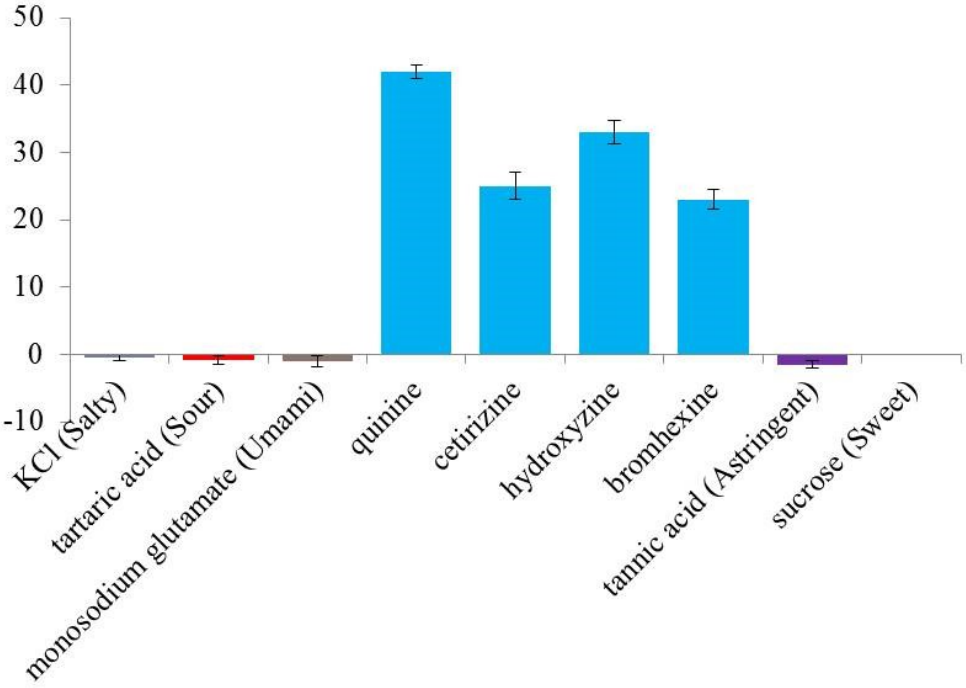

Figure 4.1: Responses of taste sensors to six tastes [66].

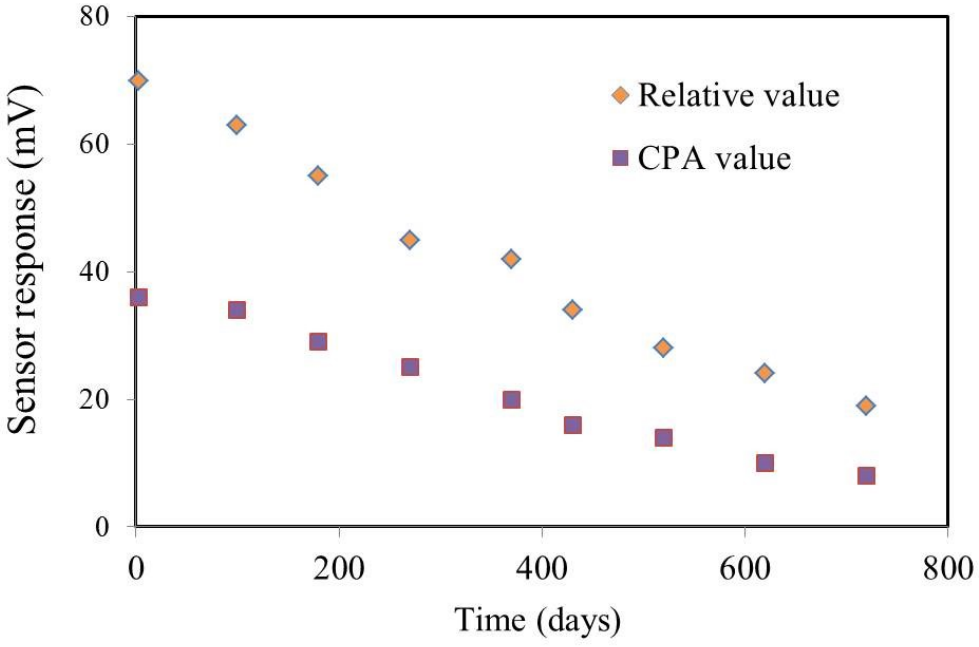

Figure 4.2: The bitterness sensor response with the preservation time

4.1.2 The current problem and the purpose of this chapter

Although the commercialized bitterness sensor (BT0) has high sensitivity and selectivity to the bitterness of medicines, the sensor response decreases with the preservation time. As shown in Figure 4.2, the relative value gradually decreases from 70 mV to 20 mV while the CPA value decreases from 36 mV to 8 mV after two years stored at room temperature and humidity in a laboratory. On the other hand, although the membrane was dissolved by THF and formed again, the response didn't recover. Therefore, we believe that the deterioration of the response is not caused by the displacement of molecules in the membrane, but due to some irreversible reactions. Among all the sensor electrodes of the taste sensor, the response deterioration only happened to BT0 sensor for the moment. This problem not only affects the performance of the BT0 sensor, but also increases the cost of transportation and preservation.

The aims of this chapter are to clarify the decrease in the response of the BT0 sensor and to improve the sensor durability to extend its lifetime.

4.2 Experiment

4.2.1 Materials

BBPA was purchased from Sigma-Aldrich, Inc. (St. Louis, MO, USA). TBAC and PADE were purchased from Tokyo Chemical Industry Co., Ltd. (Tokyo, Japan). Polyvinyl chloride (PVC), obtained from Wako Pure Chemical, Ltd. (Osaka, Japan), was used as the supporting material. The chemical structures of PADE, TBAC, and BBPA are shown in Figure 4.3. Tetrahydrofuran (THF) purchased from Sigma-Aldrich was used as the organic solvent.

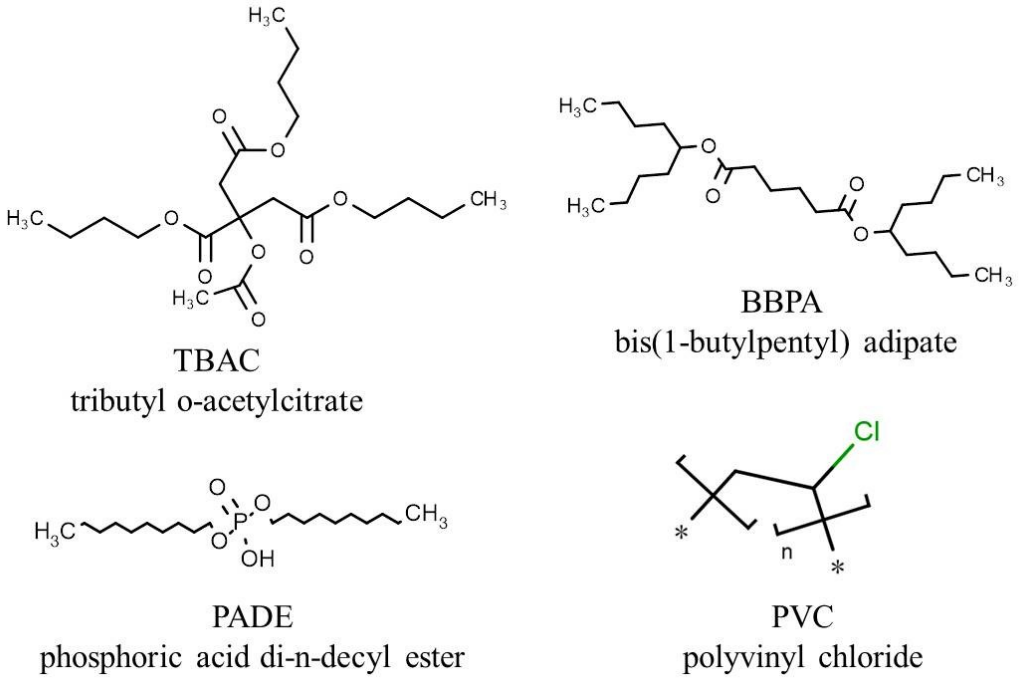

Figure 4.3: Chemical structures of PADE, TBAC, BBPA, and PVC.

Variable name (20 membranes in all)	PADE	TBAC	BBPA
Variable PADE (9)	33-278%	100%	100%
Variable BBPA (5)	100%	100%	33-200%
Variable TBAC (6)	100%	3.3-100%	100%

Table 4.1: The absolute amount of each component in the membranes

4.2.2 Accelerated deterioration process

Because it is inefficient to let BT0 sensor degrade naturally, we set up an accelerated deterioration process to reproduce a BT0 sensor after long-term deterioration in a shorter time than by natural deterioration. We investigated the characteristics of the BT0 sensor before and after the deterioration process. To find suitable conditions for accelerating the deterioration, we placed the sensor membrane in a chamber (YAMATO IG421, Tokyo, Japan) to adjust the temperature and humidity for one month. The sensor membrane was placed in a glass Petri dish without a cover in the chamber. The temperature was set to 45–80 °C. The relative humidity (RH) was set to 20% (regarded as a dry condition), 40%, 60%, or 95% RH.

4.2.3 Effect of lipid and plasticizers on deterioration rate

To determine which component most affects the response deterioration, we changed the amounts of the PADE, BBPA, and TBAC in the membrane to observe their influences on the sensor response. We defined the deterioration rate D shown in the following equation to evaluate the sensor performance:

$$D = \frac{|R_{\mathrm{after}} - R_{\mathrm{before}}|}{R_{\mathrm{before}}} \tag{4.1}$$

Here, R_{after} is the CPA value after the accelerated deterioration process and R_{before} is the CPA value before the accelerated deterioration process.

We adopted the control variate method for the sample concentrations shown in Table 4.1 Here, 100% means that the absolute amount is the same as that in the BT0 sensor.

4.2.4 Partial deteriorated BT0 sensor

In order to figure out the monomer or combination of the components causing the response deterioration, the lipid (PADE) and two plasticizers (TBAC, BBPA) were made into membrane in different combinations with PVC, respectively. The absolute amount of each component is the same as that in the BT0 sensor. Therefore, we made up six membranes in the following combinations: PADE / PVC, TBAC / PVC, BBPA / PVC, PADE / TBAC / PVC, PADE / BBPA / PVC, and BBPA / TBAC / PVC. After accelerated deterioration process, the other components without accelerated deterioration were added into the membrane to make the final concentration match BT0 membrane. Finally, the sensor membrane was used to measure 0.1 mM quinine hydrochloride sample.

4.2.5 Quantitative analysis by liquid chromatography-tandem mass spectrometry

Liquid chromatography–tandem mass spectrometry (LC-MS/MS) was used to compare the change of the amounts of PADE, TBAC, and BBPA in the membrane before and after four-week accelerated deterioration. The sample solutions were prepared in the following steps. Firstly, 0.2 g of the sensor membrane was dissolved in a 100 mL screw tube. Secondly, the polymer was precipitated by slowly adding 100 mL of acetonitrile. Thirdly, some of the prepared solution was diluted with acetonitrile (diluted 20-fold for PADE quantification or 1000-fold for BBPA and TBAC quantification). Finally, the diluted solution was filtered through a PTFE filter and used to LC-MS/MS measurement. The instrument conditions are summarized in Table 4.2.

Table 4.2: LC-MS/MS conditions [65].

LC instrument	Shimadzu LC-20A (Kyoto, Japan)
LC column	Cadenza CD-C18 (2.0 × 100 mm, 3 µm, Portland, USA)
Column temperature	50 °C
Mobile phase	A: 10 mmol/L Ammonium acetate/H_2O
	B: Acetonitrile
Flow rate	0.3 mL/min
Gradient conditions	<PADE>
	0.0 min → 10.0 min: B20% → B90%
	10.0 min → 12.0 min: B90%
	12.1 min → 20.0 min: B20%
	<BBPA/TBAC>
	0.0 min → 5.0 min: B60% → B95%
	5.0 min → 15.0 min: B95%
	15.1 min → 20.0 min: B60%
Injection volume	1 µL
MS instrument	API 4000 (AB SCIEX)
Ionization	ESI
Polarity	<PADE> negative; <TBAC/BBPA> positive
Scan type	SRM
	<PADE> Q1: m/z 377.3 → Q3: m/z 237.1
	<BBPA> Q1: m/z 399.3 → Q3: m/z 273.2
	<TBAC> Q1: m/z 403.3 → Q3: m/z 329.3

Table 4.3: GC-MS conditions [65].

GC-MS instrument	SHIMADZU QP2010 (Kyoto, Japan)
Electron ionization	70 eV
Column	Stabilwax®-MS, 30 m long, 0.25 mm I.D., 0.25 µm thick
Oven temperature	40 °C for 1 min
	40 - 270 °C at 10 °C/min
	270 °C for 4 min
Split ratio	1 : 25
Inlet temperature	270 °C
Interface temperature	280 °C
Solid phase microextraction fiber	85 µm polyacrylate film fiber

4.2.6 Products detection by gas chromatography-mass spectrometry

To reveal the physicochemical reaction occurring during the deterioration period, we measured the products released from the BT0 membrane before and after the accelerated deterioration process. The products were collected by solid-phase micro-extraction (SPME) and analyzed by gas chromatography-mass spectrometry (GC-MS). The merit of the SPME/GS-MS method is the useless of any solvent. The samples were cutoffs of BT0 membranes with a weight of 20 mg before and after the accelerated deterioration process.

4.2.7 Measurement of the amount of adsorbed quinine hydrochloride

In Chapter 3, we concluded that the CPA value is affected by both the adsorption amount and the surface charge density on the membrane. Therefore, in order to determine whether the decrease in adsorption amount was the direct cause of the response deterioration, we measured the amount of quinine hydrochloride adsorbed on the membrane using an ultraviolet-visible spectrophotometer (UV-1800, Shimadzu Corporation, Kyoto, Japan). First, the linear relationship between absorbance and concentration was obtained by measuring quinine hydrochloride solutions of known concentration. Five milliliters of 0.1 mM quinine hydrochloride solution was dropped onto the surface of a membrane in a 45 mm glass Petri dish. Then wait for the quinine hydrochloride molecules to be adsorbed on the membrane for 30 s as same as the measurement procedure of the taste sensor. 3 mL of the quinine hydrochloride solution was extracted from the glass Petri dish to measure its absorbance. Using the absorbance of the measured solution and the calibration curve, the concentration of the measured solution can be calculated. We defined the difference between the amounts of the

originally-added quinine hydrochloride solution and the solution after the 30 s adsorption process as the total amount of adsorbed quinine hydrochloride. The obtained the amount of quinine hydrochloride adsorbed per square centimeter was calculated by dividing by the area of the glass Petri dish [62,68].

4.2.8 Measurement of surface contact angle

Because the change of the lipids and plasticizers may affect the hydrophobicity of the membrane surface, we determined the change in the hydrophobicity of the membrane surface by measuring the contact angle of the membrane surface using DM500 contact angle meter (Kyowa Interface Science Co., Ltd., Saitama, Japan). We adopted the control variate method to arrange the membrane samples. Elven membranes were made with the 100% BBPA and TBAC, and 33–278% PADE. 2 μL of pure water drop was used in the measurement.

4.2.9 Fabrication of a durable Bitterness Sensor

The requirement to the durability of the improved sensor is no decrease in response after one-year natural storage. Thus, we chose the sensors meet the requirements to confirm the selectivity to the five basic taste qualities: saltiness, sourness, umami, bitterness, and sweetness. In addition, there are two requirements for the performance of the newly improved bitterness sensor for medicine: selectivity and concentration dependence. The one is the CPA value for standard quinine hydrochloride solution should be at least 30 mV and not be affected by any other basic tastes. The other one is there should be a linear relation between the sensor response and the

logarithmic of quinine hydrochloride within the intensity of the bitterness of medicines.

4.3 Results and discussion

4.3.1 Conditions of the accelerated deterioration process

In Figure 4.4, the CPA value almost didn't change at 45 °C and 20% RH (dry condition) with the storage time. On the other hand, the decrease in the CPA value became serious with the increasing humidity. This result indicated that humidity promoted the response deterioration. The response ratio decreased to about 45% after 443 days of the natural deterioration. On the other hand, the response ratio reached 45% at 45 °C and 95% RH after 28 days of the accelerated deterioration process. Thus, the deterioration process was about 16 times faster than natural deterioration. With this accelerated deterioration process, the membrane after one month of accelerated deterioration can be regarded as those after one year of natural deterioration.

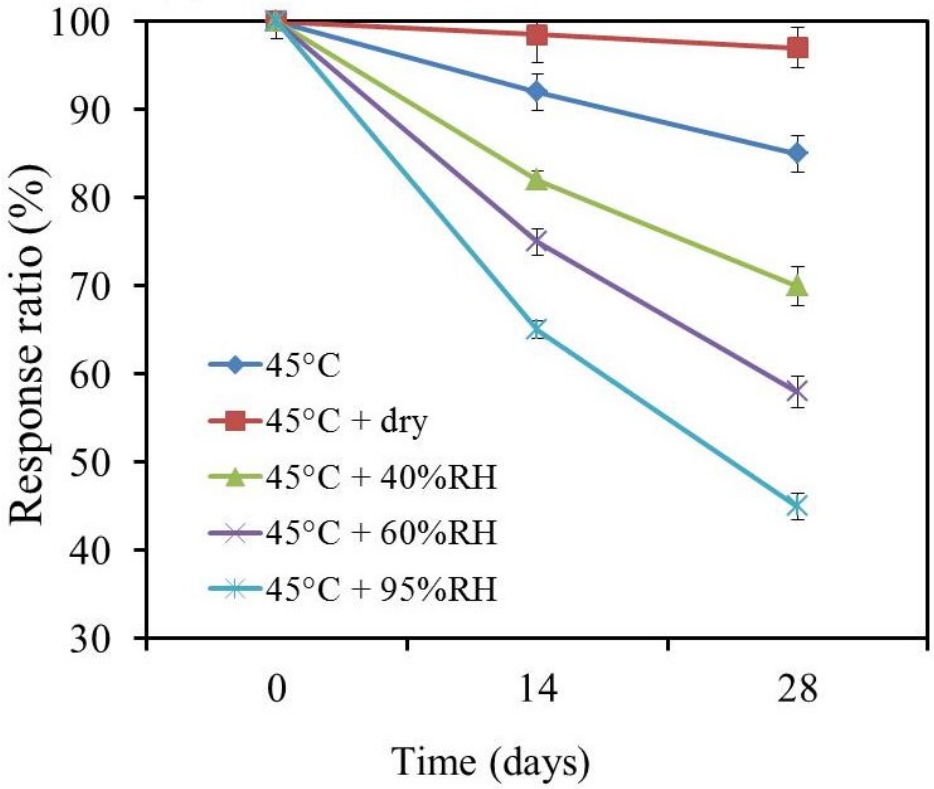

Figure 4.4: The response ratio with the preservation time (45 ºC and different humid condition) [65].

4.3.2 Effect of lipid and plasticizers on deterioration rate

Figure 4.5 showed that the deterioration rate defined by Equation (5.1) increases with the absolute amount of PADE from 33 % to 278 %. On the other hand, the deterioration rate kept almost unchanged, regardless of the absolute amount of plasticizer (Figure 4.6). Therefore, the amount of PADE makes the strongest contribution to the deterioration rate of BT0.

Figure 4.7 shows the relationship between deterioration rate and the PADE mass ratio from 0.66% to 5.36%. The circled green points represent the sensor membranes with the TBAC mass ratio under 49%. Except for the circled green points, the deterioration rate has a strong correlation with the PADE mass ratio (R^2 = 0.85). In Figure 4.7, the deterioration rate was proportional to the PADE mass ratio when the mass ratio of TBAC exceeded 49%. On the other hand, the response deterioration was suppressed when the TBAC mass ratio in the membrane was fewer than 49%.

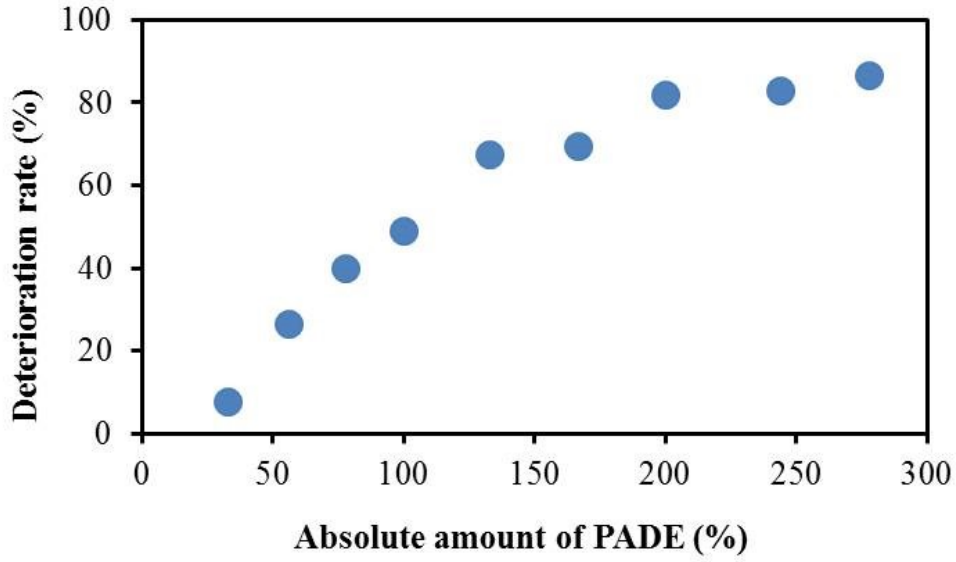

Figure 4.5: Relationship between deterioration rate and absolute amount of lipid. The amounts of TBAC and BBPA in the membranes are the same as those in BT0.

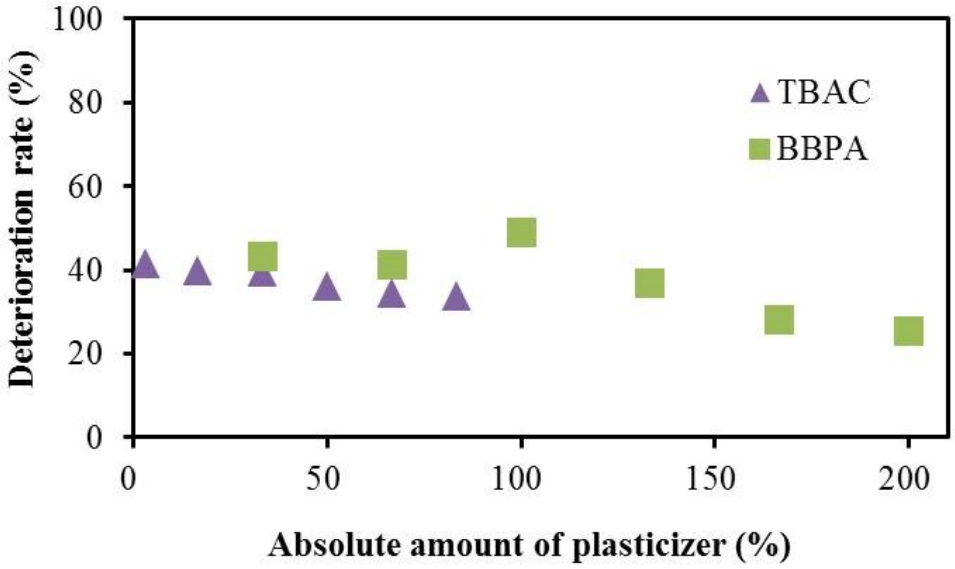

Figure 4.6: Relationship between deterioration rate and absolute amount of plasticizers. The amounts of PADE and TBAC (or BBPA) in the membranes are the same as those in BT0.

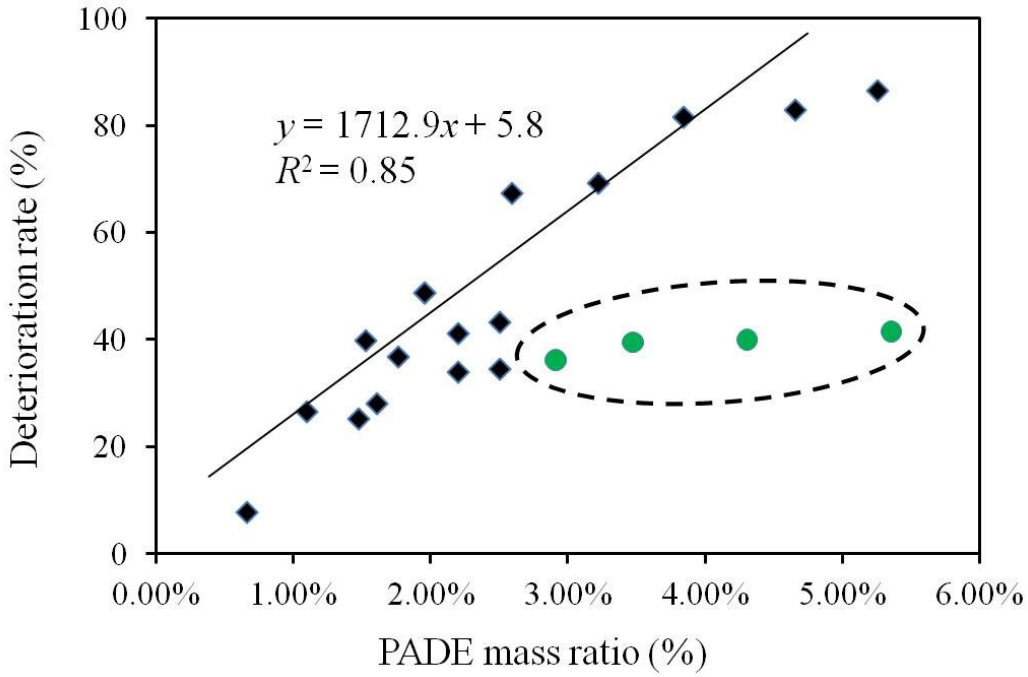

Figure 4.7: The relationship between deterioration rate and lipid mass ratio. The circled green points represent the sensor membranes with the TBAC mass ratio less than 49%. The regression equation and R^2 were calculated without the green points [65].

4.3.3 The effect of combination on the deterioration

As shown in Figure 4.8, (1) when only the lipid or the plasticizer monomer was deteriorated, the sensor response (green) didn't decrease significantly; (2) when both of the lipid and the plasticizer were deteriorated, the sensor response (yellow) decrease significantly; (3) The deterioration degree of the membrane with deteriorated TBAC and PADE was the most similar to that of BT0 membrane. These results indicated that although PADE makes the strongest contribution to the deterioration rate of BT0, the coexistence with the plasticizers is a necessary condition.

4.3.4 LC-MS/MS analysis results

Figure 4.9 shows that the amount of TBAC reduced significantly as a result of deterioration. However, the amounts of PADE and BBPA remained unchanged before and after the deterioration process. This result indicates that the reduction of TBAC may have a direct contact with the response deterioration and PADE promoted this deterioration process because of a positive correlation with the deterioration rate.

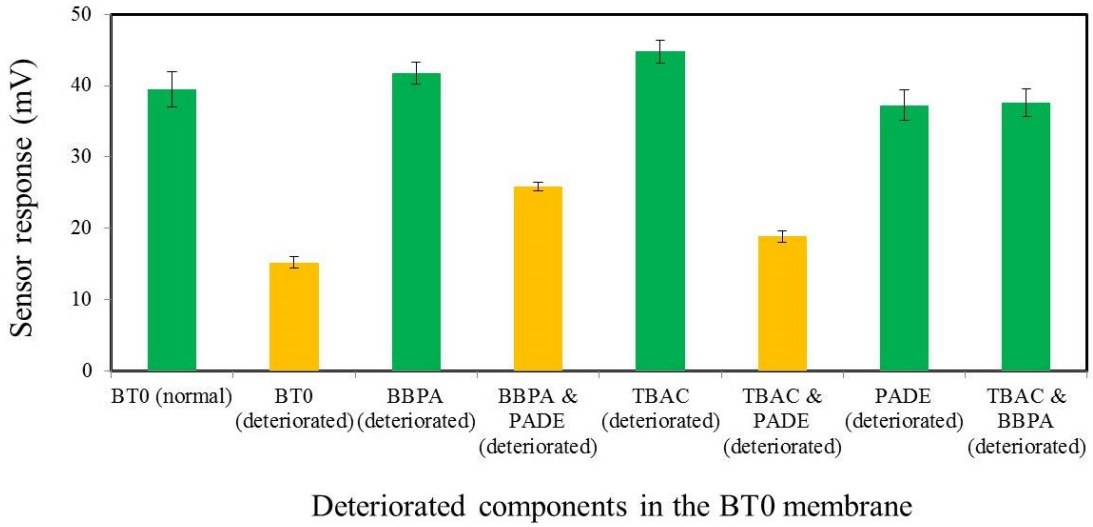

Figure 4.8: The sensor response of BT0 sensor with deteriorated components

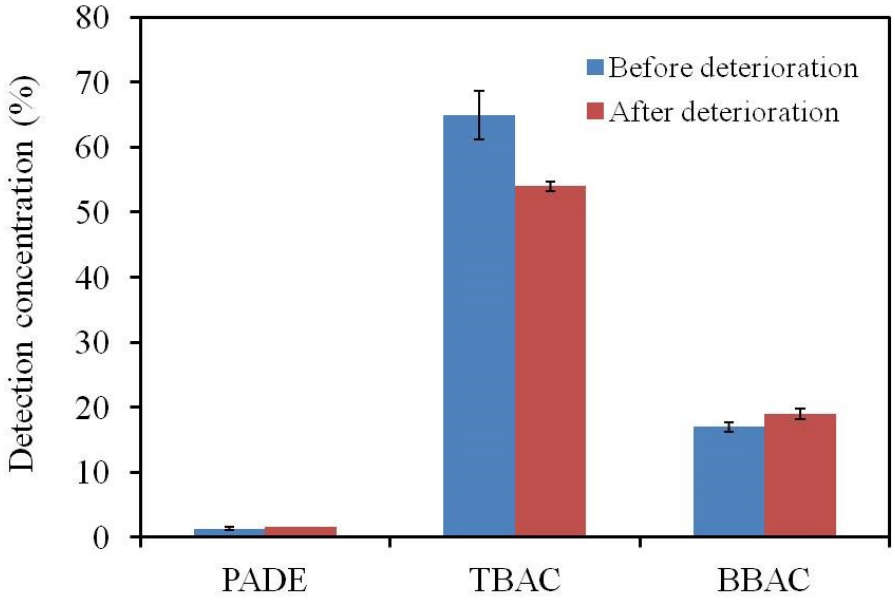

Figure 4.9: Quantitative comparison of the main components obtained by LC-MS/MS. The results are expressed as the mean ± SD (n = 3) [65].

4.3.5 GC-MS analysis of the membrane components

Decyl alcohol was detected before accelerated deterioration test, but was under the detection limit after accelerated deterioration test (Figure 4.10). There were two possibilities for the origin of decyl alcohol: (1) an impurity of PADE; (2) a derivative of PADE produced under high temperature of GC-MS condition. If the second possibility is valid, PADE is considered to reduce during deterioration process. However, the result in Figure 4.9 demonstrated that the amount of PADE didn't change during the deterioration, which negated the second possibility. On the other hand, the amount of butyl citrate increased while the amount of TBAC decreased after deterioration (Figure 4.10), indicating that butyl citrate was detected as a degradation product of the plasticizer TBAC and some TBAC molecules were hydrolyzed during the deterioration process. The chemical structures of decyl alcohol and butyl citrate were shown in Figure 4.11.

4.3.6 Amount of adsorbed quinine hydrochloride

Figure 4.12 shows the absorbance of the quinine hydrochloride with different concentrations. The wavelength of 248.6 nm was chosen to calculate the calibration curve (Figure 4.13) because the concentration of the target sample is 0.1 mM (the blue line). Figure 4.14 shows that the adsorbed amount of quinine hydrochloride didn't change before and after the deterioration. As we discussed in Chapter 3, the CPA value was affected by both the surface charge density and the amount of adsorption [35,60]. Therefore, the change in the surface charge density of the BT0 membrane probably caused the decrease in the sensor response.

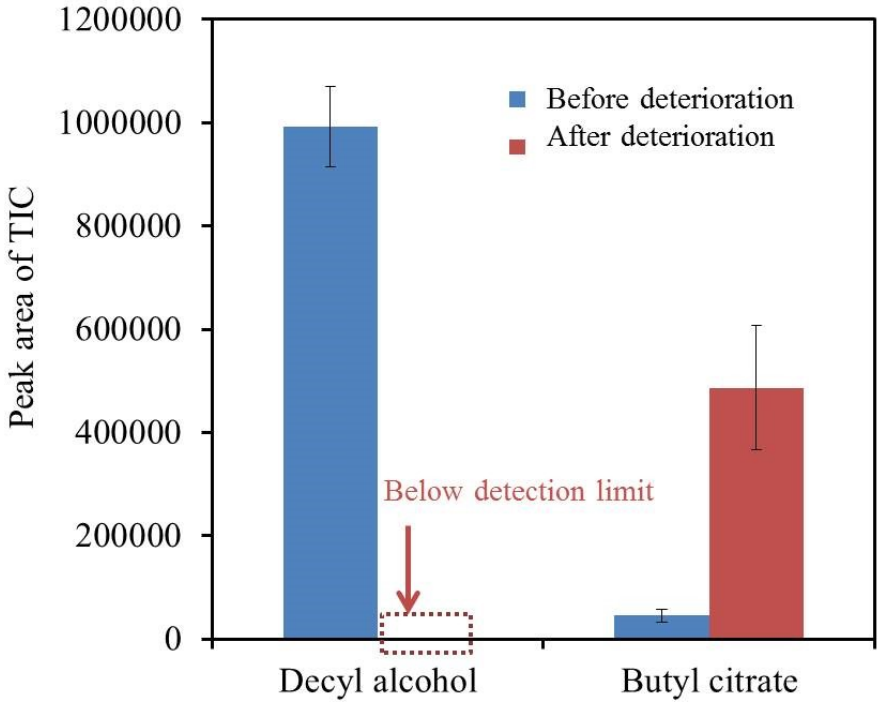

Figure 4.10: Change in the amount of butyl citrate measured by GC–MS. The results are expressed as the mean ± SD (n = 3).

Decyl alcohol

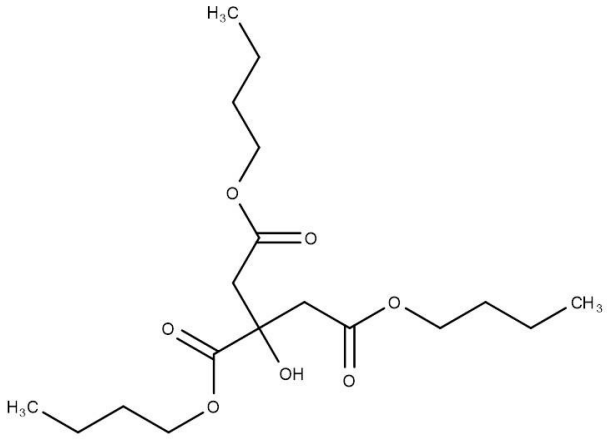

Butyl citrate

Figure 4.11: Chemical structures of decyl alcohol and butyl citrate.

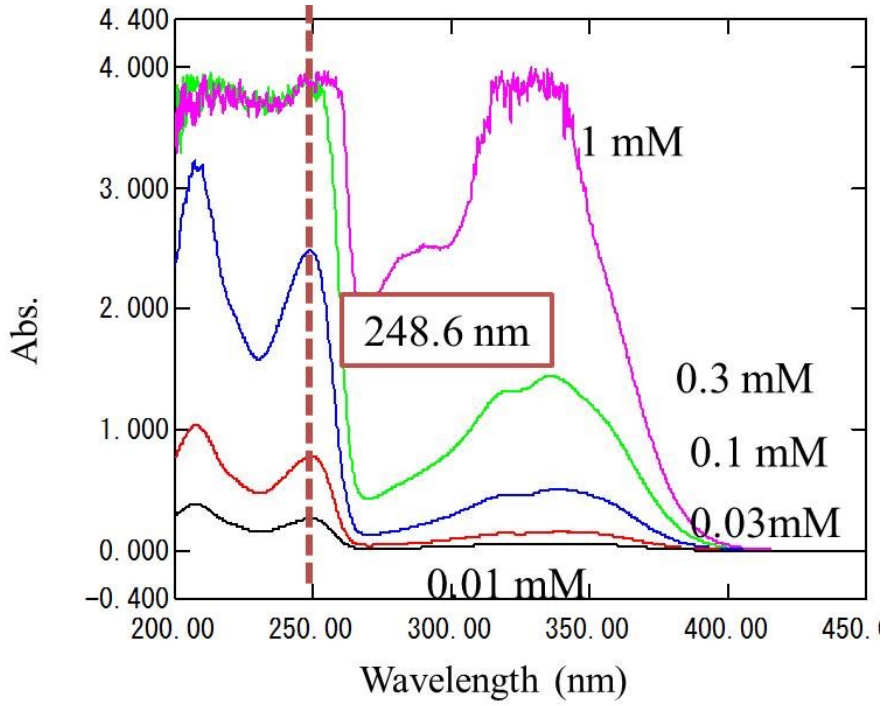

Figure 4.12: The absorbance of the quinine hydrochloride.

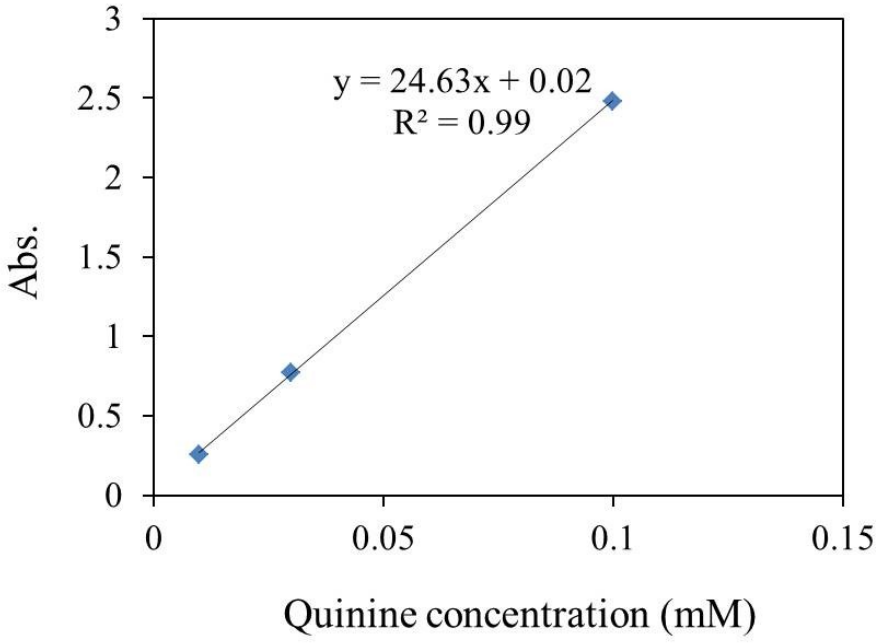

Figure 4.13: The calibration curve.

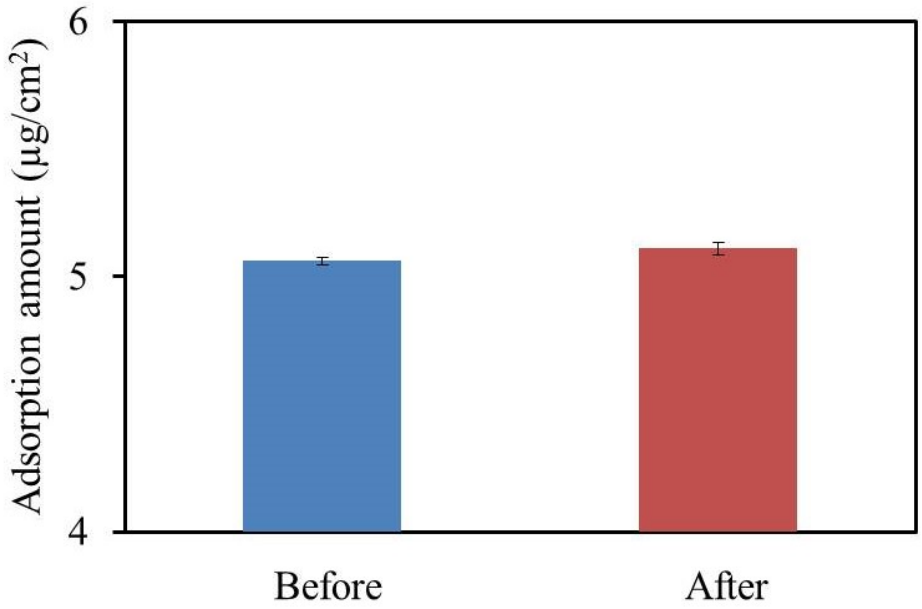

Figure 4.14: Amounts of adsorbed quinine hydrochloride before and after the accelerated deterioration process. The results are expressed as the mean ± SD (n = 3) [65].

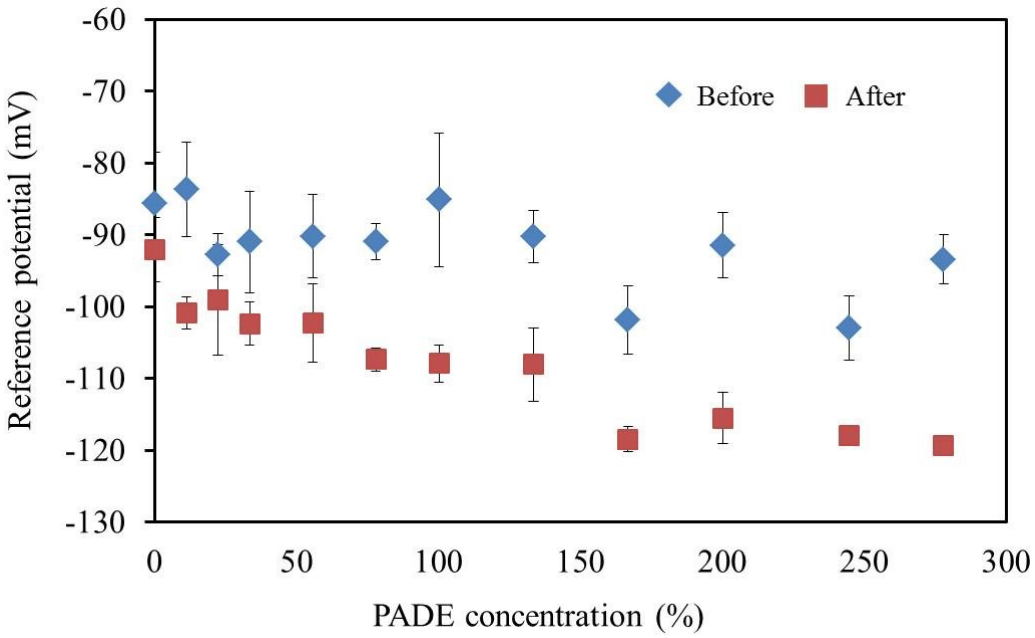

Figure 4.15: The reference potential with lipid concentration. The results are expressed as the mean ± SD (n = 4) [65].

4.3.7 Reference potential and contact angle

The reference potential (V_r) was the membrane potential in the reference solution. Basically, the negatively-charged membrane has a negative reference potential. As shown in Figure 4.15, with the increasing amount of negatively-charged PADE, the reference potential showed a tendency to increase in the negative direction. In addition, the reference potential was significantly lower after the accelerated deterioration process, which indicates that negatively-changed substances were generated on the membrane.

As shown in Figure 4.16, the contact angle decreased with the increasing amount of lipid. In addition, the contact angle decreased compared to the membrane before the deterioration. The result indicates that the surface of the membrane became more hydrophilic with the increasing amount of PADE as well as during the deterioration process. The hydrophilicity of the membrane and the negativity of the reference potential were considered to be caused by the hydrolysis of TBAC.

To summarize the reason of response deterioration of BT0 sensor, the role of PADE during the deterioration was to create an acidic condition in the membrane. Due to the acid condition, TBAC was hydrolyzed because it is a phosphate ester. From Figure 4.7, the mass ratio of PADE affects the deterioration rate more than the TBAC. Therefore, we considered that the reduction in amount of PADE would improve the durability of the sensor.

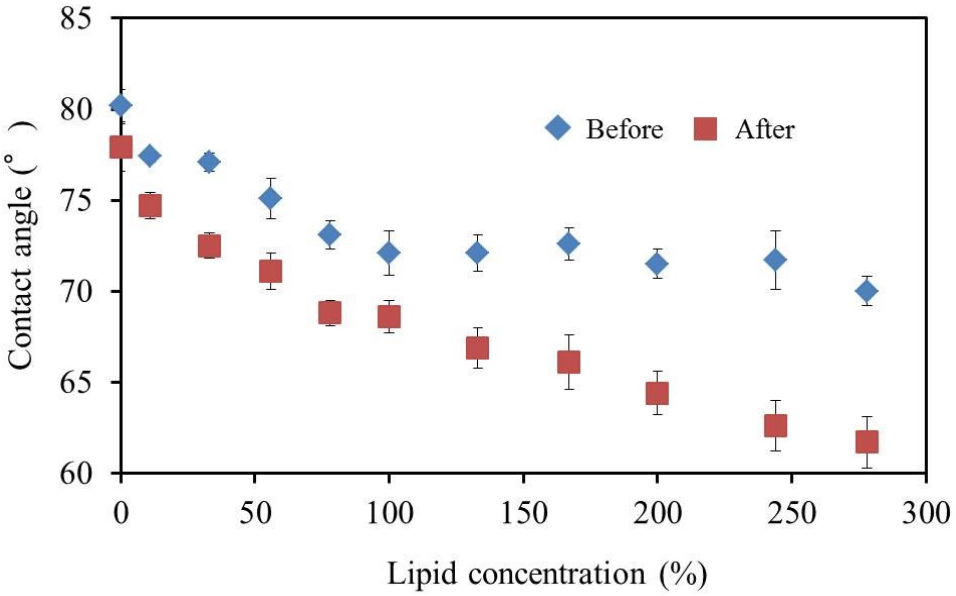

Figure 4.16: The surface contact angle with lipid concentration. The results are expressed as the mean ± SD (n = 4) [65].

4.3.8 Improvement on durability and sensitivity

As shown in Figure 4.17, we found that before the deterioration process, the sensor response increased in the beginning and kept unchanged when the amount of PADE reached 77%. On the other hand, after the deterioration, the sensor response increased in the beginning and kept unchanged when the amount of PADE reached 33%, then finally decreases with the increasing amount of PADE in the membrane after 77%. In addition, the deterioration rate of the CPA value before and after the deterioration didn't change when 33% PADE was added. This membrane could be considered as durable because of the relatively weak acidic environment. However, the CPA value was about 25 mV when 33% PADE was added, which only occupied 70% of that of the conventional BT0 sensor (about 36 mV to 0.1 mM quinine hydrochloride) and did not satisfy the required response.

As shown in Figure 4.18, the CPA value increased when the amount of the plasticizer TBAC included in the BT0 membrane was decreased. Therefore, in order to solve this problem as well as suppress the deterioration, we reduced the amount of the plasticizer TBAC included in the BT0 membrane. Although TBAC hindered the response, the existence of TBAC is necessary to match the results of bitterness sensory tests for various medicines in the sensor development stage [66]. On the other hand, the responses of sensor electrodes with 17%, 34%, and 50% TBAC didn't decrease after the accelerated deterioration and showed higher value to quinine hydrochloride than the conventional BT0 sensor [32].

As shown in Figure 4.19, the sensor only responded to bitterness (+), but not to any other basic tastes, showing good selectivity. From the viewpoint of sensitivity, the membrane with 33% PADE, 100% BBPA, and 17% TBAC met the response

requirement of over 30 mV to 0.1 mM quinine hydrochloride.

Figure 4.20 shows that the CPA value of the improved sensor was proportional to the logarithm of the concentration of quinine hydrochloride. The CPA value expresses the bitterness intensity, according to the Weber-Fechner law [69]. The improved sensor shows the same linear response range as the conventional BT0 sensor of between 0.01 and 1 mM quinine hydrochloride. Since it is the common range for sensory scores felt by humans, we chose this range to compare the sensor sensitivity. The *k* refers to the slope of the response and concentration. The improved sensor has a higher slope than the conventional sensor, which indicates that the sensitivity of improved sensor is superior to that of the conventional one.

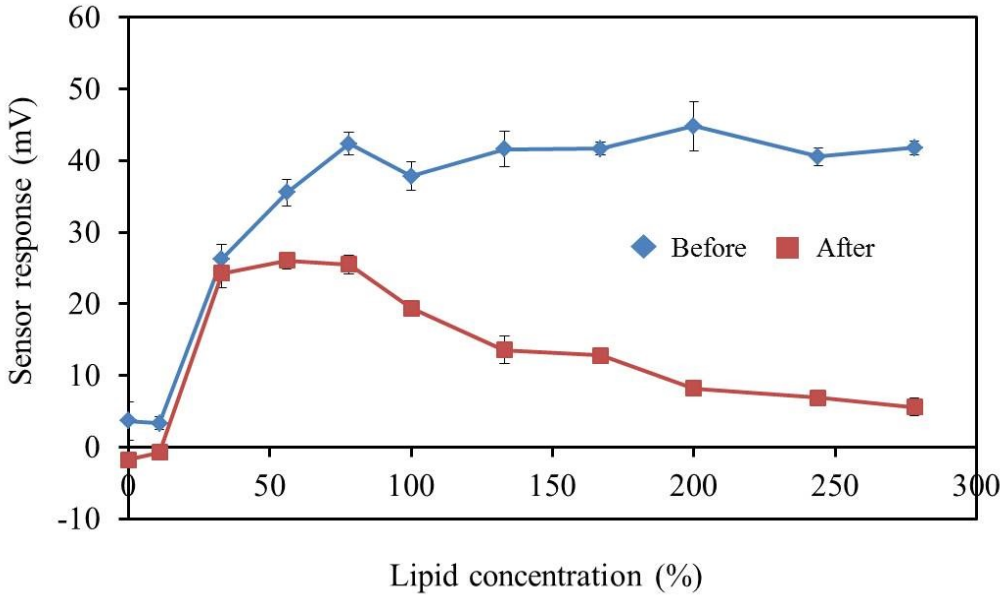

Figure 4.17: The sensor response with lipid concentration. The results are expressed as the mean ± SD (n = 4) [65].

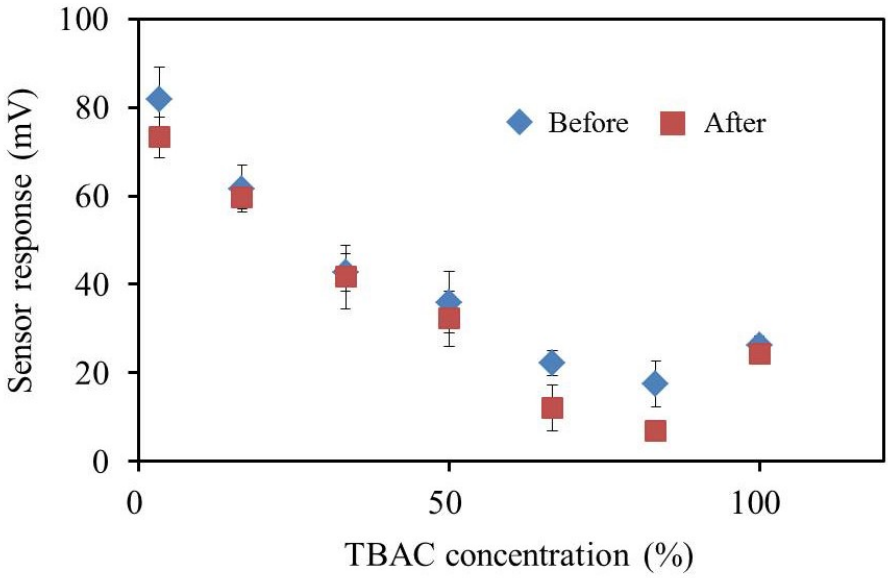

Figure 4.18: The sensor response with TBAC concentration. The results are expressed as the mean ± SD (n = 4) [65].

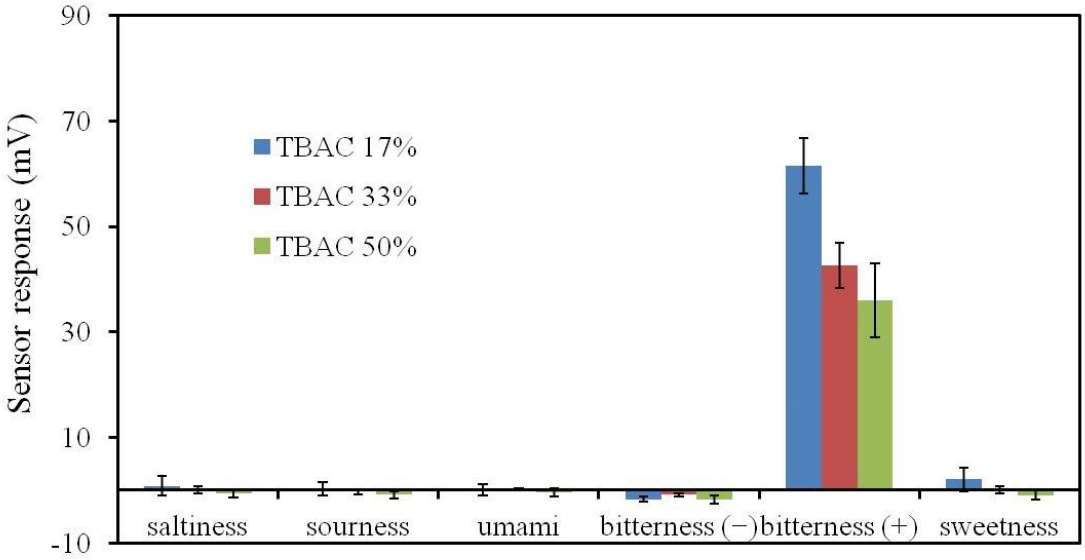

Figure 4.19: The improved sensor response to five basic tastes. The reference solution (RS) comprised 30 mM KCl, and 0.3 mM tartaric acid; the saltiness sample comprised 300 mM KCl, and 0.3 mM tartaric acid; the sourness sample comprised 30 mM KCl, and 3 mM tartaric acid; the umami sample comprised 10 mM sodium glutamate and RS; the bitterness (+) sample comprised 0.1 mM quinine hydrochloride and RS; the bitterness (−) sample comprised 0.01 vol% iso-alpha acid and RS; and the sweetness sample comprised 1 M sucrose and RS [65].

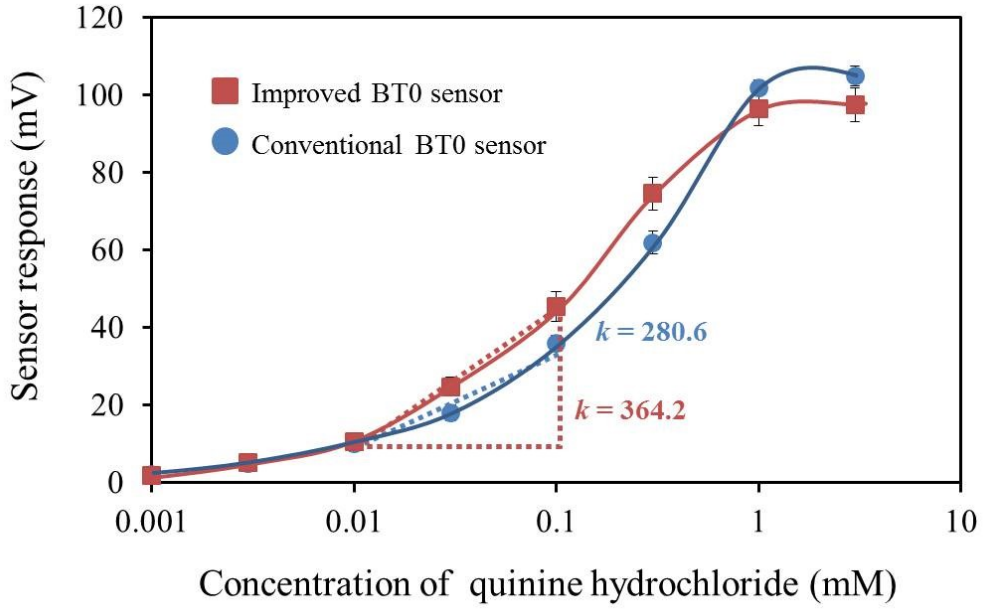

Figure 4.20: Dependence of the response of the improved bitterness sensor and conventional bitterness sensor on quinine hydrochloride concentration [65].

4.4 Conclusions

In this chapter, we investigated the reason for the deterioration in the response of the BT0 sensor. We concluded that the direct cause is the increase in the surface charge density. The results showed that the surface charge density increased because the hydrolysis of TBAC produced negatively-charged substances. Our results supported that the deterioration degree is strongly promoted by the increasing PADE because of the acidic condition generated by PADE.

The reduction of TBAC has two roles: (1) suppresses the deterioration rate; (2) improves the sensitivity of the sensor. Therefore, we improve the sensor by reducing the amounts of both PADE and TBAC in the membrane. Finally, we fabricated a new sensor membrane consisting of 33% PADE, 100% BBPA, and 17% TBAC. This sensor showed higher durability and sensitivity than the conventional BT0 sensor.

In the future, we need to measure commercially available medicines to confirm the correlation between the sensor response and the bitterness sensory score.

Chapter 5
Quantitative Evaluation of Bitterness Suppression Effect of High-potency Sweeteners Using a Taste Sensor [70]

5.1 Background

5.1.1 Bitterness suppression effect

The classification of bitterness-masking methods could be divided into three types: physical masking, biochemical masking, and functional masking [71]. As shown in Figure 5.1, physical masking adopted a polymer or microencapsulation as physical barrier to separate bitterness substances from the taste receptors. It is the most versatile method used in bitterness masking. For example, capsules separate unpleasant drugs from our tongue [72]. Biochemical masking methods are well known as chemical modification including pro-drug or cyclodextrin interact by inclusion [73]. Functional masking is the simplest method for taste masking, especially in the case of pediatric formulations and liquid formulations. Sweeteners, amino acids, flavorings and other excipient additions have been usually used as bitterness masking materials [74,75]. Although bitterness masking by sweet substances is the most conventional among all approaches, the mechanism of bitterness suppression using this method has not yet been fully explained. Manabe et al. [76] reported two experimental results in cerebrospinal fluid after feeding bitterness and sweetness solutions to rats. It is reported that diazepam binding inhibitor (DBI) was released in the brain after feeding the rat with quinine hydrochloride; on the other hand, β- endorphin was detected in the brain after feeding

the rat with sucrose and saccharin [77]. Kawai et al. [78] proposed that the balance of these substances leads to a suppression effect such as bitterness suppression.

5.1.2 Sweetener potency and high-potency sweetness

The sweetener potency of a sweetener is defined by the ratio of sweet concentrations of sucrose and the sweetener with the some sweet intensity. Sweeteners, such as sucrose (1) and glucose (0.6~0.7) are known as low-potency sweeteners. On the other hand, high-potency sweeteners refer to the sweeteners whose sweetener potency exceeding 10, such as saccharin sodium and aspartame. For some low-potency sweeteners like sucrose and xylitol, the sweetness intensity increases with concentration in both low and high concentration region. However, even though the same effect occurs at low concentrations of high-potency sweeteners, the increase in sweetness intensity slows to an eventual plateau at high concentrations of high-potency sweeteners. Therefore, we sometimes call low-potency sweeteners high-intensity sweeteners [74,79,80]. In order to combine the advantages of both low-potency sweeteners and high-potency sweeteners, pharmaceutical companies usually combine them to suppress bitterness and improve drinking ease [74,81]. The chemical structures of high-potency sweeteners are shown in Figure 5.2.

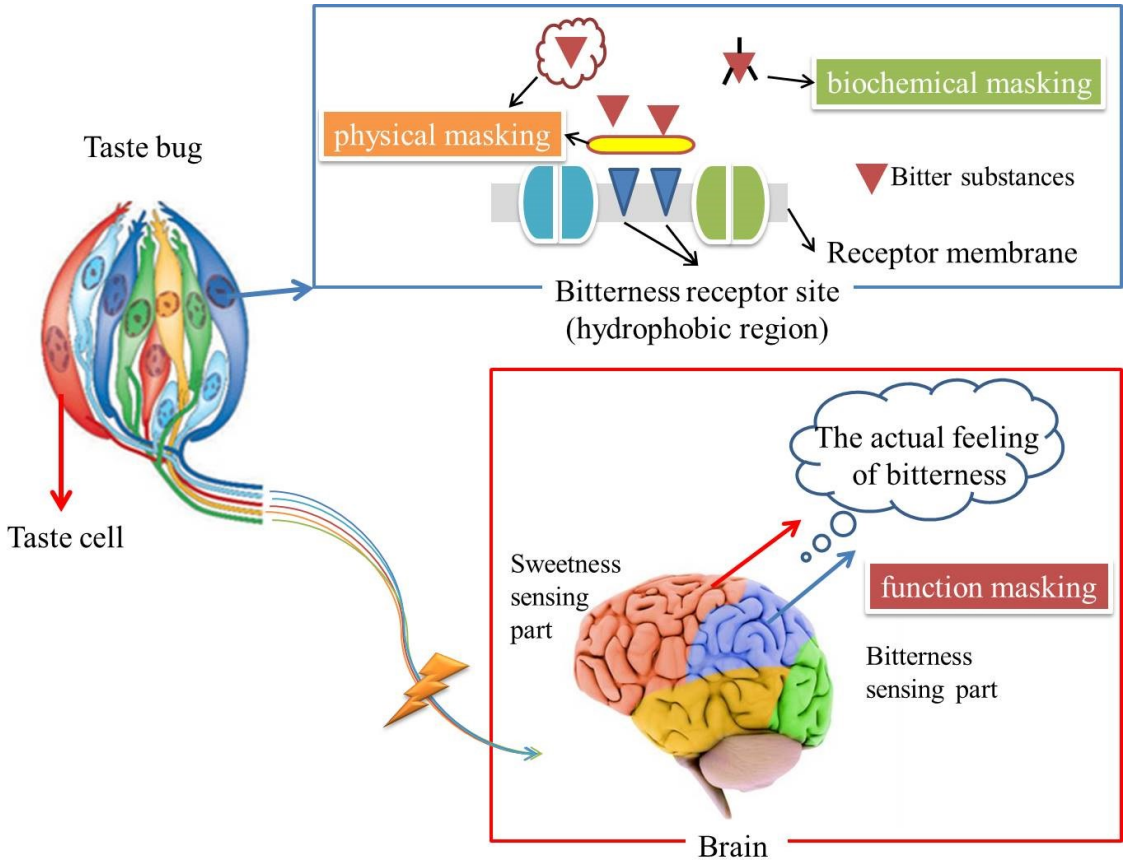

Figure 5.1: The diagram of bitterness suppression effect

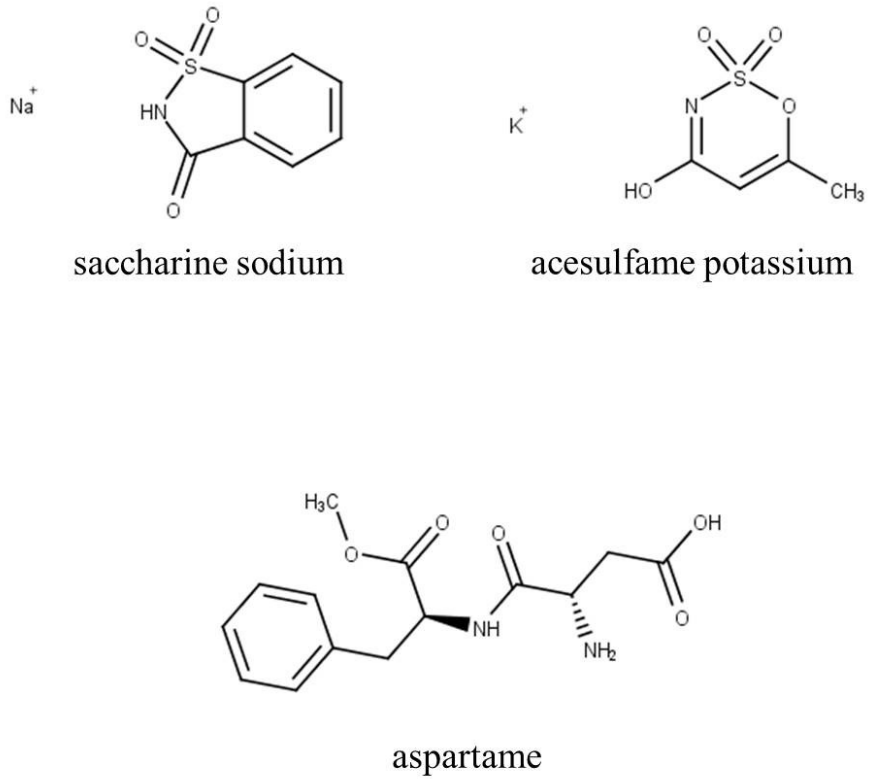

Figure 5.2: Chemical structures of high-potency sweeteners

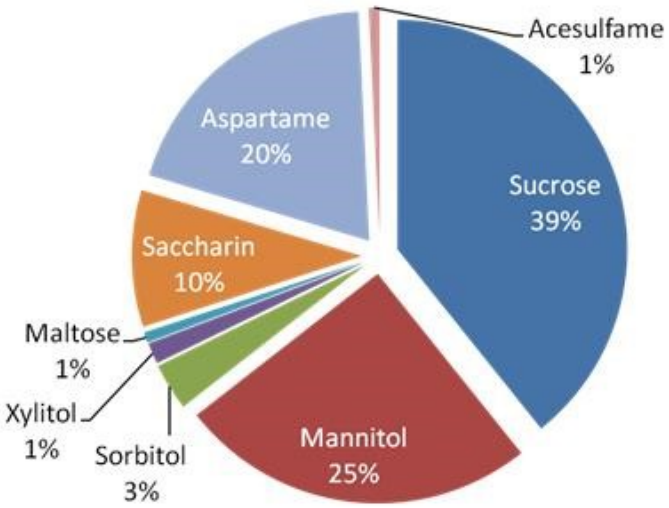

Figure 5.3: The main sweeteners used in prescription drugs [70]

5.1.3 The purpose of this chapter

The taste sensor has been used to detect the masking effect caused by sucrose when evaluating the bitterness of quinine hydrochloride and a drug substance for asthma [82]. In addition, the bitterness masking effect of a commercial bitterness masking substance (BMI-60, Kao Company, Ltd.) was also detected using taste sensor [83]. However, a quantitative method of predicting a bitterness masking effect using sweeteners has not been developed so far. According to the report of Pharmaceuticals and Medical Devices Agency (PMDA) in 2015 shown in Figure 5.3, 270 commonly used oral formulations were investigated including syrup, dry syrup, granules, fine granules, powders, etc. More than 30% include aspartame, saccharin and acesulfame, which implies a widely usage of high-potency sweeteners in pharmaceutical Industry [74].

Recently, two kinds of sweetness sensors for high-potency sweeteners have been developed. One is for positively charged high-potency sweeteners such as aspartame [84], the other one is for negatively charged high-potency sweeteners such as saccharin sodium and acesulfame potassium [80]. On the other hand, the bitterness of medicines without containing high-potency sweeteners can be evaluated using a bitterness sensor [19,32,62,66, 67,85].

In this chapter, we aim to propose an estimate formula to evaluate the masking effect of high-potency sweeteners using the outputs of the bitterness sensor for medicine and the sweetness sensors for high-potency sweeteners.

5.2 Experiment

5.2.1 Chemicals

Quinine hydrochloride was purchased from Kanto Chemical Co., Inc., Tokyo, Japan. Aspartame was donated from Ajinomoto Co., Inc. Saccharine sodium and acesulfame potassium was purchased from Tokyo Chemical Industry Co., Ltd. The chemical structures of quinine hydrochloride are shown in Figure 5.4. Saccharine sodium is negatively charged. Aspartame and quinine hydrochloride are positively charged when dissolved in solution.

5.2.2 Fabrication of sensor electrodes

The components of each sensor membrane are listed in Table 5.1. First, the lipid, plasticizer, and PVC were dissolved by THF and stirred for one hour. Secondly, the mixture solution was poured into a 90 mm glass Petri dish and wait for the THF to volatize off. Thirdly, the membrane was cut into about 1×1 cm and stuck to the sensor probe. Fourthly, 0.2 mL inner solution of 3.3 M KCl and saturated AgCl was filled into the sensor probe. Finally, the sensor electrode was completed by attaching an Ag/AgCl electrode to the sensor probe.

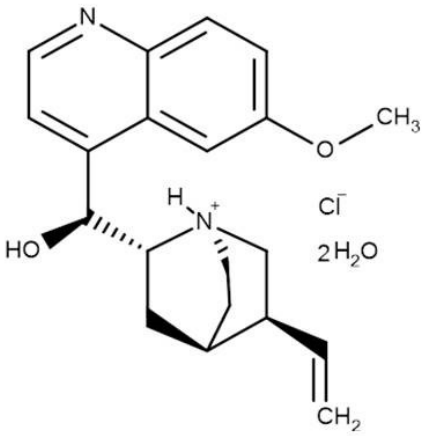

Figure 5.4: Chemical structure of quinine hydrochloride

Sensor	**Lipid**	**Plasticizer**
Bitterness sensor (BT0)	Phosphoric acid di-n-decyl ester	Bis(1-butylpentyl) adipate Tributyl O-acetylcitrate
Sweetness sensor for negatively charged sweeteners	Tetradodecylammonium bromide	Phosphoric acid tris (2-ethylhexyl) ester
Sweetness sensor for positively charged sweeteners	Phosphoric acid di (2-ethylhexyl) ester	2-Butoxyethyl oleate

Table 5.1: The membrane components of the sensors [70]

5.2.3 Matrix effect of bitterness sensor and sweetness sensors

The matrix effect is defined as the change of sensor responses caused by the coexisting substances except for the target substances [86]. In this study, high-potency sweeteners are the coexisting substances for the bitterness sensor. While the quinine hydrochloride showing bitterness is the coexisting substance for the sweetness sensor. The mixture solutions for testing bitterness sensor were prepared with 0.01 to 1.0 mM quinine hydrochloride as well as 0 to 10.0 mM aspartame or 0 to 1.0 mM saccharin sodium. The mixture solutions for testing the sweetness sensor for high-potency sweeteners were prepared with 0 to 0.10 mM quinine hydrochloride well as 0.1 to 10.0 mM aspartame or 0.01 to 1.0 mM saccharin sodium. All solutions were dissolved in the reference solution consisting of 30 mM KCl and 0.3 mM tartaric acid.

5.2.4 Sensory test of bitterness suppression

Eleven panelists (well-trained females: 23.7 ± 2.2 years old) participated in the sensory test using the method of magnitude estimation [87]. As shown in Table 5.2, quinine hydrochloride with the concentrations of 0.01, 0.03, 0.10, 0.30, 0.1 mM were used as standard bitterness solutions, corresponding to the bitterness score (τ) of 0, 1, 2, 3 and 4, respectively [88,89]. First, the panelists were asked to keep 2 ml of quinine hydrochloride solutions in their mouth each for 5 seconds. Then they were asked to keep the bitterness scores in mind. The sample solutions were composed of 0.1 mM quinine hydrochloride with aspartame or saccharine sodium. The concentrations of aspartame were 0.1, 0.3, 0.5, 1.0, 3.0, 5.0 and 10.0 mM while the concentrations of saccharine sodium were 0.01, 0.03, 0.05, 0.10, 0.30, 0.50 and 1.0 mM. Then the panelists were asked to keep each sample in their mouth for 5 seconds and answer the

bitterness scores of each sample. The design of sensory test was approved by the Ethical Committees of Mukogawa Women's University and written informed consents were obtained from all participants to make sure the safety along the test.

5.2.5 Prediction of bitterness with high-potency sweeteners

The relationship between CPA of the bitterness sensor and the bitterness of quinine hydrochloride was obtained by a single regression analysis using the results of sensory test. The part of suppressed bitterness was represented by converting the CPA of sweetness sensors for high-potency sweeteners as expressed by the second term of Equation 5.1. In order to make the model easier to understand, the sensor responses were all converted into the bitterness scores or sweetness scores. Only CPA values of these sensors were adopted in the data analysis because CPA values are more selective than relative value. The prediction model of bitterness masking effect is represented as

$$Y = Y_{\text{bitter}} - k \times Y_{\text{sweet}} + m, \quad (5.1)$$

where Y is the bitterness score of each sample; Y_{bitter} is the bitterness score of quinine hydrochloride of each sample. Y_{sweet} is the sweetness score of high-potency sweeteners involved in each sample. In this study, the sweetness score of aspartame is expressed as $Y_{\text{sweet-a}}$ and the sweetness score of saccharine sodium is expressed as $Y_{\text{sweet-s}}$.

In this chapter, we aim to calculate the parameters in this formula using SYSTAT (version No. 13.1, SYSTAT Inc.).

Standard bitterness solutions	
Quinine concentration (mM)	Bitterness score (τ)
0.01	0
0.03	1
0.10	2
0.30	3
1.00	4

Table 5.2: Standard bitterness solutions

5.3 Results and discussion

5.3.1 Sensory test of bitterness masking by high-potency sweeteners

As shown in Figure 5.5, people feel the bitterness gradually reduced when 0.1 – 10 mM aspartame was added into 0.1 mM quinine hydrochloride solutions. However, only 5 mM ($p < 0.01$) and 10 mM ($p < 0.001$) aspartame showed statistical significant differences according to Dunnett's test, comparing to the bitterness of 0.1 mM quinine hydrochloride ($\tau=2$). On the other hand, as shown in Figure 5.6, people feel almost the same bitterness when 0.01 to 0.1 mM saccharine sodium was added, but they feel the bitterness reduce significantly when 0.5 mM ($p < 0.01$) and 1 mM ($p < 0.001$) saccharine sodium were added, comparing to the bitterness of 0.1 mM quinine hydrochloride ($\tau=2$).

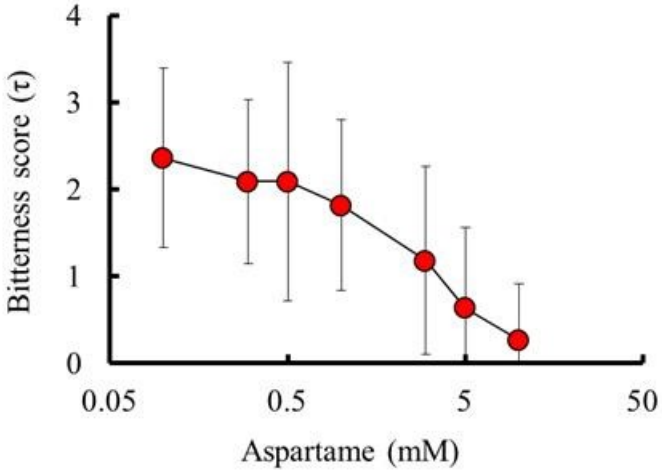

Figure 5.5: Bitterness sensory scores of 0.1 mM quinine hydrochloride and seven different concentrations of added aspartame [70].

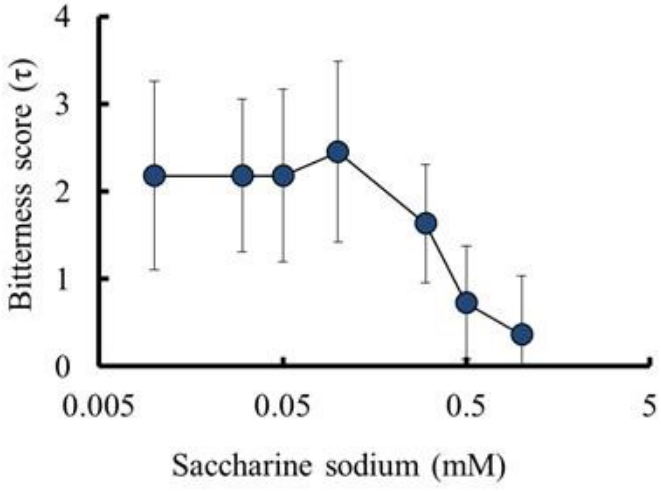

Figure 5.6: Bitterness sensory scores of 0.1 mM quinine hydrochloride and seven different concentrations of added saccharine sodium [70].

5.3.2 Matrix effect of bitterness sensor on high-potency sweeteners

As shown in Figure 5.7, when aspartame was not added into the bitterness solution, the sensor response showed good concentration dependence to the quinine hydrochloride. The CPA value is proportional to the logarithm of the concentration of quinine hydrochloride, which reflects the bitterness intensity, according to the Weber-Fechner law [69,90]. In addition, even 0.1~10 mM aspartame was added into bitterness solution, the sensor response did not change with the aspartame content. On the other hand, as shown in Figure 5.8, when saccharine sodium was added into the bitterness solution, the sensor response showed a similar result with aspartame. As a result, the bitterness sensor showed good selectivity and concentration dependence to quinine hydrochloride in mixture solutions with high-potency sweeteners. The error bars show the stand deviations (SD) of CPA values for high-potency sweeteners in all concentrations.

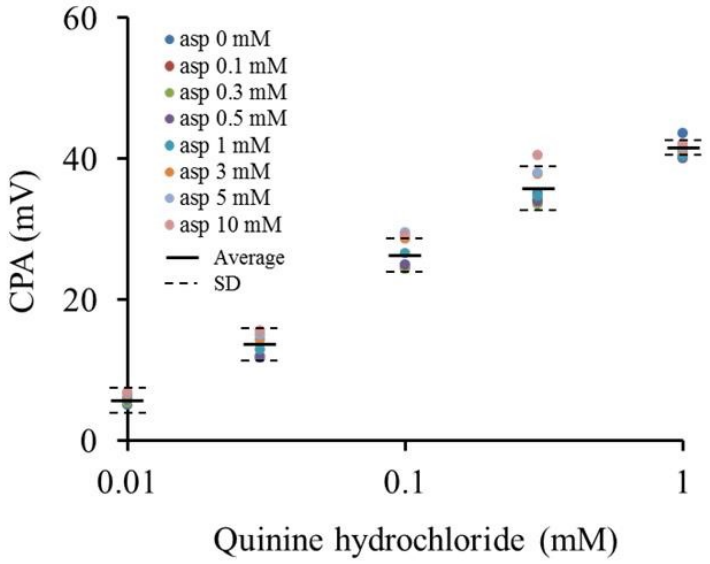

Figure 5.7: The BT0 sensor response to quinine hydrochloride and seven different concentrations of added aspartame.

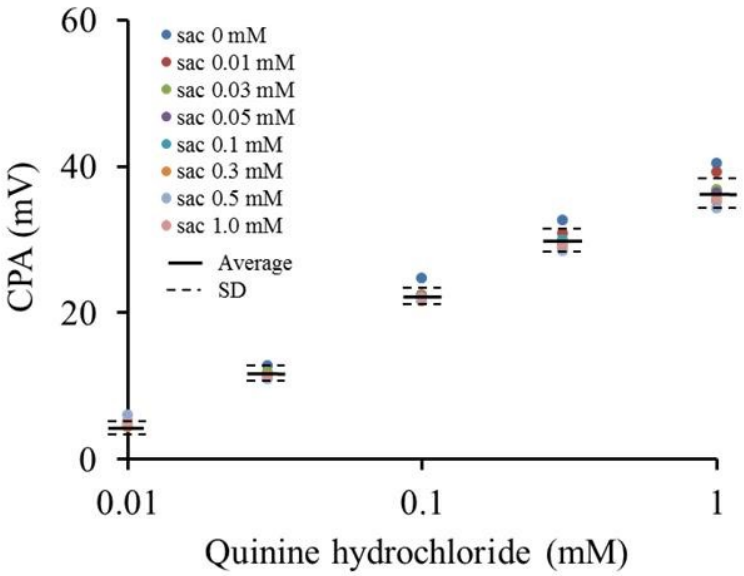

Figure 5.8: The BT0 sensor response to quinine hydrochloride and seven different concentrations of added saccharine sodium.

5.3.3 Matrix effect of sweetness sensors on quinine hydrochloride

As shown in Figure 5.9, when quinine hydrochloride was not added into the aspartame solution, the sensor response showed good concentration dependence to 1-10 mM aspartame. In addition, even 0.01~0.1 mM quinine hydrochloride was added into bitterness solution, the sensor response did not change with the quinine content. On the other hand, as shown in Figure 5.10, when quinine hydrochloride was added into the saccharine sodium solution, the sensor response showed a similar result with aspartame. As a result, the sweetness sensor showed good selectivity and concentration dependence to aspartame and saccharine sodium in mixture solutions with quinine hydrochloride.

Since both the bitter sensor and the sweetness sensors for high-potency sweeteners have a high selectivity and no response to the coexisting substances, we could build a prediction model as Equation (5.1). Firstly, we substituted the CPA of bitterness sensor B (mV) and the bitterness scores of standard solutions of quinine hydrochloride $Y_{\text{bitter}}(\tau)$ into Equation (5.2).

$$Y_{\text{bitter}} = \alpha \times B + \beta. \quad (5.2)$$

In order to figure out two coefficients α and β in Equation (5.2), we carried out a single regression analysis using the CPA of bitterness sensor of bitterness standard solutions and the corresponding bitterness scores. The result is shown in Equation (5.3).

$$Y_{\text{bitter}} = 0.098 \times B - 0.37, \quad (5.3)$$

Here, B is the CPA value of the bitterness sensor. Therefore, we could calculate the predicted bitterness score of quinine hydrochloride by substituting the CPA of bitterness sensor B into Equation (5.3).

In our previous study, we have carried out a single regression analysis to obtain the relationship between the sweetness scores of high-potency sweeteners (Y_{sweet}) and the

CPA value of sweetness sensors for high-potency sweeteners [91]. The standard sweetness solutions used sucrose with the concentrations from 0 to 1000 mM, corresponding to the sweetness score from 0 to 6. As shown in the right of Figure 5.11 (CPA value > 0), the relationship for aspartame is expressed as Equation (5.4) in 0.1 mM - 1 mM concentration area and Equation (5.5) in 1 - 10 mM concentration area:

$$Y_{\text{sweet-a}} = 1.13 \times S_a + 0.52 \qquad (-0.46 < S_a < 1.2), \tag{5.4}$$

$$Y_{\text{sweet-a}} = 0.11 \times S_a + 2.96 \qquad (S_a \geq 1.2), \tag{5.5}$$

Here $Y_{\text{sweet-a}}$ is the sweetness score of aspartame; S_a is the CPA value of sweetness sensor for aspartame (positively charged high potency sweeteners, in the mV unit). People did not feel sweetness when $S_s \leq -0.46$, because aspartame in that concentration was under human's threshold to sweetness. Therefore, we could calculate the sweetness score of aspartame by substituting the CPA value of sweetness sensors for positively charged high potency sweeteners (S_a) into Equation (5.4) or (5.5).

As shown in the left of Figure 5.11 (CPA value < 0), the red dotted line represents the sweetness scores for saccharine sodium and the blue dotted line represents the sweetness scores for acesulfame potassium [91]. In this chapter, we expressed the results of saccharine sodium and acesulfame potassium uniformly as negatively charged sweeteners Equation (5.6).

$$Y_{\text{sweet-s}} = -0.31 \times S_s - 1.48 \qquad (S_s < -4.77), \tag{5.6}$$

Here $Y_{\text{sweet-s}}$ is the sweetness score of saccharine sodium or acesulfame potassium; S_s is the CPA value of the sweetness sensor for saccharine sodium or acesulfame potassium. $Y_{\text{sweet-s}}$ would be zero when $S_s \geq -4.77$, because the concentration of saccharine sodium was under human's threshold.

Finally, we substituted the sensory score of each sample (Y), the bitterness score of

quinine hydrochloride (Y_{bitter}) and sweetness score of high-potency sweeteners (Y_{sweet}) into Equation (5.1) to calculate coefficient α, β. As a result, the bitterness estimate model aspartame is expressed as Equation (5.7). The sensory score of each sample (Y) in Figure 5.5, bitterness score of quinine hydrochloride (Y_{bitter}) in Figure 5.7 and sweetness score of high-potency sweeteners ($Y_{sweet\text{-}a}$) from Equation (5.4) and Equation (5.5) were used.

$$Y = Y_{bitter} - 0.73 \times Y_{sweet\text{-}a} + 1.62. \quad (5.7)$$

On the other hand, the bitterness estimate model for saccharine is expressed as Equation (5.8). The sensory score of each sample (Y) in Figure 5.6, the bitterness score of quinine hydrochloride (Y_{bitter}) in Figure 5.8 and the sweetness score of high-potency sweeteners ($Y_{sweet\text{-}s}$) from Equation (5.6) was used:

$$Y = Y_{bitter} - 1.34 \times Y_{sweet\text{-}s} + 2.47. \quad (5.8)$$

Because the bitterness masking effect occurred from 0.1 mM saccharine sodium, the data of saccharine sodium from 0.1 mM to 1 mM can be adopted to Equation (5.8).

As shown in Figure 5.12, when aspartame was added from 0.1 to 10 mM, the bitterness score decreased gradually. On the other hand, when saccharine sodium was added from 0.1 to 1 mM in Figure 5.13, the bitterness score decreased gradually as well. The sensual values showed good correlations with the estimate bitterness for both aspartame ($R^2 = 0.92$) and saccharine ($R^2 = 0.88$). In you look at the graph you will see that the standard deviation of sensory test was higher than the sensor response. The effectiveness of this estimate model using taste sensor was confirmed from the viewpoint of the predictability of bitterness intensity.

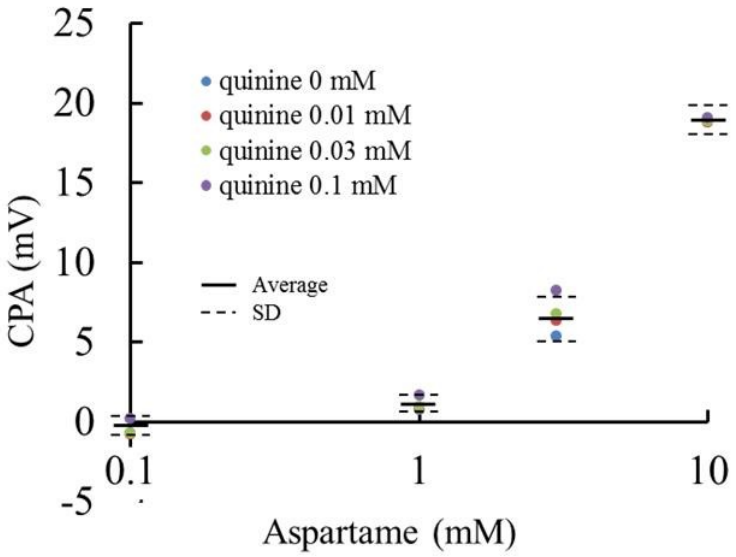

Figure 5.9: The CPA value of sweetness sensors to aspartame with added quinine hydrochloride (n = 5). The error bars show the SD of CPA values for quinine hydrochloride from 0 to 0.1 mM.

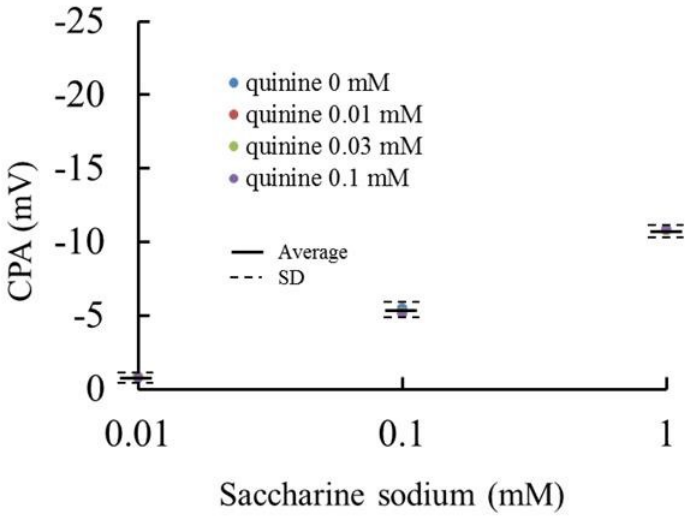

Figure 5.10: The CPA value of sweetness sensors to saccharine sodium with added quinine hydrochloride (n = 5). The error bars show the SD of CPA values for quinine hydrochloride from 0 to 0.1 mM.

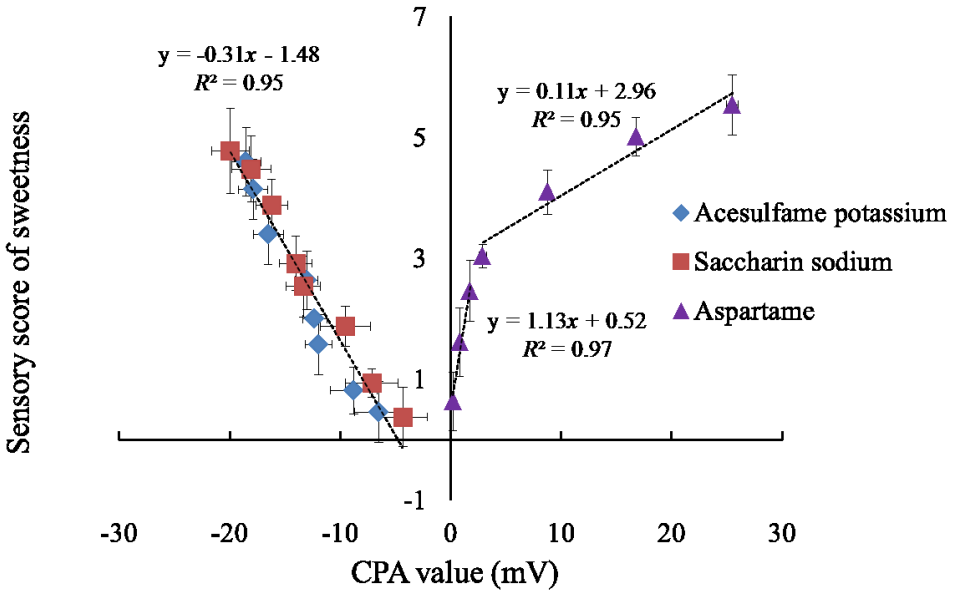

Figure 5.11: Relationship between sensory scores of sweetness and CPA values of sweetness sensors for high-potency sweeteners [70].

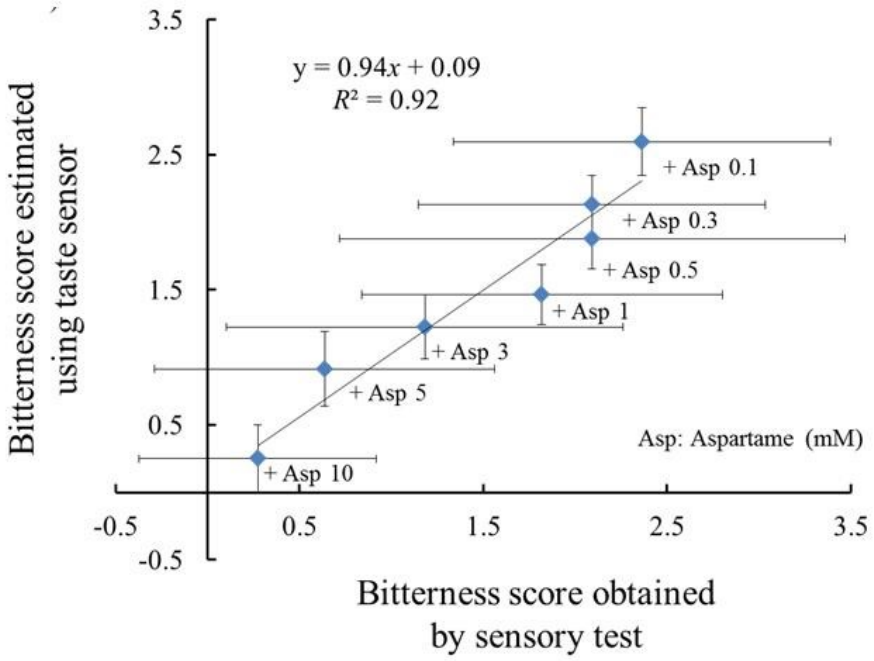

Figure 5.12: Regression analysis results using CPA values measured with BT0 and sweetness sensor for positively charged high-potency sweetener: aspartame (e.g. +Asp 0.1 means 0.1 mM aspartmae was added to quinine hydrochloride) [70].

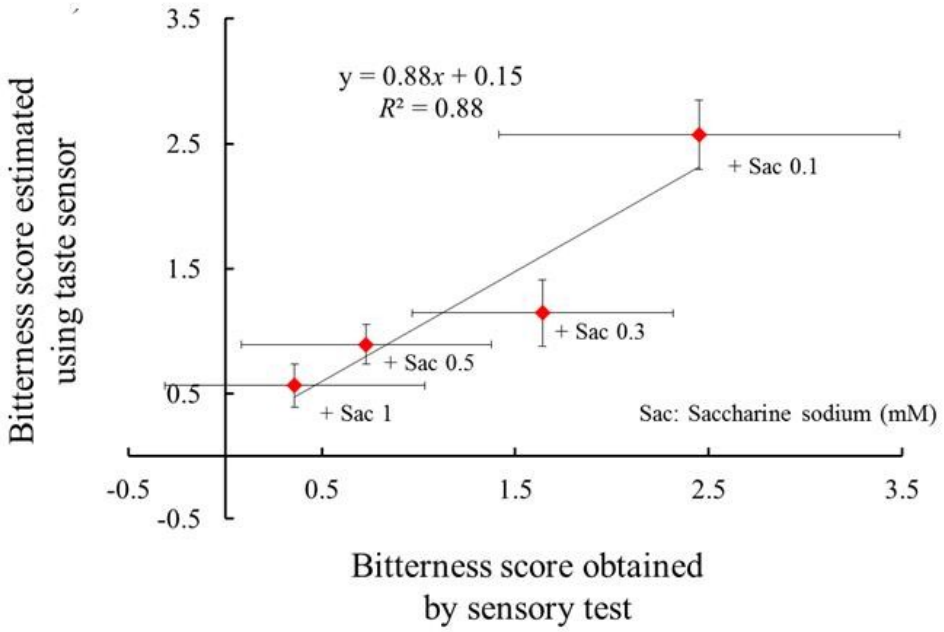

Figure 5.13 Regression analysis results using CPA values measured with BT0 and sweetness sensor for negatively charged high-potency sweetener: saccharine sodium (e.g. +Sac 0.01 means 0.01 mM saccharine sodium was added to quinine

5.4 Conclusion

The purpose of this chapter is to establish a model for predicting the bitterness of pharmaceuticals in the presence of a sweetener, so that the bitterness can be known without functional test. We presented a very easy-to-understand model, which thanks to the high selectivity of both the bitterness sensor and the sweeteners sensors for high-potency sweeteners. The results showed a good correlation between bitterness scores estimated using taste sensor and bitterness sensory scores using two estimate formulas we proposed. A future task for this study is to prove if the method is also suitable for other bitter substances such as coffee or other flavoring agents included in medicines.

Chapter 6
Conclusions

In this thesis, first, we promoted the selectivity and safety of the taste sensor for education with a lipid-impregnated membrane. Besides, we clarified the principle of MSG preconditioning process for a strongly hydrophobic lipid polymer membrane used for SDS detection. In addition, we focused on another strong hydrophobic membrane used for sensing bitterness and we improved the durability and sensitivity of the bitterness sensor. Finally, we proposed a quantitative evaluation method for bitterness masking effect of high-potency sweeteners by using the hydrophobic bitterness sensor as well as the sweetness sensor. The research objects of the study are from the shallower to the deeper. According to the research objects, the paper can be divided into three parts and the results of the research are shown below.

Part 1: Research on the development of the taste sensor for education using a simple membrane (including Chapter 2)

Chapter 2: Taste Sensor for Education with Selectivity to Salt and Citric Acid

- The selectivity of the taste sensor for education was enhanced to distinguish salt and citric acid samples.
- The safety and entertainment were enhanced by using simple stationery and optimizing the production method.
- The usefulness of the sensor set and production process were proved in the science class.

Part 2: Research on the improvement of performance (sensitivity and durability) of taste sensor (including Chapter 3 & 4)

Chapter 3: The Preconditioning for Taste Sensor with a Strongly Hydrophobic Membrane

- We concluded that the preconditioning process and time have correlation with the sensor response equipped with strongly hydrophobic membrane.
- The optimal preconditioning time was found for the pesticide sensor for SDS.
- The clarification of the principle of MSG precondition has a far-reaching significance for the design for new taste sensor for hydrophobic substances.

Chapter 4: Improved Durability and Sensitivity of Bitterness Sensing Membrane for Medicines

- We found out the reason for the deterioration in the response of the BT0 sensor.
- We fabricated a new bitterness sensor with higher durability and sensitivity than the conventional BT0 sensor.

Part 3: Research on the application of the taste sensor (including Chapter 5)

Chapter 5: Quantitative Evaluation of Bitterness Suppression Effect of High-potency Sweeteners Using a Taste Sensor

- We are first to propose the evaluation of the interaction between the tastes using two taste sensor electrodes.
- We proposed an easy-to-understand model for bitterness masking effect only using the bitterness sensor and the sweeteners sensors for high-potency sweeteners.

- The model showed a good correlation between bitterness scores estimated using taste sensor and bitterness sensory scores using two estimate formulas we proposed.

As people's quality of life requirements continue to increase, we firmly believe that the application of taste sensor in life will be more and more popular. Therefore, the performance requirements to the taste sensor itself will be higher and higher as well. From this study, we hope to arouse people’s interest and cognition of taste and engineering as well as benefit mankind by the quantification and visualization of taste. In particular, the hydrophobic bitter substances in the medicine cause a big obstacle in taking medicine. We hope to promote the standard of bitterness of medicine through the digitization of bitterness. In this way, we can help the pharmaceutical companies to create drugs that meet the tastes of different patients.

References

[1] Iwasaki, S.; Yoshizawa, H. and Kawahara, I. Ultrastructural study of the relationship between the morphogenesis of filiform papillae and the keratinization of the lingual epithelium in the rat. *J. Anat.* 1999, 195, 27-38.

[2] Mbiene, J.P. and Mistretta, C.M. Initial innervation of embryonic rat tongue and developing taste papillae: nerves follow distinctive and spatially restricted pathways. *Acta. Anat. (Basel)*. 1997, 160 (3), 139-158.

[3] Suzuki, T. Cellular mechanisms in taste buds. *Bull Tokyo Dent Coll.* 2007, 48 (4), 151-161.

[4] Roper, S.D. Taste: mammalian taste bud physiology, Reference Module in Neuroscience and Biobehavioral Psychology. ISBN: 978-0-12-809324-5.

[5] Chandrashekar, J.; Hoon, M.A.; Ryba, N.J.P.; Zuker, C.S. The receptors and cells for mammalian taste. *Nature* 2006, 444, 288-294.

[6] Running, C.A.; Craig, B.A.; Mattes, R.D. Oleogustus: The unique taste of fat. *Chem. Sens.* 2015, 40 (7), 507-516.

[7] Bachmanov, A.A.; Beauchamp, G.K. (2007). Taste receptor genes. *Annu. Rev. Nutr.* 2007, 27, 389-414.

[8] Heck, G.L.; Mierson, S.; DeSimone, J.A. Salt taste transduction occurs through an amiloride-sensitive sodium transport pathway. *Science* 1984, 223 (4634), 403-405.

[9] Avenet, P.; Lindemann, B. Amiloride-blockable sodium currents in isolated taste receptor cells. *J. Membr. Biol.* 1988, 105, 245-255.

[10] Rani, A.; Akhtar, S.; Nawaz, S.K.; Irfan, S.; Azam, S.; Arshad, M. Electrolyte disturbance and the type of malarial infection. *Iran J Public Health*. 2015, 44 (11), 1492-1497.

[11] Challisa, R.C.; Ma, M. Sour taste finds closure in a potassium channel. *Proc Natl Acad Sci U.S.A.* 2016, 113 (2), 246-247.

[12] Meyerhof, W.; Batram, C.; Kuhn, C.; Brockhoff, A.; Chudoba, E.; Bufe, B.; Appendino, G.; Behrens, M. The Molecular Receptive Ranges of Human TAS2R Bitter Taste Receptors. *Chem. Sens.* 2010, 35 (2), 157-170.

[13] Yoshida, R.; Niki, M.; Jyotaki,M.; Sanematsu, K.; Shigemura, N. and Ninomiya, Y. Modulation of sweet responses of taste receptor cells. *Seminars in Cell & Developmental Biology* 2013, 24, 226-231.

[14] Servant, G.; Tachdjian, C.; Tang, X.Q.; Werner, S.; Zhang, F.; Li, X.; Kamdar, P.; Petrovic, G.; Ditschun, T.; Java, A.; Brust, P.; Brune, N.; DuBois, G.E.; Zoller, M. and Karanewsky, D.S. Positive allosteric modulators of the human sweet taste

receptor enhance sweet taste. *Proceedings of the National Academy of Sciences of the United States of America* 2010, 107, 4746-4751.

[15] Chaudhari, N.; Pereira, E.; Roper, S.D. Taste receptors for umami: the case for multiple receptors. *Am J Clin Nutr.* 2009, 90 (3), 738-742.

[16] 村元美代, 渡辺雄二, 中川正, 水間桂子, 青木宏, 苦味感覚におよぼすストレスノ影響, *大妻女子大学紀要（家政系）* 1995, 3, 109-120.

[17] Cowart, B.J.; Yokomukai, Y.; Beauchamp, G.K. Bitter taste in aging: compound-specific decline in sensitivity. *Physiol Behav.* 1994, 56 (6), 1237-1241.

[18] Banerjee, R.; Tudu, B.; Bandyopadhyay, R.; Bhattacharyya, N. A review on combined odor and taste sensor systems. *J. Food Eng.* 2016, 190, 10-21.

[19] Tahara, Y.; Toko, K. Electronic tongues—A review. *IEEE Sens. J.* 2013, 13, 3001-3011.

[20] Bachmanov, A.A.; Beauchamp, G.K. Taste receptor genes. *Annu. Rev. Nutr.* 2007, 27, 389-414.

[21] Winquist, F. Voltammetric electronic tongues—Basic principles and applications. *Microchim. Acta* 2008, 163, 3-10.

[22] Facure, M.H.M.; Mercante, L.A.; Mattoso, L.H.C.; Correa, D.S. Detection of trace levels of organophosphate pesticides using an electronic tongue based on graphene hybrid nanocomposites. *Talanta* 2017, 167, 59-66.

[23] Ciosek, P.; Wroblewski, W. Sensor array for liquid sensing-electronic tongue systems. *Analyst* 2007, 132, 963-978.

[24] Marx, I.; Rodrigues, N.; Dias, L.G.; Veloso, A.C.A.; Pereira, J.A.; Drunkler, D.A.; Peres, A.M. Sensory classification of table olives using an electronic tongue: Analysis of aqueous pastes and brines. *Talanta* 2017, 162, 98-106.

[25] Citterio, D.; Suzuki, K. Smart taste sensors. *Anal. Chem.* 2008, 80, 3965-3972.

[26] Nunez, L.; Ceto, X.; Pividori, M.I.; Zanoni, M.V.B.; del Valle, M. Development and application of an electronic tongue for detection and monitoring of nitrate, nitrite and ammonium levels in waters. *Microchem. J.* 2013, 110, 273-279.

[27] Daikuzonoa, C.M.; Dantas, C.A.R.; Volpati, D.; Constantino, C.J.L.; Piazzetta, M.H.O.; Gobbi, A.L.; Taylor, D.M.; Oliveira, O.N., Jr.; Riul, A., Jr. Microfluidic electronic tongue. *Sens. Actuators B Chem.* 2015, 207, 1129-1135.

[28] Song, H.S.; Kwon, O.S.; Lee, S.H.; Park, S.J.; Kim, U.K.; Jang, J.; Park, T.H. Human Taste Receptor-Functionalized Field Effect Transistor as a Human-Like Nanobioelectronic Tongue. *Nano Lett.* 2013, 13, 172-178.

[29] Ha, D.; Sun, Q.; Su, K.; Wan, H.; Li, H.; Xu, N.; Sun, F.; Zhuang, L.; Hu, N.; Wang, P. Recent achievements in electronic tongue and bioelectronic tongue as taste

sensors. *Sens. Actuators B Chem*. 2015, 207, 1136-1146.

[30] Wang, P.; Liu, Q.; Wu, C.; Hsia, K.J. Electronic nose and electronic tongue, Bioinspired smell and taste sensors. 2015, Springer, Germany.

[31] Del Valle, M. Electronic tongues employing electrochemical sensors. *Electro analysis* 2010, 22, 1539-1555.

[32] Kobayashi, Y.; Habara, M.; Ikezaki, H.; Chen, R.G.; Naito, Y.; Toko, K. Advanced taste sensors based on artificial lipids with global selectivity to basic taste qualities and high correlation to sensory scores. *Sensors* 2010, 10, 3411-3443.

[33] Liu, J.; Yang, J.; Wang, W.; Fu, S.; Shi, Y.; Men, H. Automatic evaluation of sensory information for beer at a fuzzy level using electronic tongue and electronic nose. *Sens. Mater.* 2016, 28, 785-795.

[34] Lin, R.; Gao, X.; Wang, J.; Dai, L.; Kang, B.; Zhang, L.; Shi, J.; Gui, X.; Liu, P.; Li, X. Traditional human taste panel and taste sensors methods for bitter taste masking research on combined bitterness suppressants of berberine hydrochloride. *Sens. Mater.* 2017, 29, 105-116.

[35] Toko, K.; Hara, D.; Tahara, Y.; Yasuura, M.; Ikezaki, H. Relationship between the amount of bitter substances adsorbed onto lipid/polymer membrane and the electrical response of taste sensors. *Sensors* 2014, 14, 16274-16286.

[36] Ikezaki, H.; Kobayashi, Y.; Toukubo, R.; Naito, Y.; Taniguchi, A.; Toko, K. Techniques to control sensitivity and selectivity of multichannel taste sensor using lipid membranes. *Proc. Transducers* 1999, 99, 1634-1637.

[37] Cui, H.; Habara, M.; Ikezaki, H.; Toko, K. Selectivity control in a sweetness sensor using lipid/polymer membranes. *Sens. Mater*. 2005, 17, 385-390.

[38] Gouy, M. Sur la constitution de la charge électrique à la surface d'un électrolyte. *J. Phys. Theor. Appl.* 1910, 9, 457-468 (in French).

[39] Chapman, D.L. A contribution to the theory of electrocapillarity. *Phil. Mag.* 1913, 25, 475-481.

[40] Toko, K. Taste sensor with global selectivity. *Mater. Sci. Eng., C* 1996, 6, 69-82.

[41] Ikezaki, H.; Taniguchi, A.; Toko, K. Quantification of taste of green tea with taste sensor. *Trans. IEEE of Japan* 1997, 117, 465-470 (in Japanese).

[42] Ikezaki, H.; Naito, Y.; Kobayashi, Y.; Toukubo, R.; Taniguchi, A.; Toko, K. Improvement of selectivity of taste sensor by control of charge density and hydrophobicity of lipid membrane. *Technical Report of IEICE*. 2000, 100, 19-24 (in Japanese).

[43] 巫 霄，田原祐助，鍬本一至，栗焼久夫，都甲 潔，理科教育用味覚センサ，電気学会論文誌 E，2015, 135 (2), 65-70 (in Japanese).

[44] Trends in International Mathematics and Science Study (TIMSS) 2015, International Association for the Evaluation of Educational Achievement (IEA). (http:www.iea.nl)

[45] Programme for International Student Assessment (PISA) 2006, Economic Co-operation and Development (OECD). (http://www.oecd.org)

[46] 松尾勉：製作実習を伴う学生実験および新しい学生実験教材の開発と実践, available from (http://www.toray.co.jp/tsf/rika/pdf/s59_07.pdf)

[47] Arase, H.; Yasuura, M.; Tahara, Y.; Onodera, T.; Kuriyaki, H.; and Toko, K. Trial production of a taste sensor kit for education. *Technical Meeting on Chemical Sensor, IEE Japan* 2012, 6, 21-24 (in Japanese)

[48] 環境省：「化学物質の環境リスク評価第 7 巻」, available from 〈http://www.env.go.jp/chemi/report/h21-01/〉(accessed 2014/05/12)

[49] Kuwamoto, K.; Arase, H.; Yasuura, M.; Tahara, Y.; Toko, K. and Kuriyaki, H. Development of taste sensor as a teaching material comprehending science subjects in high school. *IEEJ Trans. FM* 2014, 134, 472-477 (in Japanese).

[50] Wu, X.; Kuwamoto, K.; Yasuura, M.; Yusuke, T.; Toko, K.; Kuriyaki, H. Development of Taste Sensor for Education to Measure Salt and Sour Substances. *Technical Meeting on Chemical Sensor IEEE Japan* 2014, 65-68 (in Japanese).

[51] Wu, X.; Tahara, Y.; Toko, K.; Kuriyaki, H. Fabrication of taste sensor for education. *American Institute of Physics Conference Proceedings*, 2017, 1808, 020064.

[52] Wu, X.; Ji, K.; Wang, R.; Tahara, Y.; Yatabe, R.; Toko, K. Taste sensor using strongly hydrophobic membranes to measure hydrophobic substances. *Proceedings of the 10th International Conference on Sensing Technology* 2016, Paper ID 4424977.

[53] Naito, Y.; Ikezaki, H.; Taniguchi, A.; Toko, K. Detection of agricultural chemicals using a lipid membrane sensor. *Proceedings of IEEE Sensors* 2002, 1, 331-334.

[54] Taniguchi, A.; Naito, Y.; Maeda, N.; Sato, Y.; Ikezaki, H.; Toko, K. Detection of cyanide using the taste sensor. *IEEJ Transactions on Sensors and Micromachines* 1999, 119, 587-592 (in Japanese).

[55] Naito, Y.; Ikezaki, H.; Taniguchi, A.; Toko, K. New method to detect a trace amount of organic substances using a lipid membrane sensor. *IEEJ Transactions on Sensors and Micromachines* 2001, 121, 65-69 (in Japanese).

[56] Hua, X.; Yang, J.; Wang, L.; Fang, Q.; Zhang, G.; Liu F. Development of an Enzyme Linked Immunosorbent Assay and an Immunochromatographic Assay for Detection of Organophosphorus Pesticides in Different Agricultural Products. *PLoS ONE* 2012, 7 (12), e53099.

[57] Apilux, A.; Isarankura-Na-Ayudhya, C.; Tantimongcolwat, T.; Prachayasittikul, V. Paper-based acetylcholinesterase inhibition assay combining a wet system for organophosphate and carbamate pesticides detection. *EXCLI J.* 2015, 14, 307-319.

[58] Umino, K.; Habara, M.; Toko K. Simple screening method for pesticide residues by detecting coexistent adjuvants using potentiometric measurement. *Sens. Mater.* 2012, 24, 1-11.

[59] Ministry of Economy, Trade and Industry 2008. Annual Report 2008. Statistics of chemical industry, List of statistical tables, Dynamic statistics of production surveyed by the Ministry of Economy, Trade and Industry.

[60] Harada, Y.; Noda, J.; Yatabe, R.; Ikezaki, H.; Toko, K. Research on the changes to the lipid/polymer membrane used in the acidic bitterness sensor caused by preconditioning. *Sensors*, 16 (2), 2016, 230-239.

[61] Harada, Y.; Tahara, Y.; Toko, K. Study of the relationship between taste sensor response and the amount of epigallocatechin gallate adsorbed onto a lipid-polymer membrane. *Sensors*, 15(3), 2015, 6241-6249.

[62] Fukagawa, T.; Tahara, Y.; Yasuura, M.; Habara, M.; Ikezaki, H.; Toko, K. Relationship between taste sensor response and amount of quinine adsorbed on lipid/polymer membrane. *J. Innov. Electron. Commun.* 2012, 2, 1-6.

[63] Watanabe, M.; Toko, K.; Sato, K.; Kina, K.; Takahashi, Y.; Iiyama, S. Charged impurities of plasticizer used for ion-selective electrode and taste sensor. *Sens. Mater.* 1998, 10, 103-112.

[64] Yatabe, R.; Noda, J.; Tahara, Y.; Naito, Y.; Ikezaki, H.; Toko, K. Analysis of a lipid/polymer membrane for bitterness sensing with a preconditioning process. *Sensors* 2015, 15 (9), 22439-22450.

[65] Wu, X.; Onitake, H.; Huang, Z.; Shiino, T.; Tahara, Y.; Yatabe, R.; Ikezaki, H.; Toko, K. Improved durability and sensitivity of bitterness-sensing membrane for medicines. *Sensors* 2017, 17 (11), 2541.

[66] Kobayashi, Y.; Hamada, H.; Yamaguchi, Y.; Ikezaki, H.; Toko, K. Development of an artificial lipid-based membrane sensor with high selectivity and sensitivity to the bitterness of drugs and with high correlation with sensory score. *IEEJ Trans.* 2009, 4, 710-719.

[67] Akitomi, H.; Tahara, Y.; Yasuura, M.; Kobayashi, Y.; Ikezaki, H.; Toko, K. Quantification of tastes of amino acids using taste sensors. *Sens. Actuators B Chem.* 2013, 179, 276-281.

[68] Hara, D.; Fukagawa, T.; Tahara, Y.; Yasuura, M.; Toko, K. Examination of amount of astringent substances adsorbed onto lipid/polymer membrane used in taste sensor.

Sens. Lett. 2014, 12, 1172-1176.

[69] Pfaffmann, C. The sense of taste. In Handbook of Physiology; Field, I.J., Ed.; American Physiological Society: Washington, DC, USA, 1959; 1, 507-533.

[70] Wu, X.; Onitake, H.; Haraguchi, T.; Tahara, Y. Yatabe, R.; Yoshida, M.; Uchida, T.; Ikezaki H.; Toko, K. Quantitative prediction of bitterness masking effect of high-potency sweeteners using taste sensor, *Sensors and Actuators B: Chemical* 2016, 235, 11-17.

[71] Mirajkar, R.N.; Devkar, M.S.; Kokare, D.R. Taste masking methods and agents in pharmaceutical formulations. *Int. J. Pharm.* 2012, 3, 67-70.

[72] Sugiura, T.; Uchida, S.; Namiki, N. Taste-masking effect of physical andorganoleptic methods on peppermint-scented orally disintegrating tablet of famotidine based on suspension spray-coating method. *Chem. Pharm. Bull.* 2012, 60, 315-319.

[73] Sharma, V.; Chopra, H.. Role of taste and taste masking of bitter drugs in pharmaceutical industries. *Int. J. Pharm. Pharm. Sci*. 2010, 2, 14-18.

[74] Toko, K.; Uchida, T. Taste Modification Technology of Food and Medicine, second ed., CMC Publishing, Tokyo, 2013 (in Japanese).

[75] Schiffman, S.S. Rationale for further medical and health research onhigh-potency sweeteners. *Chem. Senses*. 2012, 37, 671-679.

[76] Manabe, Y.; Kuroda, K.; Imaizumi, M.; Inoue, K.; Sako, N.; Yamamoto, T.; Fushiki, T.; Hanai, K. Diazepam-binding inhibitor-like activity in rat cerebrospinal fluid after stimulation by an aversive quinine taste. *Chem. Senses* 2000, 25, 431-439.

[77] Yamamoto, T.; Sako, N.; Maeda, S. Effects of taste stimulation on beta-endorphin levels in rat cerebrospinal fluid and plasma. *Physiol. Behav.* 2000, 69, 345.350.

[78] Kawai, T.; Kusakabe, Y. Quantitative analysis for the masking effects to bitter taste. *Rep. Nat. Food Res. Inst.* 2012, 76, 9-16.

[79] Ronald, C.D. Customizing sweetness profiles, Food Prod. Des. 2006, 15, 1-4(Available online :) http://www.gomc.com/eSub/frameset-mc.asp (accessed on 13/11/2015).

[80] Yasuura, M.; Okazaki, H.; Tahara, Y.; Ikezaki, H.; Toko, K. Development of sweetness sensor with selectivity to negatively charged high-potency sweeteners. *Sens. Actuators B Chem*. 2014, 201, 329-335.

[81] Kuhn, C.; Bufe, B.; Winnig, M.; Hofmann, T.; Frank, O.; Behrens, M.; Lewtschenko, T.; Slack, J.P.; Ward, C.D.; Meyerhof, W. Bitter taste receptors for saccharin and acesulfame K. *J. Neurosci* 2004, 24, 10260-10265.

[82] Takagi, S.; Toko, K.; Wada, K.; Yamada, H.; Toyoshima, K. Detection of

suppression of bitterness by sweet substance using a multichannel taste sensor. *J. Pharm. Sci.* 1998, 87 (5), 552-555.

[83] Takagi, S.; Toko, K.; Wada, K.; Ohki, T. Quantification of suppression of bitterness using an electronic tongue. *J. Pharm. Sci.* 2001, 90 (12), 2042-2048.

[84] Yasuura, M.; Tahara, Y.; Ikezaki, H.; Toko, K. Development of a sweetness sensor for positively charged high-potency sweeteners. *Sensors* 2014, 14, 7359-7373.

[85] Uchida, T.; Yoshida, M. Quantitative evaluation of bitterness of medicines, in: Toko, K. (Ed.), Biochemical Sensors: Mimicking Gustatory and Olfactory Senses, Pan Stanford Publishing, Singapore, 2013, 145-184.

[86] Sugitate, K.; Nakamura, S.; Orikata, N.; Mizukoshi, K.; Nakamura, M.; Toriba, A.; Hayakawa, K. Search of components causing matrix effects on GC-MS for pesticide analysis in food. *J. Pestic. Sci.* 2012, 37, 156-163.

[87] Lawless, H.T.; Heymann, H. Sensory Evaluation of Food: Principles and Practices, second ed., Springer, New York, 1992, 156-158.

[88] Ito, M.; Wada, K.; Yoshida, M.; Hazekawa, M.; Abe, K.; Chen, R.G.; Habara, M.; Ikezaki, H.; Uchida, T. Quantitative evaluation of bitterness of H1-receptor antagonists and masking effect of acesulfame potassium an artificial sweetener, using a taste sensor. *Sens. Mater*. 2013, 25, 17-30.

[89] Breslin, P.A.; Beauchamp, G.K. Suppression of bitterness by sodium: variation among bitter taste stimuli. *Chem. Senses* 1995, 20 (6), 609-623.

[90] Beider, L.M. Taste, in: L.M. Beilder (Ed.), Handbook of Sensory Physiology IV: Chemical Senses, Springer-Verlag, Heidelberg, 1971, 200–220.

[91] Onitake, H.; Tahara, Y.; Yatabe, R.; Toko, K. Evaluation of a taste sensor for high-potency sweeteners. *Jpn. J. Taste Smell Res.* 2015, 22, 419–422 (in Japanese).

Acknowledgement

First and foremost, I would like to extend my sincere gratitude to my supervisor, Prof. Kiyoshi Toko whose patient guidance, valuable suggestions and constant encouragement make me successfully complete this thesis. His conscientious academic spirit and open-minded personality inspire me both in academic study and daily life. Also I would like to thank to Associate Prof. Hisao Kuriyaki and Associate Prof. Takeshi Onodera, for their constant assistance and guidance.

Next I would like to thank to Associate Prof. Yusuke Tahara, Assistant Prof. Rui Yatabe, and Assistant Prof. Masatoshi Kouzaki who provide me lots of constructive advices with my research. A specially thank to Associate Prof. Yusuke Tahara for helping me on revising my writing materials.

Also, I would like to thank Prof. Kenshi Hayashi, Prof. Junya Suehiro and Dr. Hidekazu Ikezaki (Intelligent Sensor Technology, Inc.) for their valuable and unyielding support throughout the completion of my thesis. I appreciate Mr. Zhiqin Huang, Mr. Hideya Onitake, Mr. Takeshi Shiino for helping me to complete the experiments.

Besides, I wish to thank to Ms. Ryoko Higo, Ms. Tomoko Hidaka, Ms. Yuri Toyomasu, Ms. Kumi Shige, for helping me solve problems in my study and life. A specially thank to Ms. Ryoko Higo for her immense support to my living in Japan.

Last but not least, I would like to express my gratitude to my beloved parents and family for caring and supporting me without any complaint.

Xiao Wu
2017 in Fukuoka, Japan